2016

Improved Assessment of the Magnitude and Acceleration of Prehistoric Earthquakes in the South Carolina Coastal Plain

Emad Gheibi
University of South Carolina

IMPROVED ASSESSMENT OF THE MAGNITUDE AND ACCELERATION OF PREHISTORIC EARTHQUAKES IN THE SOUTH CAROLINA COASTAL PLAIN

by

Emad Gheibi

Bachelor of Science
Valiasr University of Rafsanjan, 2008

Master of Science
Shahid Bahonar University of Kerman, 2011

Submitted in Partial Fulfillment of the Requirements

For the Degree of Doctor of Philosophy in

Civil Engineering

College of Engineering and Computing

University of South Carolina

2016

Accepted by:

Sarah Gassman, Major Professor

Charles Pierce, Committee Member

Pradeep Talwani, Committee Member

Abbas Tavakoli, Committee Member

Cheryl L. Addy, Vice Provost and Dean of the Graduate School

DEDICATION

To my Parents, Mehran and Roshanak and my siblings, Neda and Amin.

ACKNOWLEDGEMENTS

I would like to sincerely thank my advisor, Dr. Sarah L. Gassman. Dr. Gassman is certainly a tremendous mentor for me. I would like to thank her for supporting my research and for encouraging me to grow as a research scientist. Her advice, both on research and my career have been priceless. I am also grateful because there has been a very comfortable and friendly vibe in our research group, making me more productive. I was fortunate to have accomplished faculties as committee members, Dr. Charles Pierce, Dr. Pradeep Talwani and Dr. Abbas Tavakoli. I am indebted to them for much needed advice and feedback on my work. I would also like to express gratitude to USC graduate student Miss. Samaneh Shiri for her assistance in developing the MATLAB code.

Finally, I would like to acknowledge with my gratitude the support and love of my unique family; my lovely father and mother, Mehran and Roshanak, my smart brother, Amin, and my sister's family, Neda, Majid and Armita. They all kept me going and I would not be able to accomplish my PhD without their support.

ABSTRACT

Seismically-induced soil liquefaction is one the most hazardous geotechnical phenomenon that can cause loss of life and devastating damage to infrastructure. Proper estimation of critical ground motion parameters (e.g. peak ground acceleration and earthquake magnitude) is vital for seismic design of new structures and retrofit of existing structures, especially in regions such as the South Carolina Coastal Plain (SCCP) where the frequency of re-occurrence of large earthquakes is low (studies of paleoliquefaction features have revealed seven, large, prehistoric earthquakes occurring within the last 6000 years) and the locations of potential sources are not exactly known. Moreover, due to mechanical and chemical mechanisms, phenomena known as "aging", soil resistance to liquefaction increases with time and so the age of soil deposition must be considered in liquefaction analysis of aged soil deposits in the SCCP.

In 2005, a method was developed to estimate the minimum earthquake magnitude, M, and peak ground acceleration, a_{max}, of prehistoric earthquakes using in-situ geotechnical data (e.g. cone penetration and standard penetration data), back-calculation methods (e.g. the Energy Stress and Cyclic Stress methods) and several approaches that account for soil aging by considering density changes in the soil with time. Since then, newer semi-empirical approaches have been published based on an expanded case history database of liquefaction/no liquefaction sites. Ground Motion Prediction Equations (GMPEs) have also been used in combination with back-calculation methods to estimate the earthquake magnitudes. Additional studies related to soil age

have also been published. Therefore, the purpose of this study is to use these newer approaches to further improve the current estimates of M and a_{max} at the four sites of Hollywood, Fort Dorchester, Sampit, and Gapway located in the SCCP.

The first study in this dissertation improved upon the 2005 study by using a newer semi-empirical liquefaction analysis method to update the cyclic resistance ratio (CRR) and back-calculate the minimum peak ground acceleration at Sampit and Gapway sites. The effect of aging on soil resistance was taken into account using the same methodology as in 2005. Results show that the newer method for calculating CRR produces lower peak ground accelerations than the previously used approach. The difference is most significant for lower magnitudes. Calculated average values of age-adjusted magnitude range from 5 to 7.5 and the corresponding age-adjusted peak ground acceleration range from 0.08 to 0.23g.

The newer method used in the first study was also used at the Hollywood site, a site that had not been previously studied in 2005, and has evidence of four episodes of paleoliquefaction. The results are presented in the second study of this dissertation. For the Hollywood site, it was shown that when the age of the earthquake was not considered, the magnitude ranged from 7 to 7.2 and the corresponding acceleration ranged from 0.23 to 0.35g. The minimum earthquake magnitude at the time of earthquake was found to be lower when accounting for age. As an example, for the most recent prehistoric earthquake with the age of 546±17, the minimum back-calculated magnitude ranged from 5.7 to 6.7 with corresponding acceleration ranging from 0.17 to 0.30g.

The third study of this dissertation used a newer aging approach that considers the influence of age, cementation and stress history on the CRR of the soil to back-calculate

the minimum earthquake magnitudes at the Fort Dorchester site. The new aging approach provided magnitudes that ranged from 5.1 to 6.2 and were in general agreement with previously used methods that considered the effect of aging on only the CPT tip resistance values. Also, when the size of the fault was considered, the maximum magnitude was found to be 5.6 and the corresponding peak ground acceleration ranged from 0.21 to 0.36 g.

The fourth study of this dissertation presents the results from a statistical analysis performed on the available geotechnical data set to find a relation between the updated obtained cyclic resistance ratio values. Significant correlation between equivalent clean sand tip resistance and the cyclic resistance ratio at the time of earthquake was shown using descriptive statistics, summary statistics and regression analysis on the current measurements of field test data.

The fifth study of this dissertation used four proper GMPEs for the east coast of the US combined with the Cyclic Stress method to predict the minimum earthquake magnitude and peak ground acceleration at the Hollywood, Fort Dorchester, Sampit and Gapway sites and find a regional assessment of a_{max}-M in the SCCP. Results were compared with previously found values using the Cyclic Stress and Energy Stress methods. It was shown that when the source of the earthquake is associated with the Charleston Source, the minimum earthquake magnitudes for the prehistoric earthquakes that occurred between about 546 to 1021 years ago and between 3548 to 5038 years ago were estimated to range from 6.6 to 7.5 and 6.1 to 7.2, respectively. For the earthquakes associated with the Sawmill Branch Fault that occurred about 3500 years ago or earlier, the minimum earthquake magnitudes were estimated to range from 5 to 6.3.

TABLE OF CONTENTS

DEDICATION iii

ACKNOWLEDGEMENTS iv

ABSTRACT v

LIST OF TABLES xii

LIST OF FIGURES xv

LIST OF SYMBOLS xvii

LIST OF ABBREVIATIONS xix

CHAPTER 1: INTRODUCTION 1

1.1 RESEARCH TOPIC I – EVALUATION OF NEW METHODS TO CALCULATE CRR FOR BACK-ANALYSIS OF PEAK GROUND ACCELERATION 3

1.2 RESEARCH TOPIC II – EFFECT OF AGING ON BACK-CALCULATED EARTHQUAKE MAGNITUDES AND PEAK GROUND ACCELERATION 4

1.3 RESEARCH TOPIC III – EVALUATION OF NEWER AGING APPROACHES FOR BACK-ANALYSIS OF EARTHQUAKE MAGNITUDES 5

1.4 RESEARCH TOPIC IV –STATISTICAL ANALYSIS OF POST-EARTHQUAKE CYCLIC RESISTANCE RATIOS 5

1.5 RESEARCH TOPIC V – REGIONAL ASSESSMENT OF THE a_{MAX}-M FOR THE CHARLESTON AREA 6

1.6 LIST OF PAPERS AND STRUCTURE OF DISSERTATION 7

CHAPTER 2: BACKGROUND AND LITERATURE REVIEW 9

2.1 SUMMARY OF PALEOLIQUEFACTION STUDIES IN THE SCCP 9

2.2 GEOTECHNICAL FIELD TESTS 11

2.3 Liquefaction Analysis Methods 15

2.4 Paleoearthquake Evaluation Methods 22

2.5 Time-Dependent (Aging) Phenomenon 32

2.6 Summary 38

Chapter 3: Reassessment of Prehistoric Earthquake Accelerations at Sampit and Gapway Sites in the South Carolina Coastal Plain 40

3.1 Introduction 41

3.2 Sites Investigated 43

3.3 Methods 44

3.4 Results 51

3.5 Conclusion 54

Chapter 4: Magnitudes of Prehistoric Earthquakes at the Hollywood, South Carolina Site 55

4.1 Introduction 56

4.2 Site Studied 58

4.3 Framework for Age and Disturbance Correction 61

4.4 Results 66

4.5 Conclusions 70

Chapter 5: Application of Geotechnical Data to Determine a Charleston-Area Prehistoric Earthquake Magnitude 72

5.1 Introduction 73

5.2 Site Description 75

5.3 Geotechnical Field and Laboratory Data 76

5.4 Methodology 85

5.5 Results 91

5.6 Summary and Conclusions 96

Chapter 6: Using Regression Model to Predict Cyclic Resistance Ratio at South Carolina Coastal Plain (SCCP) 97

6.1 Introduction 98

6.2 Site Studied 100

6.3 Methodology 101

6.4 Data Analysis 103

6.5 Results 104

6.6 Conclusions 109

Chapter 7: Application of GMPEs to Estimate the A_{MAX}-M of Prehistoric Earthquakes for the Charleston Area 112

7.1 Introduction 113

7.2 Site Studied 116

7.3 Framework for Age correction 116

7.4 Paleoliquefaction Back-Analysis Procedure 119

7.5 Results 124

7.6 Conclusion 146

Chapter 8: Conclusion 148

8.1 Summary and Conclusions 149

8.2 Future Research 152

References 154

Appendix A: Copyright Permissions to Reprint 167

A1 Chapter 3 Copyright Permission 168

A2 Chapter 4 Copyright Permission 169

A3 CHAPTER 6 COPYRIGHT PERMISSION 170

A4 CHAPTER 7 COPYRIGHT PERMISSION 171

LIST OF TABLES

Table 3.1 Average Values of Current, Post- and Pre- Earthquake Tip resistance Data for Source Sand Layer Corrected for Aging and Disturbance 46

Table 3.2 Estimated Magnitudes of Prehistoric Earthquake Episodes in SCCP 48

Table 3.3 Average Values of $(q_{c1N})_{cs\ (pre)}$ corresponding to $q_{c1(pre)}$ from Table 3.1 51

Table 3.4 Comparison of $CRR_{M=7.5}$ found from two methods 52

Table 3.5 Peak Ground Acceleration for Source Sand Layer 53

Table 3.6 Estimated Peak Ground Accelerations of Prehistoric Earthquake Episodes in the SCCP 54

Table 4.1 Average values of Age-Corrected Tip Resistance for Source Sand Layer 63

Table 4.2 Average Values of Age-Corrected Blow Counts for Source Sand Layer 63

Table 4.3 Average Values of $(q_{c1N})_{cs\ (pre)}$ Corresponding to $q_{c1(pre)}$ 66

Table 4.4 Earthquake Magnitudes 67

Table 4.5 Average Values of $CRR_{M=7.5}$ 67

Table 4.6 Peak Ground Acceleration for Source Sand Layer 68

Table 4.7 Estimated Peak Ground Accelerations 70

Table 5.1 Source Sand Layer Depth, Elevation, Thickness, and Water Table Depth 80

Table 5.2 Source Sand Index Test Results 82

Table 5.3 CPT Results for the Source Sand Layer Susceptible to Liquefaction 84

Table 5.4 Post-Earthquake Values of q_{c1} and $(N_1)_{60}$ and CRR for the Source Sand Layer 92

Table 5.5 Peak Ground Acceleration for Source Sand Layer 94

Table 5.6 Earthquake Magnitude (M) for the Age of 3500 Year B.P. 95

Table 6.1 Average Values of Current Tip Resistance in the Source Sand Layer 102

Table 6.2 Age of Sand Blows at Each Test Location 103

Table 6.3 Frequency Distribution of (a) Age and (b) Fines Content 104

Table 6.4 N, Mean, Standard Deviation, Minimum, and Maximum for Variables 105

Table 6.5 N, Means, Standard Deviation, Minimum, and Maximum for Variables by Fines Content Levels.....106

Table 6.6 Pearson Correlation.....107

Table 6.7 Multiple Regression Models for Equivalent Clean Sand Tip Resistance on Cyclic Resistance Ratio at the Time of Earthquake for Approach 1 and 2 and Different Percentages of Change in Relative Density.....108

Table 7.1 Average Values of q_{c1} and CRR for the Source Sand Layer that Have Been Corrected for Age 119

Table 7.2 Ground Motion Prediction Models Used for Back-Calculations.....123

Table 7.3 Average Values of a_{max} for Source Sand Layer. 125

Table 7.4 Minimum a_{max}-M for Each Test Location at the Hollywood Site, Found Using the Combined Methods of Cyclic Stress and GMPEs for Different Earthquake Episodes. 131

Table 7.5 Minimum a_{max}-M for Each Test Location at the Fort Dorchester Site, Found Using the Combined Methods of Cyclic Stress and GMPEs for Different Earthquake Episodes. 133

Table 7.6 Minimum a_{max}-M for Each Test Location at the Sampit Site, Found Using the Combined Methods of Cyclic Stress and GMPEs for Different Earthquake Episodes. 135

Table 7.7 Minimum a_{max}-M for Each Test Location at the Gapway Site, Found Using the Combined Methods of Cyclic Stress and GMPEs for Different Earthquake Episodes. 137

Table 7.8 Range of minimum a_{max}-M at Each Test Location Found Using the Combined Methods of Cyclic Stress and GMPEs. 139

Table 7.9 Range of Minimum a_{max}-M at Each Test Location.....142

Table 7.10 Summary of Estimated Minimum Peak Ground Acceleration and Earthquake Magnitude at the Hollywood, Fort Dorchester, Sampit and Gapway Sites……. ..143

LIST OF FIGURES

Figure 2.1 Locations of Paleoliquefaction Features in the South Carolina Coastal Plain. 10

Figure 2.2 Normalized CPT Soil Behavior Type Chart. 13

Figure 2.3 Relation Between Epicentral Distance and Earthquake Magnitude. 24

Figure 2.4 Relation Between Blow Count Number and Seismic Energy Intensity Function. 25

Figure 2.5 Combination of GMPE and Liquefaction Evaluation Methods for a Hypothetical Site. 27

Figure 2.6 Paleoliquefaction Sites in the Wabash Valley. 27

Figure 2.7 Regional Assessment of Vincennes Earthquake Strength Using (a) Somerville et al. 2001, (b) Atkinson and Boore 1995, (c) Toro et al. 1997, and (d) Campbell 2001, 2003 GMPEs. 28

Figure 2.8 Comparison of Ground Motion Predictions. 30

Figure 2.9 Comparison of Ground Motion Predictions. 30

Figure 2.10 SEM Images of Ottawa Sand Grain Surface, Image Width (a) 160 μm, (b) 100 μm, and (c) 10 μm.. 34

Figure 2.11 Variation in C_D Due to the Postliquefaction Densification, Δe_R. 36

Figure 2.12 (a) Effect of Particle Size on Blow Counts in Sands. (b) Effect of Aging on Blow Counts 37

Figure 2.13 Deposit Resistance Factor, K_{DR}, as a Function of Time 38

Figure 3.1 CPT Profiles at the Sampit and Gapway Sites 45

Figure 4.1 CPT and SPT Profiles at the Hollywood Sites 60

Figure 4.2 Soil Profile at Hollywood 61

Figure 5.1 Geology of the Fort Dorchester Area 76

Figure 5.2 Locations of Field Tests and Profile Alignments 77

Figure 5.3 Subsurface Profile of the Northern East-West Alignment 78

Figure 5.4 Subsurface Profile of the North-South Alignment 79

Figure 5.5 Index Properties of Soils from Vibracores 83

Figure 6.1 Locations of Paleoliquefaction Features in South Carolina Coastal Plain 100

Figure 7.1 An Example of a_{max}-M Combination to Trigger Liquefaction 121

Figure 7.2 Combined GMPE and Liquefaction Evaluation Methods.....122

Figure 7.3 Relation Between a_{max} and M for Each Test Location at Hollywood Site:
(a) HWD-4, (b) HWD-5, and (c) HWD-6 127

Figure 7.4 Relation Between a_{max} and M for Each Test Location at Fort Dorchester
Site: (a) FD-1, (b) FD-2, (c) FD-3, and (d) FD-7 127

Figure 7.5 Relation Between a_{max} and M for Each Test Location at Sampit Site:
(a) SAM-1, (b) SAM-2, and (c) SAM-3.....128

Figure 7.6 Relation Between a_{max} and M for Each Test Location at Gapway Site:
(a) GAP-1, (b) GAP-2, and (c) GAP-3.....128

Figure 7.7 Combination of the Cyclic Stress Method and GMPEs to Find the
Minimum amax and M for Each Test Location at the Hollywood Site:
(a) HWD-4, (b) HWD-5, and (c) HWD-6 130

Figure 7.8 Combination of the Cyclic Stress Method and GMPEs to Find the
Minimum a_{max} and M for Each Test Location at the Fort Dorchester Site:
(a) FD-1, (b) FD-2, (c) FD-3, and (d) FD-7 132

Figure 7.9 Combination of the Cyclic Stress Method and GMPEs to Find the
Minimum a_{max} and M for Each Test Location at the Sampit Site:
(a) SAM-1, (b) SAM-2, and (c) SAM-3.....134

Figure 7.10 Combination of the Cyclic Stress Method and GMPEs to Find the
Minimum a_{max} and M for Each Test Location at the Gapway Site:
(a) GAP-1, (b) GAP-2, and (c) GAP-3.....136

Figure 7.11 Minimum Earthquake magnitudes for Prehistoric Earthquakes
In SCCP Found Using GMPEs 145

LIST OF SYMBOLS

a_{max} Peak ground acceleration.

B_q Normalized cone pore pressure ratio.

C_B Correction factor for borehole diameter in SPT.

C_C Compression index.

C_E *or* $ER_m/60$ Energy ratio correction factor.

C_N Overburden normalization factor.

C_Q Correction parameter for overburden pressure.

C_R Correction factor for rod length in SPT.

C_S Correction factor for sampler in SPT.

C_α Secondary compression index.

ER_m Measured delivered energy ratio in SPT.

F Normalized friction ratio.

F_S Sleeve friction in CPT.

I_C Soil behavior type index in CPT.

K_C Correction factor for the effect of grain characteristics in CPT.

K_{DR} Liquefaction resistance correction factor.

K_σ Overburden correction factor.

M Earthquake magnitude.

N_m Measured blow counts in SPT.

N_{60} Blow count for an energy ratio of 60% in SPT.

$(N_1)_{60}$ Corrected SPT blow count for the effect of energy and overburden pressure.

P_a Atmospheric pressure = 100kPa.

Q Stress normalized cone penetration resistance in CPT.

q_c Cone penetration tip resistance in CPT.

q_{c1N} Normalized value of q_{c1} for the effect of overburden pressure in CPT.

$(q_{c1N})_{cs}$ Equivalent clean sand value of tip resistance in CPT.

R *or* R_h Hypocentral distance.

R_e Epicentral distance.

r_d Correction factor for soil column flexibility.

T Seismic intensity.

t_R Time to the end of primary consolidation.

U_2 Pore water pressure

U_0 Hydrostatic pore pressure

Z Depth of Soil

σ_{vc} Total vertical stress

$\sigma`_{vc}$ Total vertical stress

ΔD_R Change in relative density

List of Abbreviations

BP ..... Before Present

BPT ..... Becker Penetration Test

CPT ..... Cone Penetration Test

CRR ..... Cyclic Resistance Ratio

CSR ..... Cyclic Stress Ratio

ENA ..... Eastern North America

FC ..... Fines Content

FD ..... Fort Dorchester

FHS ..... Four Hole Swamp

GAP ..... Gapway

GMPE ..... Ground Motion Prediction Equation

HWD ..... Hollywood

MSF ..... Magnitude Scaling Factor

PEER ..... Pacific Earthquake Engineering Research Center

PGA ..... Peak Ground Acceleration

PGV ..... Peak Ground Velocity

PL ..... Liquefaction probability

PSA ..... Pseudo-absolute Acceleration Spectra

PZ ..... Piezometer

RA ..... Fault Rupture Area

REG ..... Regression

R_{rup} .....Distance to Fault Rapture

SAM..... Sampit

SBF ..... Sawmill Branch Fault

SCCP..... South Carolina Coastal Plain

SPT..... Standard Penetration Test

TMH.....Ten Mile Hill

WF..... Wood Stock Fault

WNA ..... Western North America

VC ..... Vibracore Soil Core

V_S ..... Shear Wave Velocity

CHAPTER 1

INTRODUCTION

Seismically-induced soil liquefaction is one the most hazardous geotechnical phenomenon that can cause loss of life and devastating damage to infrastructure. In 1964, earthquakes in Nigata, Japan (M=7.5) and Alaska, USA (M=9.2) destroyed numerous buildings and structures and initiated studies to understand soil liquefaction. Since then, there have been major advances in both understanding and practice with regard to assessment and mitigation of hazards associated with seismically induced soil liquefaction (Seed and Idriss 1971 and 1982, Robertson and Wride 1998, NCEER 2001, etc.). One major outcome from these studies has been the development of empirical correlations that are extensively used to determine liquefaction resistance of sand deposits from in-situ soil indices (e.g. $(N_1)_{60}$ from the standard penetration test (SPT) and $(q_c)_1$ from the cone penetration test (CPT)).

In regions such as the South Carolina Coastal Plain (SCCP), where the frequency of large earthquakes is low and the locations of potential sources are not exactly known, the study of liquefaction evidence produced from prehistoric earthquakes plays an important role in understanding the regional seismic hazard and estimating critical ground motion parameters (e.g. peak ground acceleration and earthquake magnitude) for modern seismic design. Such paleoliquefaction studies in the SCCP have revealed more than 100 sand blows associated with at least seven, large, prehistoric earthquakes occurring within the last 6000 years (Talwani and Schaeffer 2001, Martin and Clough

1994, Obermeier et al. 1987, Weems et al. 1986 and Talwani and Cox 1985). The soil deposits associated with these sand blows are older than Holocene age (<10,000 years old) (Talwani and Cox 1985 and Weems et al. 1986) and studies have shown that the cyclic resistance ratio (CRR) of soil increases with time due to mechanical and chemical mechanisms (Mitchell and Solymar 1984, Dowding and Hryciw 1986, Skempton 1986 and Mesri et al. 1990), a phenomenon known as "aging." Therefore, using empirical correlations that are primarily based on studies of recent earthquakes in California and Japan where the soil deposits are of Holocene age to determine liquefaction resistance of old sand deposits in the SCCP (>100,000 years old) is not strictly valid.

Recently, a method was developed by Leon et al. 2005 to consider the effect of aging on the cyclic resistance ratio of aged soil deposits in the SCCP. In-situ geotechnical data (penetration resistance and shear wave velocity reported by Hu et al. 2002 a,b) from two sites (Gapway and Sampit) near Georgetown, South Carolina and two sites near the Ten Mile Hill Air Force Base north of Charleston, South Carolina were used to back calculate prehistoric minimum earthquake magnitudes and peak ground accelerations using Seed's simplified method (as reported in Youd and Idriss 1997) and time-dependent approaches of Mesri et al. 1990 and Kulhawy and Mayne 1990. Using this methodology, Leon et al. 2006 found that neglecting the effect of aging resulted in a 60% underestimation of CRR.

Since the study of Leon et al. 2005, newer methods for liquefaction analysis with consideration to aged soil deposits have been published. For example, Seed's simplified method of liquefaction analysis has been reexamined using additional liquefaction/no liquefaction case histories (Moss et al. 2006 and Idriss and Boulanger 2008) and Green et

al. 2005 used Ground Motion Prediction Equations (GMPEs) in combination with Cyclic Stress methods to back-calculate the earthquake magnitudes of the Vincennes Earthquake that occurred around 6100 years B.P. in the Wabash Valley. Furthermore, Hayati and Andrus 2009 studied data from over 30 sites in 5 countries and proposed a newer aging approach that considers the effect of aging on CRR.

Therefore, the main goal of this study is to use these newer approaches to find a combination of minimum magnitude, M, and peak ground acceleration, a_{max}, for the prehistoric earthquakes associated with the aged soil deposits in the SCCP. In-situ geotechnical data from the cone penetration test (CPT) and standard penetration test (SPT) (including tip resistance, sleeve friction, pore water pressures and blow counts) obtained in the vicinity of prehistoric sand blows (see Hu et al. 2002 a,b and Hasek 2016) at the SCCP sites of Hollywood (HWD), Fort Dorchester (FD), Sampit (SAM), and Gapway (GAP) will be used in this work. The following five research topics are explored in this dissertation:

1.1 RESEARCH TOPIC I – EVALUATION OF NEW METHODS TO CALCULATE CRR FOR BACK-ANALYSIS OF PEAK GROUND ACCELERATION

Due to the significant impact of the liquefaction evaluation methods on assessment of the cyclic resistance ratio and factor of safety, using the proper liquefaction method has received considerable attention (e.g. Cetin et al. 2004, Moss et al. 2006 and Idriss and Boulanger 2008). The first study in this dissertation presents a reassessment of the prehistoric earthquake peak ground accelerations at the Sampit and Gapway sites using the newer semi-empirical method of liquefaction analysis (to update the CRR) proposed by Idriss and Boulanger 2008 with the time-dependent approaches of Mesri et al. 1990 and Kulhawy and Mayne 1990 that were used by Leon et al. 2005. The source

sand at these sites is estimated to be 450,000 years old (Weems and Lemon 1984). The age of sand blows are associated with earthquakes occurring about 546±17 and 1021±30 years B.P. at Sampit and about 3548±66 and 5038±166 years B.P. at Gapway sites (Talwani and Schaeffer 2001). Readers are referred to Chapter 3 of this dissertation for more information about this work, which provides an overview of the previously used methods for back-analysis of minimum earthquake magnitudes at the Sampit and Gapway sites and illustrates how using the newer approach changed the results.

1.2 RESEARCH TOPIC II –EFFECT OF AGING ON BACK-CALCULATED EARTHQUAKE MAGNITUDES AND PEAK GROUND ACCELERATION

The second study of this dissertation addresses the back-calculation of the minimum earthquake magnitude and required acceleration for liquefaction initiation at the time of earthquake at the Hollywood site using the newer semi-empirical method of liquefaction analysis proposed by Idriss and Boulanger 2008 and the time-dependent approaches of Mesri et al. 1990 and Kulhawy and Mayne 1990 that were used by Leon et al. 2005. The source sand at the Hollywood site is estimated to be 120,000 to 130,000 years old (Weems et al. 1986) and the age of the sand blows have been associated with earthquakes occurring 546±17 years B.P., 1021±30 years B.P., 3548±66 years B.P. and 5038±166 years B.P. (Talwani and Schaeffer 2001). Results from the study were compared to earlier back-calculations by Martin and Clough 1994 that did not consider the effect of aging. Readers are referred to Chapter 4 of this dissertation for more information about this work, which provides a review of related studies, research contribution, description of aging approaches and the methodologies used to back-calculate the magnitudes in detail.

1.3 RESEARCH TOPIC III – EVALUATION OF NEWER AGING APPROACHES FOR BACK-ANALYSIS OF EARTHQUAKE MAGNITUDES

Minimum earthquake magnitude and peak ground acceleration of prehistoric earthquakes at the Fort Dorchester site is investigated using the newer aging approach of Hayati and Andrus 2009 with the newer liquefaction analysis methods of Idriss and Boulanger 2008 studied in Research Topics 1 and 2. The aging approach of Hayati and Andrus 2009 uses an updated liquefaction resistance correction factor (that considers the influence of age, cementation and stress history) to find the deposit resistance-corrected CRR; whereas, the two aging approaches of Mesri et al. 1990 and Kulhawy and Mayne 1990 use relations between observed increases in penetration resistance and relative density to modify the CPT tip resistance or SPT blow counts for the effect of aging. The source sand at the Fort Dorchester site is about 200,000 years old (McCarten et al. 1984; Weems and Lemon 1984) and the discovered sand blow is associated with an earthquake having a minimum age of 3500 or 6000 years B.P. (Talwani et al. 2011). Readers are referred to Chapter 5 of this dissertation for more information about this work, which describes the studied site and the aging approaches in detail.

1.4 RESEARCH TOPIC IV –STATISTICAL ANALYSIS OF POST-EARTHQUAKE CYCLIC RESISTANCE RATIOS

Empirical liquefaction potential assessment correlations are developed based on analyzing experimental studies and case studies. Running statistical analyses on the smaller liquefaction data sets leads to extend meaningful correlations that can be used as a larger data base to predict liquefaction at the sites where complete sets of data are not available. The fourth study of this dissertation addresses performing descriptive statistics, summary statistics and regression analysis on the current measurements of field test data

(CPT tip resistance values) at the SCCP sites of FD, HWD, SAM, GAP and FHS to predict the cyclic resistance ratio of the soil at the time of prehistoric earthquakes in the South Carolina Coastal Plain. Readers are referred to Chapter 6 of this dissertation for more information about this work, which describes the studied sites and the statistical analysis in detail.

1.5 RESEARCH TOPIC V –REGIONAL ASSESSMENT OF a_{MAX} -M FOR THE CHARLESTON AREA

Chapter 7 of this dissertation presents the research aimed to form a regional assessment of the a_{max}-M in the Charleston, SC area. The Hayati and Andrus 2009 aging approach is applied to the Sampit, Gapway, and Hollywood sites (first studied in Chapters 3 and 4 using the aging approaches of Mesri et al. 1990 and Kulhawy and Mayne 1990). This is necessary to further investigate the effect of the new aging approach on the minimum earthquake magnitudes and accelerations back-calculated using the site-specific geotechnical method (Cyclic Stress method) at all four sites.

Four regionally proper Ground Motion Prediction Equations (GMPEs) for the east coast of the US (Toro et al. 1997, Tavakoli and Pezeshk 2005, Atkinson 2008' and Pezeshk et al. 2011) are used to estimate the minimum earthquake magnitude and peak ground acceleration at the Hollywood, Fort Dorchester, Sampit, and Gapway sites and compare the results with previously found values using the site-specific geotechnical method (Cyclic Stress method) and Energy Stress methods. Readers are referred to Chapter 7 of this dissertation for more information about this study.

1.6 LIST OF PAPERS AND STRUCTURE OF DISSERTATION

This dissertation includes results that have been published or submitted to peer-reviewed conferences and journals. One additional paper is in preparation. The five completed articles that appear in the dissertation as separate chapters include:

1. Gheibi, E., and Gassman, S.L. (2014). "Reassessment of prehistoric earthquake accelerations at Sampit and Gapway sites in the South Carolina Coastal Plain." *Network for Earthquake Engineering Simulation (distributor),* Paper, DOI:10.4231/D3PV6B73Z
2. Gheibi, E., and Gassman, S.L. (2015). "Magnitudes of prehistoric earthquakes at the Hollywood, South Carolina, Site." *Geotechnical Special Publication,* 256: 1246-1256, DOI: 10.1061/9780784479087.112
3. Gheibi, E., Gassman, S.L., and Tavakoli, A. (2014). "Using regression model to predict cyclic resistance ratio at South Carolina Coastal Plain (SCCP)." *Advanced Analytics (distributor),* Paper, DOI: 10.13140/2.1.4893.4081
4. Gheibi, E., and Gassman, S.L. (2016). "Application of GMPEs to estimate the minimum magnitude and peak ground acceleration of prehistoric earthquakes at Hollywood, SC." *Engineering Geology,* 214: 60-66. DOI: 10.1016/j.enggeo.2016.09.016
5. Gheibi, E., Gassman, S.L., Hasek, M., and Talwani, P. (2017). "Assessment of paleoseismic shaking that caused sand blow at Fort Dorchester, SC." *Bulletin of Earthquake Engineering,* Submitted.

The format of this dissertation follows a manuscript style and the remaining chapters are organized as follows: Chapter 2 provides a brief overview of geotechnical

in-situ testing, liquefaction potential assessment methods, paleoearthquake evaluation methods and time dependent mechanisms ("aging"). Chapters 3, 4, 5, 6 and 7 include the five original research papers mentioned above. Finally, conclusions are presented in Chapter 8.

CHAPTER 2

BACKGROUND AND LITERATURE REVIEW

This chapter presents the necessary background information related to the data and methods used in this study. First, an overview of the paleoliquefaction studies in the South Carolina Coastal Plain (SCCP) is provided. A brief explanation of the procedures used to analyse the previously collected Cone Penetration Test (CPT) and Standard Penetration Test (SPT) data in the SCCP sites is also presented. Time dependent mechanisms that are associated with aging phenomenon are explained and methods that consider the effect of time dependent mechanism on soil strength are discussed. The liquefaction analysis methods that were used to evaluate the liquefaction potential at the SCCP sites are described in addition to the methods to back-analyse the earthquake magnitude and peak ground acceleration of the prehistoric earthquakes including Magnitude Bound method, Energy Stress method and Ground Motion Prediction Equations (GMPEs).

2.1 SUMMARY OF PALEOLIQUEFACTION STUDIES IN THE SCCP

Cox 1984 discovered a sand blow at Warrens Crossroads located at 40 km west of Charleston, South Carolina. Following his findings, Obermeier et al. 1987 conducted series of research to discover the extent of paleoliquefaction features associated with the prehistoric earthquakes in the soils of SCCP and the areas which experienced paleoliquefaction. More studies have been performed during the past thirty years to determine the location and age of sand blows in the SCCP. Talwani et al. 1999 and

Talwani and Schaeffer 2001 discussed the discovery of more than fifty sand blows associated with earthquakes that date back as far as 6,000 years. Figure 2.1 indicates location of paleoliquefaction features discovered in the South Carolina Coastal Plain area.

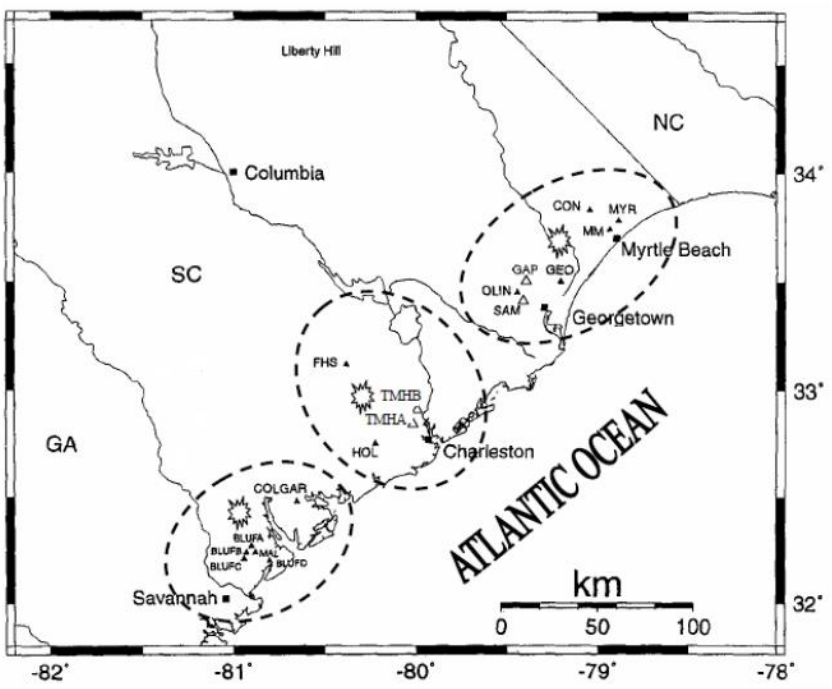

Figure 2.1 Locations of paleoliquefaction features in the South Carolina Coastal Plain (adapted from Hu et al. 2002a).

Hu et al. 2002a used geotechnical data (CPT, SPT, Vs, and soil index properties) to evaluate the liquefaction potential at three sites of Sampit (SAM), Gapway (GAP) and Ten Mile Hill (TMHA and TMHB) located in the SCCP. Leon et al. 2005 and 2006 assessed liquefaction potential at the time of earthquake at these sites using a time-dependent approach and two methods of Mesri et al. 1990 and Kulhawy and Mayne 1990 to account for the age of soil.

The focus of this research is to estimate a proper combination of a_{max}-M for the prehistoric earthquakes that liquefied soils at five sites of Hollywood (HWD), Fort Dorchester (FD), Sampit (SAM), Gapway (GAP) and Four Hole Swamp (FHS) in the SCCP. Back-calculation is performed using geotechnical data (CPT, SPT and soil index properties), time-dependent approaches that consider the effect of aging on increase in soil resistance against liquefaction, liquefaction analysis methods (site-specific method) and Ground Motion Prediction Equations. Readers are referred to Chapter 3 for more detailed information regarding the description of the Sampit and Gapway sites and Chapter 4 and 5 for the Hollywood and Fort Dorchester sites, respectively.

2.2 GEOTECHNICAL FIELD TESTS

2.2.1 Cone Penetration Test (CPT)

Cone penetration test is a method used to delineate soil stratigraphy and determine geotechnical properties of soil such as: cone penetration tip resistance, q_c, sleeve friction, f_s, pore water pressure, u_2. The test consists of hydraulically penetration of an electric piezocone into the soil at a constant rate of 2cm/sec (ASTM D5778-12 (2012)). The test provides continues record of penetration resistance along the soil profile. CPT measurements are used to determine soil type using Figure 2.2, Equations 2.1, 2.2 and 2.3.

$$Q = \left(\frac{q_c - \sigma_{vc}}{P_a}\right)\left(\frac{P_a}{\sigma'_{vc}}\right)^n \tag{2.1}$$

where Q is stress normalized cone penetration resistance, σ_{vc} is the total vertical stress, σ'_{vc} is the effective vertical stress, P_a is the atmospheric pressure, and the exponent n

varies from 0.5 in sands to 1 in clays (Robertson and Wride 1998). Normalized friction ratio, F, and normalized cone pore pressure ratio, B_q, are is determined as follows:

$$F = \left(\frac{f_s}{q_c - \sigma_{vc}}\right).100\% \tag{2.2}$$

$$B_q = \left(\frac{u_2 - u_0}{q_c - \sigma_{vc}}\right) \tag{2.3}$$

where u_0 is hydrostatic pore pressure. Soil behavior type index, I_c, is used to correlate fines content and liquefaction resistance of soil as presented by Robertson and Wride 1998 in Equation 2.4.

$$I_C = [(3.47 - \log(Q))^2 + (\log(F) + 1.22)^2]^{0.5} \tag{2.4}$$

Robertson 2009 pointed out the influence of soil sensitivity and overconsolidation ratio on the parameters F and Q respectively (shown in Figure 2.2) and updated the approach to determine value of n as in Equation 2.5:

$$n = 0.381\ (I_C) + 0.05\left(\frac{\sigma'_{vc}}{P_a}\right) - 0.15 \qquad where\ n \leq 1 \tag{2.5}$$

Robertson 1990 suggested using normalized CPT soil Behavior type chart shown in Figure 2.2 to determine soil type. Zone 5, 6 and 7 are potential zones for soil liquefaction according to Robertson and Wride 1998. Soil in zone 5, 6 and 7 in Figure 2.2 is mostly consists of sand mixtures with little fines. Robertson and Wride 1998 criteria

for soil liquefaction is F<1% and $(q_{c1N})_{cs}$<160. They also defined the boundaries in Figure 2.2 using I_c values as follows; clays (I_c>2.95), silts (2.05≤I_c≤2.95) and sands (I_c<2.05). In general Robertson and Wride 1998 criteria for soil liquefaction is I_c≤2.6 and B_q ≤0.5 but considering the concerns proposed by Youd et al. 2001 and Hayati and Andrus 2008, soils with I_c<2.4 and B_q<0.4 are susceptible to liquefaction and soils fall in the range of I_c>2.6 and B_q>0.5 are considered as the nonliquefiable soils. Soils between these criteria are considered as moderately liquefiable and additional testing is required to define the liquefaction susceptibility.

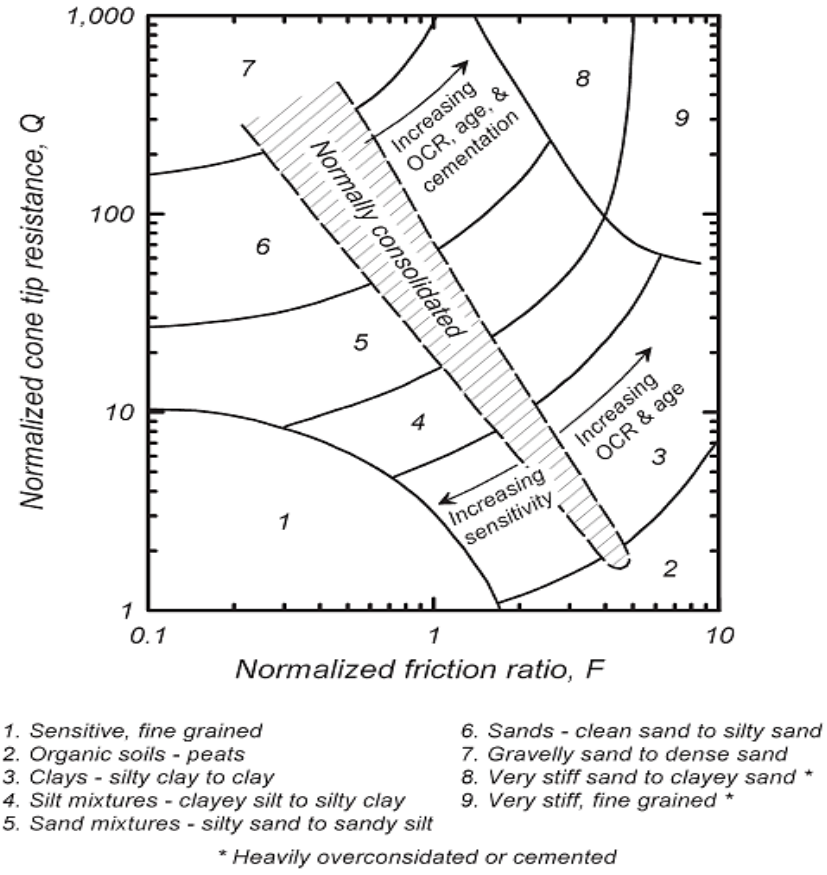

Figure 2.2 Normalized CPT soil behavior type chart (adapted from Robertson 1990).

2.2.2 Standard Penetration Test (SPT)

Standard penetration test is a widely used method to determine soil strength and compactness. A 140-pound hammer connected to drill rods and a split spoon sampler falls freely and repeatedly through a distance of 760 mm (30in) to drive a standard split spoon into the ground for 150 mm (6in) (ASTM D1586-11 (2011)). Number of blow counts for sampler penetration at each interval (6in) is recorded. Sum of the blow count numbers for second and third intervals is reported as the "Standard Penetration Resistance" or the N value. Soil samples collected from split spoon sampler are disturbed due to the penetration method but are proper for the index geotechnical testing. SPT is widely used throughout the world because of its simplicity and economic efficiency. The important advantage of using SPT is collection of soil samples but the test provides non-continues data in depth of soil profile which is an important disadvantage. It is shown that temperature has significant effect on dynamic properties of the material (Gheibi et al. 2016) and soil strength parameters also may vary by the change in soil temperature (Moradi et al. 2015, 2016, Baser et al. 2016, McCartney et al. 2015) or environmental effects that cause electro consolidation in soil deposits (Malekzadeh and Sivakugan 2016, Saeedi et al. 2012). Moreover, blow count numbers are significantly affected by parameters such as hammer type, blow rate, overburden pressure, drill length and type of anvil. Depending upon type of equipment and operation environment 10-70% of the energy (the 140-Ib hammer drops from 30in height) transferred to the drill rod stem by each impact is lost by the frictional and mechanical resistances. Seed et al. 1984 considered N_{60} as the standard for SPT as:

$$N_{60} = N_m \frac{ER_m}{60} \tag{2.6}$$

where N_m is the measured blow count, ER_m is the measured delivered energy ratio as a percentage, $ER_m/60$ is the energy ratio and N_{60} is the blow count for an energy ratio of 60%. In addition to the energy ratio correction, C_E ($ER_m/60$), Youd et al. 2001 recommended applying correction factor for borehole, C_B, correction factor for rod length, C_R, and correction factor for sampler, C_S, to the N_{60} in Equation 2.7.

$$N_{60} = C_E C_B C_R C_S N_m \tag{2.7}$$

C_R accounts for the effect of rod length on the energy transferred to the sampling rods. Youd et al. 2001 recommended range of 0.75 for rods shorter than 3m to C_R=1 for rod lengths of 10m for liquefaction analysis. C_B and C_S factors will be unnecessary if appropriate standard borings are used. Sampler in the SPT might strike a large particle in the depth of soil which leads to the change in soil strength parameters (Khabiri et al. 2016) and cause a jump in the number of blow counts in the corresponding depth, whereas a uniform increase in the blow counts indicates the soil condition.

2.3 LIQUEFACTION ANALYSIS METHODS

Soil liquefaction analysis can be conducted using 1) stress-based, 2) strain-based, and 3) energy-based methods (Gheibi and Bagheripour 2010, Gheibi and Bagheripour 2011, and Gheibi et al. 2011). Stress-based method is the most commonly used method and is conducted using two approaches; 1) methods based on the laboratory test results on the undisturbed soil samples and 2) methods based on the empirical correlations using the

field test results such as SPT, CPT and shear wave velocity (V_S). Laboratory methods are not common for research purposes because of the problems associated with undisturbed sample preparation accuracy, cost and difficulty (Cetin et al. 2004). Seed and Idriss 1971 initiated the simplified method to evaluate liquefaction potential by the means of factor of safety against liquefaction. Cyclic stress ratio, CSR, and cyclic resistance ratio, CRR, in saturated soil are compared during the earthquake to determine the factor of safety. Please note that dynamic behavior of saturated clay and unsaturated sands are different during the earthquake (Ghavami et al. 2016, Khosravi et al. 2016, and Shooshpasha et al. 2011). The Seed and Idriss 1971 simplified method has been modified and extensively used in the past few decades (i.e. Youd and Idriss 1997, Idriss 1999). Brief description of the three recent CPT based liquefaction analysis methods in the literature (including key equations and assumptions) are summarized in the following sections.

2.3.1 CPT Based Liquefaction Analysis Methods

2.3.1.1 Robertson and Wride 1998

The Seed and Idriss 1971 simplified method was used to determine the CSR:

$$CSR = \frac{\tau_{ave}}{\sigma'_{vc}} = 0.65\left(\frac{a_{max}}{g}\right)\left(\frac{\sigma_{vc}}{\sigma'_{vc}}\right)r_d \qquad (2.8)$$

where a_{max} is the maximum ground acceleration at surface, σ_{vc} is the vertical stress and σ'_{vc} is the vertical effective stress at depth z. r_d is the reduction factor that considers the flexibility of soil column based on the recommendations of Seed and Idriss 1971 and Liao and Withman 1986.

$$r_d = 1 - 0.00765 * Z \qquad Z \leq 9.15m \tag{2.9}$$

$$r_d = 1.174 - 0.0267 * Z \qquad 9.15 < Z \leq 23m \tag{2.10}$$

Robertson and Wride 1998 defined the CRR for the 7.5 Richter earthquake magnitudes using equivalent clean sand value of tip resistance ($(q_{C1N})_{CS}$) and following equations:

$$CRR_{7.5} = 93\left[\frac{(q_{C1N})_{CS}}{1000}\right]^3 + 0.08 \qquad 50 \leq (q_{C1N})_{CS} < 160 \tag{2.11}$$

$$CRR_{7.5} = 0.833\left[\frac{(q_{C1N})_{CS}}{1000}\right]^3 + 0.05 \qquad (q_{C1N})_{CS} < 50 \tag{2.12}$$

$$(q_{C1N})_{cs} = K_C q_{C1N} \tag{2.13}$$

$$q_{C1N} = \frac{q_{c1}}{p_{a2}} = \left(\frac{q_c}{p_{a2}}\right) C_Q \tag{2.14}$$

$$C_Q = (P_a/\sigma'_{vc})^n \tag{2.15}$$

where P_a is 100 kPa and C_Q is the correction parameter for overburden pressure with the maximum value of 2. Stress normalized cone penetration resistance (Q), normalized friction ratio (F) and soil behavior type index (I_c) in Equations 2.1, 2.2 and 2.4 were used to determine n and K_c (correction factor for the effect of grain characteristics). The parameter n in Equation 2.15 is considered to be one and 0.5 for clay type soils and sandy soils, respectively. Iterative procedure is used to define n with the first estimation of n=1 in Equation 2.1 and applying the obtained Q values in Equation 2.4. q_{c1N} will be equal to Q if the calculated I_c is greater than 2.6 but if the I_c is less than 2.6 then n is assumed to be 0.5 in Equation 2.1. If the recalculated I_c remains less than 2.6 then n=0.5 will be used

in Equation 2.15 else, n=0.75 is used in both equations 2.15 and 2.1. K_c is also function of soil behavior index (I_c) and is calculated using the following procedure:

$$K_C = 1 \qquad I_c < 1.64 \tag{2.16}$$

$$K_C = 0.403{I_c}^4 + 5.581{I_c}^3 - 21.63{I_c}^2 + 33.75I_C - 17.88 \qquad I_c > 1.64 \tag{2.17}$$

$$K_C = 1 \qquad 1.64 < I_c < 2.36 \ \ and \ F < 0.5\% \tag{2.18}$$

$$I_c \geq 2.64 \ \ Likely \ non \ liquefiable \ if \ F > 1\% \tag{2.19}$$

2.3.1.2 Moss et al. 2006

Moss et al. 2006 analyzed the CPT results from liquefied and non-liquefied cases to develop deterministic and probabilistic approach of soil liquefaction evaluation. Following sections address their equations to define the CSR and CRR for both deterministic and probabilistic approaches. CPT tip resistance, q_c, and sleeve friction, f_s, were normalized using the following equations:

$$q_{c,1} = C_q . q_C \qquad and \qquad f_{s,1} = C_f . f_s \tag{2.20}$$

$$C_q = (\frac{P_a}{\sigma'_v})^c \qquad and \qquad C_f = (\frac{P_a}{\sigma'_v})^s \tag{2.21}$$

$$C = f1.(\frac{R_f}{f3})^{f2} \qquad and \qquad R_f = \frac{f_s}{q_c} * 100\% \tag{2.22}$$

$$f1 = x_1 . q_c^{x_2}, \quad f2 = -(y_1 . q_c^{y_2} + y_3), \quad f3 = abs(\log(10 + q_c))^{z_1} \tag{2.23}$$

where x_1=0.78, x_2=-0.33, y_1=-0.32, y_2=-0.35, y_3=0.49 and z_1=1.21. Moss et al. 2006, defined the reduction factor, r_d, as a function of earthquake magnitude, M_w, and peak ground acceleration, a_{max}, using Equations 2.24 and 2.25.

$$r_d = \frac{\left[1 + \frac{-9.147 - 4.173.a_{max} + 0.652.M_w}{10.567 + 0.089e^{0.089(-d.3.28 - 7.760.a_{max} + 78.576)}}\right]}{\left[1 + \frac{-9.147 - 4.173.a_{max} + 0.652.M_w}{10.567 + 0.089e^{0.089(-7.760.a_{max} + 78.576)}}\right]} \quad d < 20m \tag{2.24}$$

$$r_d = \frac{\left[\frac{1 + \frac{-9.147 - 4.173.a_{max} + 0.652.M_w}{10.567 + 0.089e^{0.089(-d.3.28 - 7.760.a_{max} + 78.567)}}}{1 + \frac{-9.147 - 4.173.a_{max} + 0.652.M_w}{10.567 + 0.089e^{0.089(-7.760.a_{max} + 78.567)}}}\right]}{} - 0.0014.(d.3.28 - 65)\ d > 20_i \tag{2.25}$$

Finally, the cyclic resistance ratio, CRR, was calculated using Equation 2.26 and 2.27. For the deterministic approach, Moss et al. 2006 recommended the liquefaction probability of 15%, PL=15%, based on the prior thresholds of CPT and SPT-based analyses.

$$P_L = \varphi\left(-\frac{\left(\begin{matrix}q_{c,1}^{1.045} + q_{c,1}(0.110R_f) + (0.001R_f) + c(1 + .850R_f) - \\ 7.177.\ln(CSR) - 0.848.\ln(M_w) - 0.002.\ln(\sigma_v') - 20.923\end{matrix}\right)}{1.632}\right) \tag{2.26}$$

$$CRR = exp\left(\frac{\left(\begin{matrix}q_{c,1}^{1.045} + q_{c,1}(0.110R_f) + (0.001R_f) + c(1 + .850R_f) - \\ 0.848.\ln(M_w) - 0.002.\ln(\sigma_v') - 20.923 + 1.632.\varphi_{(P_L)}^{-1}\end{matrix}\right)}{7.177}\right) \tag{2.27}$$

2.3.1.3 Idriss and Boulanger 2008

Idriss and Boulanger 2008 used additional liquefaction/no liquefaction case histories and reexamined the original procedures and proposed revised relations for the parameters involved in calculating CSR and CRR. For the study herein, their procedure was used to back-calculate the minimum earthquake magnitude and peak ground

acceleration at the sites with paleoliquefaction features; Sampit, Gapway, Hollywood, Fort Dorchester and Four Hole Swamp. Following sections provide updated equations to calculate CSR and CRR based on the CPT results. Reduction factor, r_d, was determined using the Idriss 1999 approach for the depths less than 20m. For the depths more than 20m the site response analysis was recommended by Idriss and Boulanger 2008.

$$r_d = \exp(\alpha(z) + \beta(z)M) \qquad Z < 20m \tag{2.28}$$

$$\alpha(z) = -1.012 - 1.126 \sin\left(\frac{z}{11.73} + 5.133\right), \quad \beta(z) = 0.106 + 0.118\, sin\left(\frac{z}{11.28} + 5.142\right) \tag{2.29}$$

CPT tip resistance increase with depth and so q_c values were normalized using Equations 2.30 and 2.31 to obtain a dimensionless value of penetration resistance in sand to an equivalent effective stress of one atmosphere.

$$q_{c1} = C_N q_c\,, \qquad q_{c1N} = \frac{q_{c1}}{P_a} \tag{2.30}$$

$$C_N = \left(\frac{P_a}{\sigma'_{vc}}\right)^{1.338 - 0.249.(q_{c1N})^{0.264}} \leq 1.7 \qquad 21 < q_{c1N} < 254 \tag{2.31}$$

Cyclic stress ratio for the earthquake magnitude of 7.5 and at depth where effective vertical stress is equal to 1 atm was obtained using the simplified procedure for liquefaction potential evaluation and Equation 2.32 to 2.35.

$$CSR_{M=7.5,\sigma'_{vc}=1} = CSR_{M,\sigma'_{vc}} * \frac{1}{MSF} * \frac{1}{K_\sigma} = 0.65 * r_d * \left(\frac{\sigma_{v0} * a_{max}}{\sigma'_{v0} * g}\right) * \frac{1}{MSF} * \frac{1}{K_\sigma} \tag{2.32}$$

$$MSF = 6.9\ \exp\left(\frac{-M}{4}\right) - 0.058 \leq 1.8 \tag{2.33}$$

$$K_\sigma = 1 - C_\sigma \ln\left(\frac{\sigma'_{vc}}{P_a}\right) \leq 1.1 \tag{2.34}$$

$$C_\sigma = \frac{1}{37.3 - 8.27(q_{C1N})^{0.264}} \leq 0.3, \qquad q_{C1N} \leq 211 \tag{2.35}$$

Note that following the procedure used in Idriss and Boulanger 2008, $(q_{c1N})_{cs}$ was used in Equations 2.31 and 2.35. Cyclic resistance ratio was also calculated using Equation 2.36.

$$CRR_{M=7.5,\sigma'_{vc}=1} = exp\left\{\frac{(q_{c1N})_{cs}}{540} + \left(\frac{(q_{c1N})_{cs}}{67}\right)^2 - \left(\frac{(q_{c1N})_{cs}}{80}\right)^3 + \left(\frac{(q_{c1N})_{cs}}{114}\right)^4 - 3\right\} \tag{2.36}$$

where $(q_{c1N})_{cs}$ is the equivalent clean-sand value of the tip resistance and is obtained using Equation 2.37 and 2.38.

$$(q_{c1N})_{cs} = q_{c1N} + \Delta q_{c1N} \tag{2.37}$$

$$\Delta q_{c1N} = \left(5.4 + \frac{q_{C1N}}{16}\right) * \exp\left\{1.63 + \frac{9.7}{FC + 0.01} - \left(\frac{15.7}{FC + 0.01}\right)^2\right\} \tag{2.38}$$

Finally, Factor of safety against liquefaction was obtained as the ratio of CRR to CSR.

$$FS_{liq} = \frac{CRR_{M,\sigma'_{vc}}}{CSR_{M,\sigma'_{vc}}} \quad or \quad FS_{liq} = \frac{CRR_{M=7.5,\sigma'_{vc}=1}}{CSR_{M=7.5,\sigma'_{vc}=1}} \tag{2.39}$$

2.4 PALEOEARTHQUAKE EVALUATION METHODS

The main goal in paleoearthquake analysis is to back-calculate the minimum earthquake magnitude, M, and peak ground acceleration, a_{max}, required for liquefaction initiation. Paleoliquefaction features are used in the regions such as South Carolina that encounter infrequent earthquakes and the exact locations of the prehistoric earthquake faults are not known, to determine the a_{max} and M. Recently, Obermeier et al. 2001, Olson et al. 2005, Green et al. 2005 and Leon et al. 2005 have conducted paleoearthquake studies in the SCCP sites.

Obermeier et al. 2001 reviewed most of the methods used for back-analysis of the earthquake magnitudes. They concluded selection of the appropriate method depends on the data available at the liquefaction sites. Olson et al. 2005 studied different approaches and corresponding uncertainties for back-analysis of earthquake magnitudes. They summarized the existing methods into two main categories; 1) Cyclic Stress method and 2) Magnitude Bound method. Uncertainties for Cyclic Stress method include; validity of in-situ testing techniques, factors related to liquefaction susceptibilities, factors related to seismicity, factors related to field observations and ground failure mechanisms. The Magnitude Bound method is also limited by the need for calibration from historic earthquakes in the same tectonic settings.

Following the study of Olson et al. 2005, Green et al. 2005 used Ground Motion Prediction Equations in combination with the Cyclic Stress method (considering the uncertainties discussed by Olson et al. 2005) to back-calculate the earthquake magnitude of the prehistoric Vincennes Earthquake that occurred around 6100 years B.P. in the Wabash Valley. Leon et al. 2005 also used Magnitude Bound and Energy-Stress methods

to back-calculate the prehistoric earthquake magnitudes and used Seed's Cyclic Stress method, Ishihara method and the Martin and Clough method to back-calculate the peak ground acceleration at the SCCP. The following sections provide information about the paleoearthquake magnitude evaluation method that was used in Leon et al. 2005 and the Ground Motion Prediction Equations, as used by Green et al. 2005.

2.4.1 Paleoearthquake Magnitude Evaluation

Magnitudes of prehistoric earthquakes are estimated based on the paleoliquefaction evidences. Because of the uncertainties associated with paleoearthquake back-analysis methods, finding magnitudes using different methods increase the confidence in interpretation of the results. Following the approaches used in Leon et al. 2005, two methods are discussed in this section for back-analysis of earthquake magnitude; 1) Magnitude Bound method and 2) Energy-Stress method

2.4.1.1 Magnitude Bound Method

The Magnitude Bound method correlate the earthquake magnitude, M, to the distance from tectonic source to farthest liquefied site as discussed by Ambraseys 1988. Figure 2.3 indicate the world wide data of many historical earthquakes. To estimate range of farthest distance of liquefaction, origins of the data from various tectonic plates were analysed. Ambraseys 1988 also used Equation 2.40 to correlate earthquake magnitude and the maximum epicentral distance, R_e (cm), at which liquefaction had been observed.

$$M = -0.31 + 2.65 * 10^{-8} R_e + 0.99(logR_e) \quad (2.40)$$

The method was used herein because it was used in previous studies by Talwani and Schaeffer 2001 and Leon et al. 2005 for similar sites in the SCCP; however, it is

important to note that it was developed based on active shallow crustal settings dissimilar to the eastern U.S. and is a method independent of age and the in-situ soil properties.

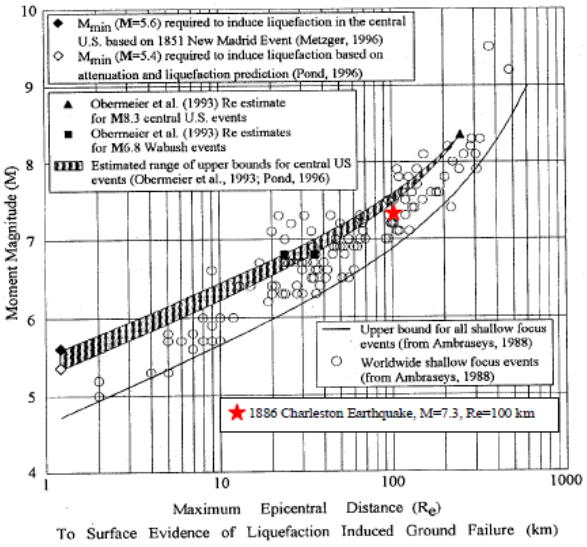

Figure 2.3 Relation between epicentral distance and earthquake magnitude. (adapted from Pond and Martin, 1997)

2.4.1.2 Energy-Stress Method

The earthquake magnitude in the Energy-Stress method is described in terms of energy center location and strength properties, $(N_1)_{60}$. Pond 1996 defined the seismic intensity, T, as a function of hypocentral distance, R (km), and earthquake magnitude, M as in Equation 2.41:

$$T = 10^{1.5M}/R^2 \qquad (2.41)$$

Pond and Martin 1997, used the data from liquefied and non-liquefied sites to find the boundary for liquefied sites as a function of seismic intensity and penetration resistance, $(N_1)_{60}$, as shown in Figure 2.4. The boundary between the two areas is formulated as:

$$(N_1)_{60} = (\frac{T}{1.445})^{0.165} \quad (2.42)$$

Hu et al. 2002b, combined Equations 2.41 and 2.42 and derived Equation 2.43 to define earthquake magnitude as a function of hypocentral distance, R, and corrected blow count numbers, $(N_1)_{60}$.

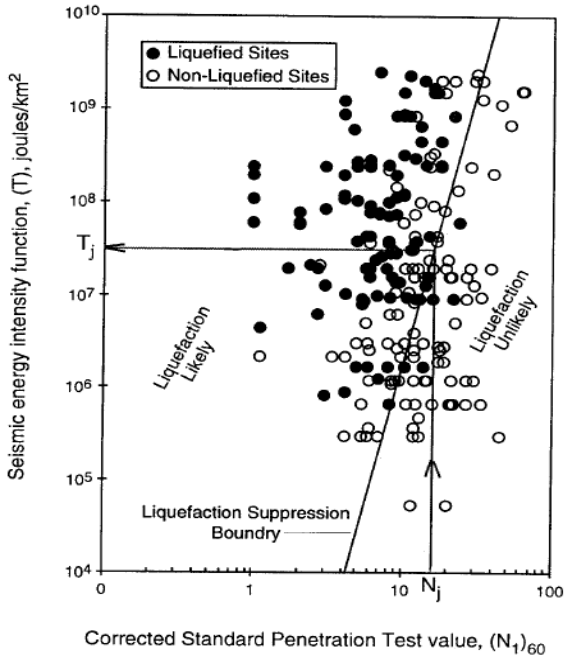

Figure 2.4 Relation between blow count number and seismic energy intensity function. (after Pond and Martin, 1997)

$$M = \frac{2}{3}\log[1.445R^2(N_1)_{60}^{6.06}] \quad (2.43)$$

The post-earthquake number of blow counts, $(N_1)_{60\ (post)}$, at the Sampit and Gapway sites in Chapter 3, Hollywood Site in Chapter 4 and Fort Dorchester Site in Chapter 5 were used in Equation 2.43 to Back-calculate the earthquake magnitudes.

2.4.2 Ground Motion Prediction Equation

Risk assessment plays a significant role in designing important structures. GMPEs are used to estimate the ground motion parameters required for risk assessment such as peak ground acceleration (PGA) and pseudo-spectral acceleration (PSA). Selecting the appropriate GMPE leads to a more robust risk assessment and increases the safety factors in design purposes. Similar to the site-specific geotechnical method (Cyclic Stress method), GMPE defines a_{max} as a function of earthquake magnitude (M) and site-to-source distance (R**)**. As there are many combinations sufficient to induce liquefaction, the results of both methods are combined by the intersection of the results to provide a reasonable combination of a_{max}-M. This concept is shown in Figure 2.5. The solid line is the range of possible a_{max}-M combinations for liquefaction initiation obtained using the site-specific geotechnical method and the dashed line represents the a_{max}-M combinations for liquefaction initiation found using GMPE. The intersection point is the minimum potential a_{max}-M combination to initiate liquefaction.

Green et al. 2005 used four Ground Motion Prediction Equation, namely Somerville et al. 2001, Atkinson and Boore 1995, Toro et al. 1997, and Campbell 2001, 2003 in combination with the Cyclic Stress method to back-calculate the earthquake magnitude of the prehistoric Vincennes Earthquake that occurred around 6100 years B.P. in the Wabash Valley. Many paleoliquefaction sites have been discovered in the Wabash Valley as shown in Figure 2.6. They concluded that the liquefaction features were associated with the prehistoric Vincennes Earthquake which was determined to have magnitude of about 7.5.

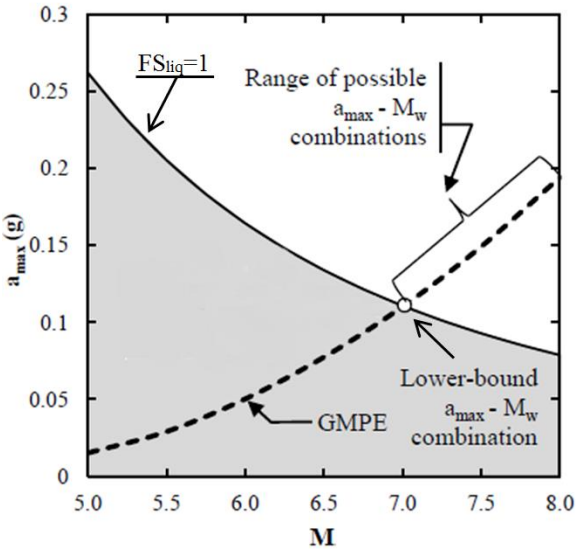

Figure 2.5 Combination of GMPE and liquefaction evaluation methods for a hypothetical site (adapted from Green et al. 2005)

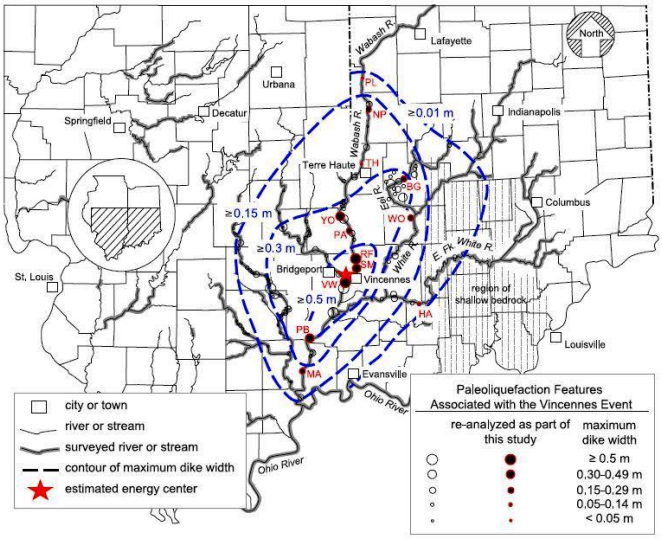

Figure 2.6 Paleoliquefaction sites in the Wabash Valley (adapted from Green et al. 2005)

Figure 2.7 presents the regional assessment of paleoseismic strength of shaking of the Vincennes Earthquake using four used GMPEs. As shown, acceleration values at each site were obtained as a function of site-to-source distance.

Green et al. 2013 also studied the application of GMPEs to evaluate the accuracies of back-calculation methods for the modern 2010-2011 Canterbury (New Zealand) earthquake sequence. They used five GMPEs, namely McVerry et al. 2006, Boore and Atkinson 2008, Chiou and Youngs 2008, Ambrahamson and Silva 2008, and Bradley 2010 models and figured out back-analysis methods determine the seismic parameters accurately if the earthquake source location and mechanism are known; the earthquake magnitude was estimated to be 7.1 and 6.3 for the Darfield 2010 and Christchurch 2011 earthquakes respectively.

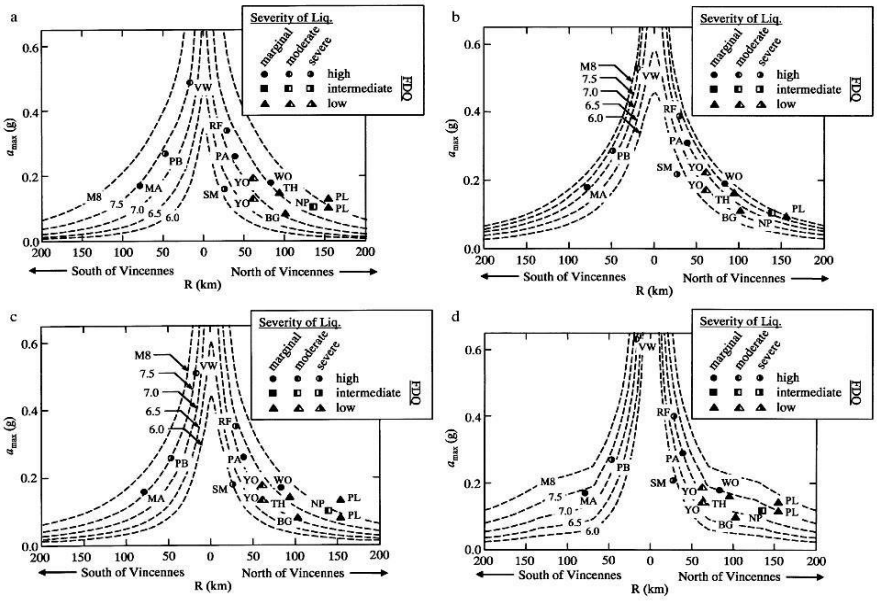

Figure 2.7 Regional assessment of Vincennes earthquake strength using (a) Somerville et al. 2001, (b) Atkinson and Boore 1995, (c) Toro et al. 1997, and (d) Campbell 2001, 2003 GMPEs. (adapted from Green et al. 2005)

The U.S. Geological Survey (USGS) (Petersen et al. 2014) updated hazard map report includes nine updated regionally proper ground motion models for the central and eastern United States. A brief introduction to four of these models will be discussed

below. Two of these are new models that were not in the previous 2008 USGS report: Pezeshk et al. 2011 and Atkinson 2008'. The Toro et al. 1997 and Tavakoli and Pezeshk 2005 models have similar site classification to the SCCP sites based on the National Earthquake Hazards Reduction Program (NEHRP) site classification.

Toro et al. 1997 used stochastic ground motion models and derived four sets of attenuation equations for the central and eastern part of the North America. They updated previous studies using more ground motion data, more realistic modeling of crustal effects and more quantitative process to derive the median predictions. They noted that their model may overestimate ground motion parameters at sites near the rupture of a large earthquake. This limitation is not significant for most sites in the central and eastern United States because the distances from the earthquakes are usually more than one or two source dimensions. Wave propagation and fracture prediction mechanism can be developed using the recent studies of Salimi-Majd et al. 2016 and Regueiro et al. 2014 that proposed a failure criterion to predict failures for different type of materials. Figure 2.8 shows the comparison of this model with two attenuation equations of AB87 and Atkinson and Boore 1995 (AB95). The Toro et al. 1997 model was developed for the earthquake magnitudes in the range of 5 to 8 and the closest distance to the rupture (R_{jb}) up to 500km. As shown in Figure 2.8, for a given distance, peak ground acceleration is defined as a function of earthquake magnitude which typically forms a relation like the dashed line in Figure 2.5 used in back-calculation analysis.

Figure 2.9 also presents the comparison of predicted accelerations as a function of earthquake magnitudes and rupture distances for three models of P11, TP05 and A08'.

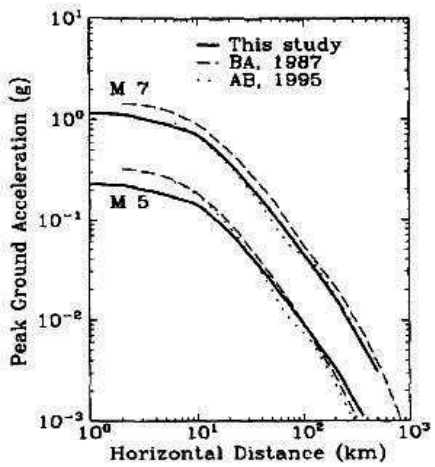

Figure 2.8 Comparison of ground motion predictions (adapted from Toro et al. 1997)

The lower and upper curves for each model are the earthquake magnitudes of 5 and 7 respectively. Similar to the Toro et al. 1997 model, the relation between earthquake magnitude and peak ground acceleration at a given distance for each model will be similar to the dashed line in Figure 2.5.

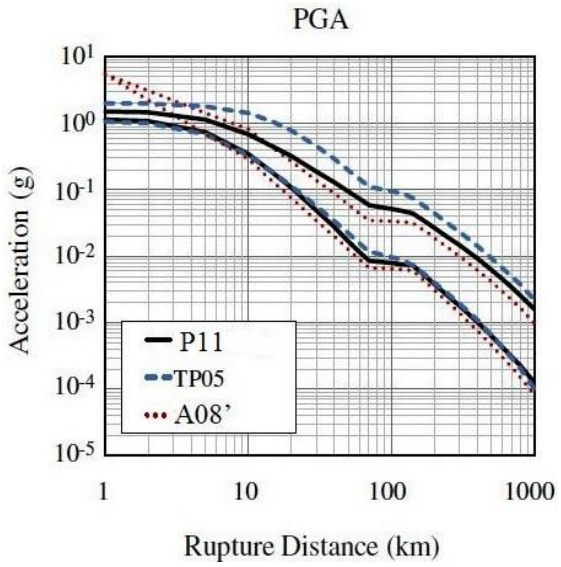

Figure 2.9 Comparison of ground motion predictions (adapted from Pezeshk et al. 2011)

Tavakoli and Pezeshk 2005 used a Hybrid-empirical model to predict the ground motion relationships for eastern North America (ENA) using ground motion parameters from western North America (WNA). They revised the Campbell 2003 attenuation model using a Hybrid-empirical model and changed the magnitude-dependent stress drop in the WNA and ENA regions which have different seismological parameters. They used empirical attenuation models in a host region (WNA) and hybrid models to transform attenuation relationship to a target region (ENA). They considered effects of focal depth and stress drop on ground motion. Furthermore, they developed an empirical model to obtain ground motions at different distances; they used a single corner-frequency source model for the far-field ground motions and a double corner-frequency source model for the short distances. The proposed attenuation relationship is valid for earthquake magnitudes from 5 to 8.2 and closest distance to the fault rupture (R_{rup}) less than 1000km.

Atkinson 2008 defined GMPE for a particular measure of horizontal-component ground motions as a function of earthquake mechanism, distance from source to site, local average shear-wave velocity and fault type. Equations were developed to obtain ground acceleration, peak ground velocity (PGV) and 5%-damped pseudo-absolute acceleration spectra. He performed regression analysis on the Pacific Earthquake Engineering Research Center (PEER) NGA strong motion database. Atkinson and Boore 2011 developed an adjustment factor to be multiplied by the Boore and Atkinson 2008 GMPE (applicable for WNA) to obtain A08' GMPE applicable for ENA. The adjustment factors were obtained using the ENA data directly. The A08' GMPE is similar to the hybrid empirical approaches and provides a reliable model with a wide range of magnitudes (4 to 8) and closest distance to the rupture (R_{jb}) (1 to 500 km).

Pezeshk et al. 2011 used empirical Hybrid method and five GMPEs for the western North America generated by Pacific Earthquake Engineering Research Center to derive an updated approach for the eastern North America. In the Hybrid empirical method, adjustment factors between the WNA and ENA reflect the regional differences in source, path and site. Pezeshk et al. 2011 mapped ground motion models from the WNA onto the ENA based on the seismological regional properties. They developed an alternative GMPE applicable for earthquake magnitudes from 5 to 8 and distances to the fault rapture (R_{rup}) less than 1000 km. Their model was compatible with other GMPEs developed for the earthquakes in ENA.

The four discussed GMPEs will be used in combination with the site-specific geotechnical method and age-adjusted values of Cyclic Resistance Ratio (CRR) in Chapter 7 to find the minimum earthquake magnitude and peak ground acceleration of the prehistoric earthquakes at the Hollywood, Fort Dorchester, Sampit and Gapway sites

2.5 TIME-DEPENDENT (AGING) PHENOMENON

Effect of time on increase in soil penetration resistance in SPT and CPT have been studied following the use of ground modification methods by Mitchell 1986, Schmertmann 1987 and Mesri et al. 1990. Penetration resistance in SPT and CPT increases with time (Mitchell and Solymar 1984, and Skempton 1986). More studies are required to evaluate the effect of aging on elastic behavior of soils using the similar studies by Moahmmadi and Shahabi 2015 and 2012 that developed a constitutive to simulate soil behaviors. Aging mechanism in sands and discussion of aging methods are described in the following sections:

2.5.1 Aging Mechanism in Sands

Mechanical and chemical mechanisms are known as two major mechanisms that cause aging in sands. Macro-interlocking of sand particles, micro-interlocking of surface roughness and internal stress arching during secondary consolidation are three major reasons for mechanical mechanisms. Moreover, chemical mechanism consists of dissolution and precipitation of silica. Youd and Hoose 1977, discovered cementing and compaction in sand deposits as a reason for increase in resistance against liquefaction. Shahsavari and Sivathayalan 2014, Shahsavari et al. 2014, and Shahsavari and Grabinsky 2014 also studied the effect of post liquefaction and overconsolidation on liquefaction susceptibility of the Fraser River. Mitchell and Solymar 1984, and Mitchell 1986, explained formation of silica acid gel on particle surfaces and cementing bonds at interparticle contacts as the chemical mechanism in sands over periods that cause increase in strength of sands due to aging.

For dry sands, Joshi et al. 1995 and Mesri et al. 1990, correlated the increase in penetration resistance to the macro-interlocking of the particles and micro-interlocking of surface roughness due to external loads during the secondary compression. Schmertmann 1991, described increase in effective stresses including grain slippage, dispersive particle movements and internal stress arching as the phenomenon that cause aging in sand and clay particles. Moreover, Arango and Migues 1966, concluded that the high resistance in aged soils is attributed to the particle interlocking.

Michalowski and Nadukuru 2015, studied microscopic characterization of the sand grains using Scanning Electron Microscopy (SEM) and Atomic Force Microscopy

to explain the gradual increase in the soil strength with time. Figure 2.10 indicates the surface roughness of Ottawa sand in different scales.

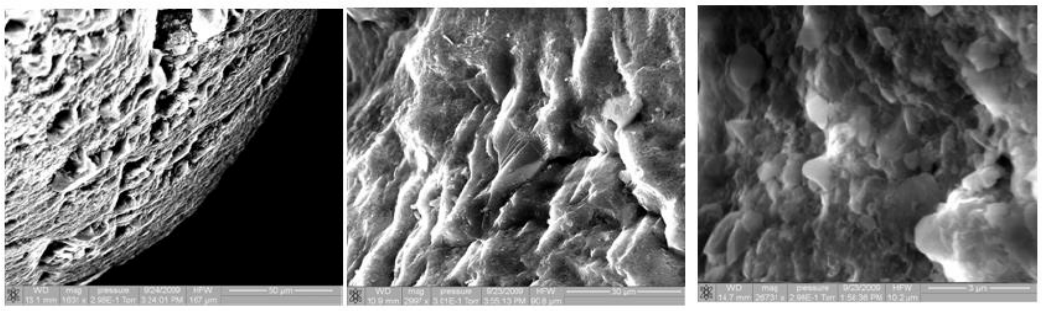

Figure 2.10 SEM images of Ottawa sand grain surface: (a) image width 160 μm, (b) 100 μm, and (c) 10 μm. (after Michalowski and Nadukuru 2015)

As shown in Figure 2.10, roughness of texture is independent of scale. They concluded that contact in grains with surface morphology (shown in Figure 2.10) causes intense fracturing in the initial stages of loading until stopping the applied load. They referred the time dependent process of interaction as contact fatigue and observed the increase in soil resistance after several days while the interlocking forces increase with time. The technique developed by Salamat-Taleb et al. 2013 can also be used to perform lower length scale analysis to estimate size-dependent behavior of soils particles.

2.5.2 Methods to Account for Aging

Several investigations have revealed that liquefaction resistance of sands increases with time. Youd and Hoose 1977 were among the first researchers who analysed the liquefaction reports and noticed the liquefaction probability is higher in sediments deposited within the past few hundred years compare to the Holocene (<10,000 yrs) sediments. Seed et al. 1975 and Seed 1979, addressed the time period under sustained load or age of the deposit as one of the factors that significantly affect the

liquefaction potential of sands. Seed 1979 concluded that the samples subjected to longer periods of loading have more resistance against liquefaction. Based on his findings, cyclic strength resistance of undisturbed samples obtained from an old fill are 50 to 100 times greater than the freshly deposited samples. Mitchell and Solymar 1984, also detected the increase in stiffness and strength of soil against penetration up to 100 percent more than the initial penetration resistance value. Skempton 1986, observed reflection of the aging effect in higher blow count over several months. In this study, Mesri et al. 1990, Kulhawy and Mayne 1990, and Hayati and Andrus 2009 approaches were used to account for the effect of aging on penetration tip resistance and blow count numbers.

2.5.2.1 Mesri et al. 1990

The Mesri et al., 1990 relation is based on an observed increase in penetration resistance after ground densification by blasting, vibrocompaction and dynamic compaction in clean sands and is a function of time, t, the change in relative density, ΔD_R, and the ratio of the secondary compression index to the compression index, C_α/C_c, in Equation 2.44. Mesri et al. 1990, concluded that continues rearrangement of the sand particles in the secondary compression step leads to the decrease in the relative density which causes increase in penetration resistance.

$$\frac{q_c}{(q_c)_R} = \left(\frac{t}{t_R}\right)^{C_D \cdot C_a/C_c} \tag{2.44}$$

where $(q_c)_R$ and t_R are the cone penetration resistance and time at the end of primary consolidation. q_c is the cone penetration resistance at any time $t>t_R$, C_D is the empirical parameter related to the soil densification obtained using Figure 2.11.

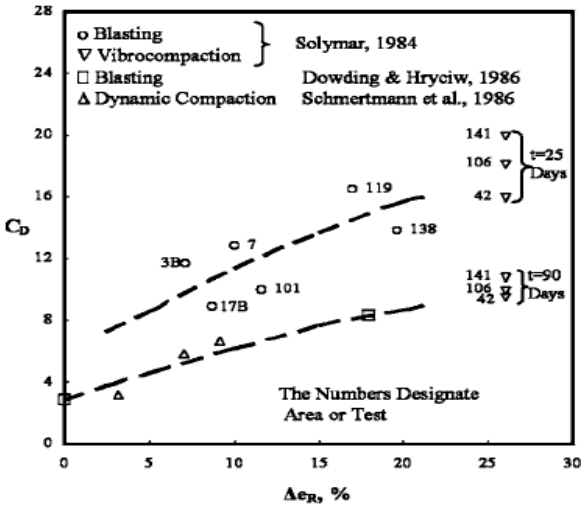

Figure 2.11 Variation in C_D due to the post-liquefaction densification, Δe_R, (after Mesri et al., 1990).

To account for the changes in post-earthquake soil consolidation, Ellis and De Alba 1999 and Stark et al. 2002 estimated the change in relative density, ΔD_R, to be between 5% and 10%.

2.5.2.2 Kulhawy and Mayne 1990

The Kulhawy and Mayne 1990 method is based on collected SPT blow count, $(N_1)_{60}$, and relative density data, D_R, as a function of soil particle size, D_{50} for the normally consolidated sands as shown in Figure 2.12.a and Equation 2.45

$$\frac{(N_1)_{60}}{D_R^2} = 60 + 25 log D_{50} \qquad (2.45)$$

They also developed their study on aged fine to medium overconsolidated sands from four geologic periods and proposed a correction factor, C_A, to describe the influence of aging (t) on the $(N_1)_{60}/Dr^2$ ratio.

$$C_A = 1.2 + 0.05\log(\frac{t}{100}) \quad (2.46)$$

Leon et al. 2005, applied the coefficient C_A to the CPT penetration data and described the following equation to correlate the current penetration resistance to the post-earthquake values of penetration resistance, $q_{c1\ (post)}$, and $(N_1)_{60\ (post)}$.

$$\frac{(N_1)_{60}}{(N_1)_{60\ (post)}} = \frac{q_{c1}}{q_{c1\ (post)}} = C_A \quad (2.47)$$

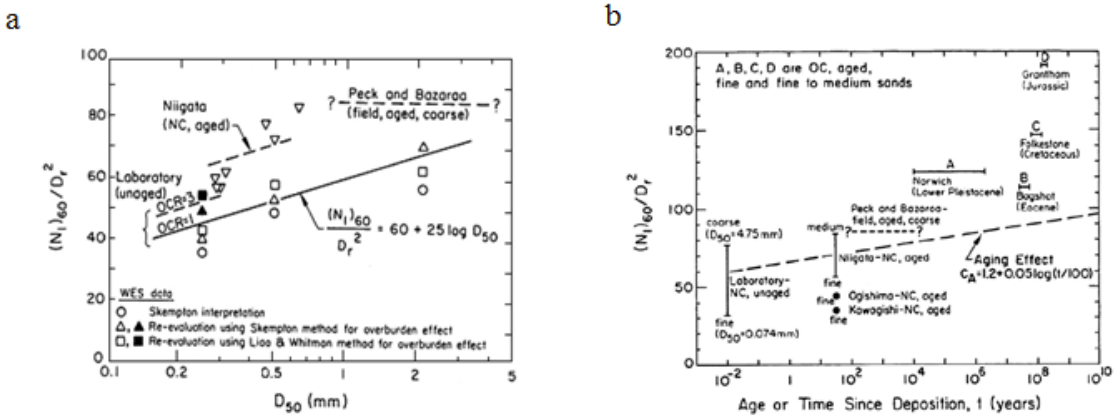

Figure 2.12 (a) Effect of particle size on blow counts in sands. (b) effect of aging on blow counts, (after Kulhawy and Mayne 1990)

2.5.2.3 Hayati and Andrus 2009

Hayati and Andrus 2009 analysed the laboratory and field data from more than 30 sites to update factors used in liquefaction analysis of aged soils. They performed regression analysis to evaluate effect of aging, cementation and stress history on CRR and liquefaction analysis. The methodology of Hayati and Andrus 2009 uses updated liquefaction resistance correction factor, $K_{DR,}$ given in Equation 2.48, where t is the time

since initial deposition or critical disturbance in years, to find CRR_k (the deposit resistance-corrected CRR) from Equation 2.49.

$$K_{DR} = 0.13.\log(t) + 0.83 \quad (2.48)$$

$$CRR_K = CRR.K_{DR} \quad (2.49)$$

Results of cyclic tests on laboratory samples suggest an increase of 0.12 per log cycle of time which is in a good agreement with the factor 0.13 in Equation 2.48 obtained from combining analysis of the laboratory and field tests. As shown in Figure 2.13, coefficient of determination, r^2, for Equation 2.48 is 0.62. Hayati and Andrus 2009, also updated the reference age to 23 years (when K_{DR}=1) as it was assumed to be 10 years in Hayati et al. 2008.

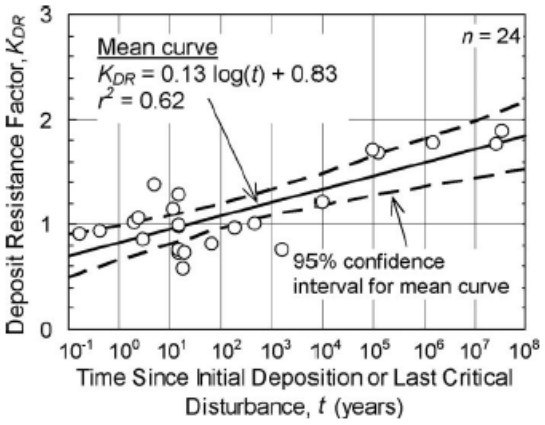

Figure 2.13, Deposit resistance factor, K_{DR}, as a function of time. (after Hayati and Andrus 2009)

2.6 SUMMARY

This chapter presented a summary of paleoliquefaction studies in the SCCP. Geotechnical in-situ testing procedures including CPT and SPT were discussed.

Liquefaction analysis methods developed based on the CPT results including Robertson and Wride 1998, Moss et al. 2006, and Idriss and Boulanger 2008 were summarized. The earthquake magnitudes of the prehistoric earthquakes in the South Carolina Coastal Plain were not recorded at time of earthquake and so paleoseismic evaluation methods and aging phenomenon were introduced to consider the effect of increase in soil resistance in back-analysis of the prehistoric earthquake magnitude and peak ground acceleration. The Magnitude Bound method, Energy Stress method and Ground Motion Prediction Equations were discussed as the approaches used in this study to back-calculate the minimum earthquake magnitude and peak ground acceleration. The Mesri et al. 1990, Kulhawy and Mayne 1990, and Hayati and Andrus 2009, approaches were used in this study to consider the effect of aging and readers are referred to Chapter 3 for more detailed information regarding the description of Sampit and Gapway sites and Chapter 4, and 5 for Hollywood, Fort Dorchester sites respectively.

CHAPTER 3

REASSESSMENT OF PREHISTORIC EARTHQUAKE ACCELERATIONS AT SAMPIT AND GAPWAY SITES IN THE SOUTH CAROLINA COASTAL PLAIN[1]

[1] Gheibi, E., and Gassman, S. L. (2014). Network for Earthquake Engineering Simulation (distributer), Paper, DOI: 10.4231/D3PV6B73Z. Reprinted here with permission of publisher.

ABSTRACT

Current empirical procedures to evaluate soil liquefaction susceptibility are applicable for relatively young Holocene soil deposits (<10,000 years) and do not consider the increase in cyclic resistance ratio over time. Particle rearrangement, interlocking and cementation are aging phenomenon that can cause increase in liquefaction resistance. For this study, in situ geotechnical data (cone penetration tests with pore pressure measurements and laboratory index tests) in the vicinity of prehistoric sand blows at Sampit and Gapway sites in the South Carolina Coastal Plain were used to reassess the back analysis of prehistoric earthquake magnitudes and maximum ground accelerations using newer, semi-empirical approaches than were used in previous analyses. The geotechnical data were used with paleoliquefaction evaluation methods that consider the effect of soil age and disturbance to estimate the magnitude and maximum ground acceleration needed for liquefaction at the time of the prehistoric earthquakes. Results show that the newer method for calculating acceleration produces lower peak ground accelerations than the previously used approach. The difference is most significant for lower magnitudes. Calculated average values of age-adjusted magnitude range from 5 to 7.5 Richter and age-adjusted peak ground acceleration for this variation of M range from 0.08 to 0.23g.

3.1 INTRODUCTION

Paleoliquefaction analysis plays an important role in studying the paleoseismicity in regions such as the South Carolina Coastal Plain (SCCP) where the frequency of re-occurrence of earthquakes is low and the locations of potential sources are not exactly known. Studies of paleoliquefaction features (e.g. sand blows) found in the SCCP over the past two decades have revealed at least seven, large, prehistoric earthquakes occurring

within the last 6000 years with an average occurrence rate, based on the three most recent events, of about 500 years (Talwani and Schaeffer 2001). Hu et al. 2002a,b used site-specific geotechnical data (penetration resistance and shear wave velocity) in the vicinity of these paleoliquefaction features to back-calculate the magnitude and peak ground accelerations of the prehistoric earthquakes needed for liquefaction to occur. The back-calculations were based on empirical correlations using Seed's Simplified Method (Seed and Idriss 1971) as reported in Youd and Idriss 1997, that are extensively used to determine liquefaction resistance of sand deposits from in-situ soil indices (e.g. $(N_1)_{60}$ from the standard penetration test (SPT) and $(q_c)_1$ from the cone penetration test (CPT)). However, these correlations are primarily based on studies of recent earthquakes in Japan, China and the west coast region of the U.S. where the soil deposits are of Holocene age (<10,000 years old). Because the sand deposits encountered in the SCCP are older than 100,000 years, Leon et al. 2005, developed a method to account for the effect of time-dependent mechanisms ("aging") on the back-calculated magnitudes and peak ground accelerations and obtained an approximately 0.9 unit reduction in magnitude and 15% reduction in peak ground acceleration. Neglecting the effect of aging resulted in a 60% underestimation of CRR (Leon et al. 2006). To obtain peak ground surface acceleration, both Hu et al. 2002b, and Leon et al. 2005, used the empirical correlations from Seed's Simplified method (Seed and Idriss 1971, and Youd and Idriss 1997).

However, since the time Seed's original method was put forth, in-situ index testing has been improved, the analysis framework has been refined, and additional liquefaction/no liquefaction case histories have been added to the database. This led Idriss and Boulanger 2008, to reexamine the original procedures and propose revised

relations for the stress reduction factor (r_d), earthquake magnitude scaling factor for cyclic stress ratios (MSF), overburden correction factor for cyclic stress ratios (K_σ), and the overburden normalization factor for penetration resistances (C_N). Therefore, for the study herein, the back-calculated magnitudes and peak ground accelerations of the prehistoric earthquakes at the Sampit and Gapway sites are reassessed using the newer semi-empirical approach of Idriss and Boulanger 2008, and the time-dependent approach of Leon et al. 2005, to obtain the accelerations.

3.2 SITES INVESTIGATED

In-situ testing was performed at the Sampit and Gapway sites between 1997 and 2010. The Sampit site is located about 4.8 km west-northwest of Georgetown, SC and is approximately 9 km southwest of the Gapway (GAP) site. Both sites are on the eastern flank of a mid-Pleistocene-age beach ridge and overlapping Holocene swamp deposits.

At the Sampit site, sand blows were found at three locations (SAM-02, SAM-04 and SAM-05) and were associated with earthquake episodes that occurred about 546, 1021 and 1648 years ago respectively (Talwani and Schaeffer 2001). Hu et al. 2002a, reported the results for the in-situ tests (seismic cone penetration tests (SCPT) and standard penetration tests (SPT)) performed at six locations (SAM-01 to SAM-06). Three additional SCPT tests (which are used in this research to back calculate the peak ground acceleration) were performed in 2010. SAM-SCPT-1 is in the vicinity of the sand blow at SAM-04. In general, the soil profile at Sampit consists of 2.0 m of silty sand underlain by 5.0 m of sand, 2.7 m of clay, and silt beginning at a depth of 10 m below the ground surface. As shown in Figure 3.1, the source sand layer is located between about 2.0 to 7.0 m and has a thickness that varies across the site from 4.65 to 6.15 m. The soil within this

layer has been classified as poorly graded sand (SP) (Hu et al. 2002a and Williamson 2013).

At the Gapway site, sand blows were found at three locations (GAP-02, GAP-03, and GAP-04). GAP-02 and GAP-03 were associated with earthquakes that occurred 3548 and 5038 years ago (Talwani and Schaeffer 2001), respectively. The sand blow discovered at GAP-04 is assumed to be associated with the same earthquake as the nearby sand blow found at GAP-03 (Leon et al. 2005). Hu et al. 2002a reported the results for the in-situ tests performed at five locations (GAP-01 to GAP-05). Three additional SCPT tests were performed in 2010. GAP-SCPT-1 is in the vicinity of the sand blow at GAP-04. GAP-SCPT-2 and GAP-SCPT-3 are in the vicinity of the sand blows at GAP-03 and GAP-02, respectively. In general, the soil profile at Gapway consists of 1 m of sand that overlies 0.3 m of clay, 1 m of sand, 2.4 m of clay, and sand below a depth of 4.6 m. As shown in Figure 1, the source sand layer is found between 1.2 to 2.1 m depth and varies in thickness from 0.72 to 1.75 m across the site. The source sand has been classified as poorly graded sand with 5 to 7% fines (SP-SM or -SC). The source sand is estimated to be 450,000 years old at both sites (Weems and Lemon 1984).

3.3 METHODS

3.3.1 Accounting for Soil Aging and Disturbance

The methodology of Leon et al. 2005, was used to correct the cone penetration tip resistance, q_{c1}, for 1) aging of the soil and 2) disturbance due to post-liquefaction consolidation (primary) and densification (or loosening). The method is based on the idea that the empirical correlations for liquefaction evaluation applicable for young or freshly deposited soils can be used for the older soil deposits as long as the parameters involved

(SPT, CPT, V_s, and CRR) are modified appropriately to account for the effect of aging. By correcting the *in situ* currently recorded in situ geotechnical data for aging, the corresponding data immediately after the earthquake (for the sites that liquefied) or deposition (for the sites that did not liquefy) are determined and termed "post-earthquake". These data are further corrected for disturbance from the earthquake to obtain the "pre-earthquake" data.

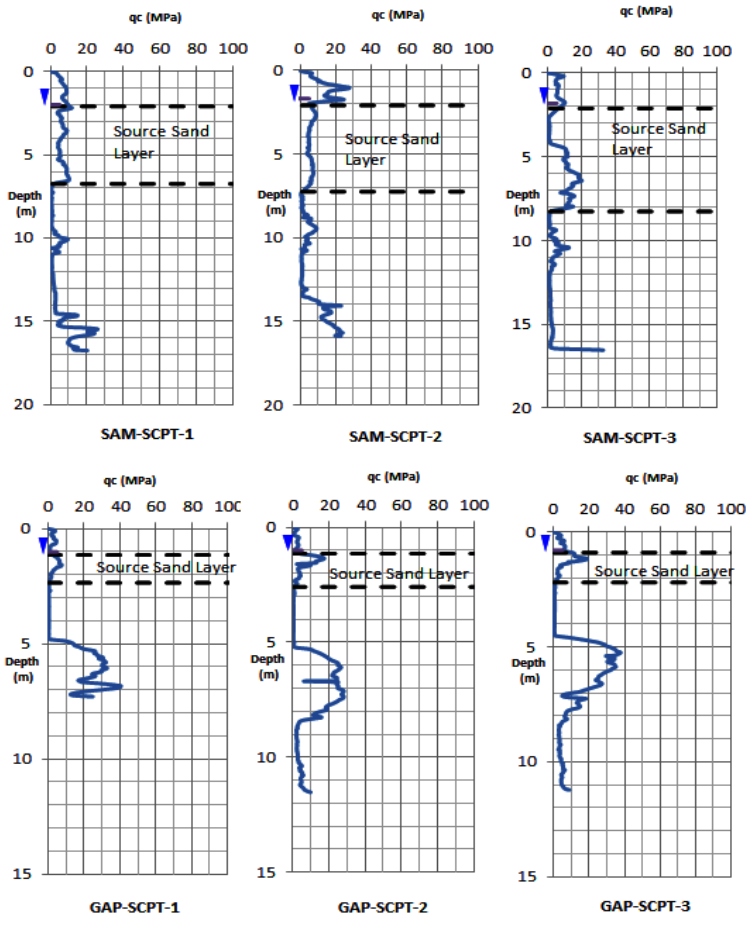

Figure 3.1 CPT profiles at the Sampit and Gapway sites.

Leon et al.'s method accounts for disturbance due to the liquefaction event and post-liquefaction aging using two different approaches. Approach 1 is based on the

relations offered by Mesri et al. 1990, for both the age and disturbance correction and Approach 2 is based on work by Kulhawy and Mayne 1990, for the age correction and Seed et al. 1988, for the disturbance correction. Change in relative density (ΔD_R) is considered to be 5% and 10% between the pre-($q_{c1\ (pre)}$) and post-($q_{c1\ (post)}$) earthquake state. Following Leon et al. 2005 for the CPT locations in vicinity of discovered sand blows, the age of earthquake is used when correcting for age to obtain $q_{c1\ (post)}$;whereas, for CPT locations where sand blows were not discovered, the age of soil deposit is used. The average $q_{c1\ (pre)}$ and $q_{c1\ (post)}$ values of tip resistance found using this method and the six most recent CPT profiles at Sampit and Gapway are summarized in Table 3.1. The results show that the age and disturbance-corrected values of tip resistance are less than current measurements, thus showing the increase in soil resistance with time.

Table 3.1 Average values of current, post- and pre- earthquake tip resistance data for source sand layer corrected for aging and disturbance.

Location	**Age (years)**[†]	**$q_{c1(current)}$ (MPa)**	**Average $q_{c1\ (post)}$ (MPa)**				**Average $q_{c1(pre)}$ (MPa)**			
			Approach 1		**Approach 2**		**Approach 1**		**Approach 2**	
			ΔDR 5%	ΔDR 10%	ΔDR 5%	ΔDR 10%	ΔDR 5%	ΔDR 10%	ΔDR 5%	ΔDR 10%
SAM-CPT-1	1,021	10	3	3	8	8	6	4	8	7
SAM-CPT-2	450,000	9	2	1	7	7	2	1	7	7
SAM-CPT-3	450,000	13	2	1	9	9	2	1	9	9
GAP-CPT-1	5,038	7	2	2	6	6	4	2	5	5
GAP-CPT-2	5,038	8	2	2	6	6	4	3	6	6
GAP-CPT-3	3,548	4	1	1	3	3	2	1	3	3

[†]Age of earthquake from Talwani and Schaeffer 2001.

3.3.2 Back-Calculation of the Earthquake Magnitude

The earthquake magnitude has been back-calculated by using the "Magnitude Bound" method and by using the "Energy-Stress" method for sites in the SCCP (Hu et al.

2002b and Leon et al. 2005). The Magnitude Bound method relates the earthquake magnitude, M, to the epicentral distance (Re) as discussed by Ambraseys 1988:

$$M = -0.31 + 2.65 * 10^{-8} R_e + 0.99(logR_e) \quad (3.1)$$

Hu et al. 2002b, derived a relationship using the Energy-Stress method based on the work of Pond and Martin 1997. This is a relationship between the seismic intensity at the site in terms of magnitude, M, in Richter, hypocentral distance, R_h, in km, and liquefaction susceptibility represented by $(N_1)_{60}$:

$$M = \frac{2}{3}\log[1.445R^2(N_1)_{60}^{6.06}] \quad (3.2)$$

This relationship is assumed to be applicable for world-wide tectonic conditions, but Obermeier and Pond 1999, recognized that the magnitude could be constrained further knowing localized information such as stress drop, focal depth, the degree of liquefaction susceptibility on the extent of liquefaction, and the attenuation of bedrock shaking.

Magnitudes back-calculated from previous studies are summarized in Table 3.2. The results from the "Magnitude Bound" method indicate a magnitude of 7.0 to 7.2 (assuming a source near Charleston (Re=100 to 140 Km)) or 6.3 to 6.8 (assuming a source northeast of Charleston (Re= 10 to 35 Km)) as found by Talwani and Schaeffer 2001, and Hu et al. 2002b. The results from the "Energy Stress" method range from 5.5 to 7.0 (northeast source) and 6.8 to 7.8 (Charleston source) when soil age was not taken

into account and from 4.3 to 6.4 (northeast source) and 5.5 to 7.2 (Charleston source) when soil age was taken into account (Leon et al. 2005). Given the range of values from these two methods, the peak ground acceleration for different magnitudes at each site was subsequently obtained for M=5, 6, 7.5 Richter.

Table 3.2 Estimated magnitudes of prehistoric earthquake episodes in SCCP.

Earthquake Magnitude								
Episode	**Age†, Years B.P.**	**Source**	**Associated Sand blow**	**Re or R (Km)**	**Talwani & Schaeffe,2001**		**Hu et al. 2002b**	**Leon et al. 2005**
					Empirical	**Magnitude Bound**		
A	546±17	Charleston	SAM-02	100-140	7+	7.0	7.4 to 7.6	6.2 to 7.0
B	1021±30	Charleston	SAM-04	100-140	7+	7.0	7.4 to 7.6	6.2 to 6.8
C	1648±74	Northeast	SAM-05	10-35	~6	6.3 to 6.8	6.3 to 7.0	5.1 to 6.4
C'	1683±70	Charleston	SAM-05	100-140	7+	7.2	7.6 to 7.8	6.4 to 7.2
D	1996±212	South	…	…	~6	5.7	…	…
E	3548±66	Charleston	GAP-02	100-140	7+~6	7.0	6.8 to 7.0	5.6 to 6.4
F	5038±166	Northeast	GAP-03	10-35	~6	…	5.5 to 6.2	4.3 to 5.6
F'	5038±166	Charleston	GAP-03	100-140	7+	…	6.8 to 7.0	5.5 to 6.2

†Age of earthquake from Talwani and Schaeffer, 2001.

3.3.3 Evaluation of Peak Ground Acceleration

Idriss and Boulanger 2008, defined the cyclic resistance ratio for a given earthquake ($CRR_{M,\sigma'VC}$) with the following equation:

$$CSR_{M,\sigma'_{vc}} = CRR_{M=7.5,\sigma'_{vc}=1} * MSF * K_{\sigma} = 0.65 * r_d * \left(\frac{\sigma_{v0} * a_{max}}{\sigma'_{v0} * g}\right) \quad (3.3)$$

where a_{max} is the maximum ground acceleration at surface, σ_{v0} is the vertical stress and σ'_{v0} the vertical effective stress at depth z, and r_d is the reduction factor that considers the

flexibility of soil column. A coefficient of 0.65 is applied to consider the significant cycles during the earthquake. The magnitude scaling factor (MSF) is used to consider the earthquakes with the magnitudes other than 7.5. K_σ is the overburden correction factor which has effect on SPT blow counts $(N_1)_{60}$, and normalized cone penetrometer resistance $(q_{c1N})_{cs}$ for calculation of CRR. The revised relations of MSF, r_d, K_σ and C_N proposed by Idriss and Boulanger 2008, were used in this study.

Idriss and Boulanger 2008, also re-evaluated the CPT-based liquefaction correlation using an expanded case history database of liquefaction/no liquefaction sites and adjusted the relation to reflect the number of equivalent cycles that had occurred up to the time when liquefaction was triggered for cases where liquefaction occurs early in shaking. The CPT-based approach was also modified to account for the effects of non-plastic fines content on the liquefaction resistance. The relation between CRR and $(q_{c1N})_{cs}$ is given by:

$$CRR_{M=7.5,\sigma'_{vc}=1} = exp\left\{\frac{(q_{c1N})_{cs}}{540} + \left(\frac{(q_{c1N})_{cs}}{67}\right)^2 - \left(\frac{(q_{c1N})_{cs}}{80}\right)^3 + \left(\frac{(q_{c1N})_{cs}}{114}\right)^4 - 3\right\} \quad (3.4)$$

where $(q_{c1N})_{cs}$ is the equivalent clean-sand value of the corrected tip resistance and can be computed as follows:

$$(q_{c1N})_{cs} = q_{c1N} + \Delta q_{c1N} \quad (3.5)$$

$$\Delta q_{c1N} = \left(5.4 + \frac{q_{C1N}}{16}\right) * exp\left\{1.63 + \frac{9.7}{FC + 0.01} - \left(\frac{15.7}{FC + 0.01}\right)^2\right\} \quad (3.6)$$

where FC is the fines content percentage and q_{c1N} is the normalized value of q_{c1} by Pa (q_{c1N}=q_{c1}/Pa) to obtain a dimensionless value of penetration resistances in sand to an equivalent σ'_{v0} of one atmosphere (Pa=1.06 tsf=101 kPa). q_{c1} is the corrected value of tip penetration resistance for overburden pressure and is defined using Equation 3.7 and 3.8.

$$q_{c1} = q_c * C_N \tag{3.7}$$

$$C_N = (\frac{P_a}{\sigma'_{v0}})^{\beta} \leq 1.7 \,, \beta = 1.338 - 0.249(q_{C1N})^{0.264} \,, \quad 21 \leq q_{C1N} \leq 254 \tag{3.8}$$

An iterative procedure is needed to determine the C_N and q_{c1} because as it is indicated in these equations, C_N depends on q_{c1} and q_{c1} depends on C_N. In this research 100 times of iteration is done to achieve q_{c1N}. To calculate $CSR_{M,\sigma'_{vc}}$, MSF and K_σ parameters are applied to $CRR_{M=7.5,\sigma'_{vc}=1}$. The overburden correction factor, K_σ, is achieved using the following equation:

$$K_\sigma = 1 - C_\sigma \ln\left(\frac{\sigma'_{v0}}{P_a}\right) \leq 1.1; \;\; C_\sigma = \frac{1}{37.3 - 8.27(q_{C1N})^{0.264}} \leq 0.3, \;\; q_{C1N} \leq 211 \tag{3.9}$$

For reference, Leon et al. 2005, found CRR using the following relations where, $(q_{c1N})_{cs}$ was found from Youd and Idriss 1977:

$$CRR_{7.5} = 0.05 + 0.833[\,(q_{c1N})_{cs}/1000] \qquad If\ (q_{c1N})_{cs} < 50 \tag{3.10}$$

$$CRR_{7.5} = 0.08 + 93[\,(q_{c1N})_{cs}/1000]^3 \qquad If\ 50 \leq (q_{c1N})_{cs} < 160 \tag{3.11}$$

The $(q_{c1N})_{cs}$ values that correspond to the $q_{c1(pre)}$ values from Table 3.1 were found from Idriss and Boulanger 2008, and compared to those from previous studies using Leon et al. 2005, are shown in Table 3.3. The differences in $(q_{c1N})_{cs}$ found from Idriss and Boulanger 2008 and Leon et al. 2005, range from 0 to 59 (average of 15).

Table 3.3 Average values of $(q_{c1N})_{cs\ (pre)}$ corresponding to $q_{c1(pre)}$ from Table 3.1.

Location	**Age (years)**	**$q_{c1(current)}$ (MPa)**	**Average $(q_{c1N})_{cs\ (pre)}$**							
			Approach 1				**Approach 2**			
			ΔDR 5%		ΔDR 10%		ΔDR 5%		ΔDR 10%	
			[8]	[5]	[8]	[5]	[8]	[5]	[8]	[5]
SAM-CPT-1	1,021	10	62	74	38	46	75	89	73	87
SAM-CPT-2	450,000	9	16	20	10	12	64	79	64	79
SAM-CPT-3	450,000	13	23	24	15	15	92	94	92	94
GAP-CPT-1	5,038	7	38	54	23	32	53	74	52	72
GAP-CPT-2	5,038	8	42	85	25	50	59	118	58	116
GAP-CPT-3	3,548	4	25	33	15	20	33	44	32	43

3.4 RESULTS

Using the age-corrected values of $(q_{c1N})_{cs}$ from Table 3.3, the calculated values of $CRR_{M=7.5}$, representing those at the time of the earthquake for SAM-CPT-1, and GAP-CPT-1, -2, and -3 (or deposition for SAM-CPT-2,-3) using the newer relations of Idriss and Boulanger 2008, in Equation 3.4 are compared with those found using Equation 3.10 and 3.11, used in previous studies (Leon et al. 2005), in Table 3.4.

The maximum ground acceleration, a_{max}, found using Equation 3.3 and the CRR values in Table 3.4 are summarized for earthquake magnitudes M=5, M=6 and M=7.5 in Table 3.5.

Table 3.4 Comparison of $CRR_{M=7.5}$ found from two methods.

Location No.	**Age (years)**	**$CRR_{M=7.5}$ (Average of Approach 1 and 2)**			
		ΔDR =5%		**ΔDR =10%**	
		Eqn 10	Eqn 4	Eqn 10	Eqn 4
SAM-CPT-1	1,021	0.14	0.10	0.12	0.09
SAM-CPT-2	450,000	0.10	0.07	0.10	0.07
SAM-CPT-3	450,000	0.13	0.10	0.13	0.10
GAP-CPT-1	5,038	0.12	0.08	0.11	0.07
GAP-CPT-2	5,038	0.13	0.09	0.12	0.08
GAP-CPT-3	3,548	0.09	0.06	0.08	0.06

The accelerations found using the previous method are shown for comparison. For a stronger earthquake in magnitude, less acceleration is needed for the soil to be liquefied. Using the Idriss and Boulanger 2008, procedure for the Sampit site, the peak ground accelerations range from 0.15 to 0.23g for M=5 and 0.08 to 0.12 g for M=7.5 while the previous method leads to a range from 0.30 to 0.46g and 0.10 to 0.16g for M=5 and M=7.5, respectively. The Youd and Idriss 1997, method which is used in the Leon's 2005, work results in higher values of acceleration which is not conservative particularly for lower earthquake magnitudes. Using the newer method reduces the acceleration values about 50% for M=5 and 23% for M=7.5. For the Gapway site, the calculated accelerations range from 0.15 to 0.20g for M=5 and 0.08 to 0.11g for M=7.5 and range from 0.29 to 0.43g for M=5 and 0.10 to 0.15g when M=7.5. For the cases when relative density changes more during the earthquake (ΔDR=10%) less acceleration is needed for soil to be liquefied due to higher amount of disturbance.

Finally, the site-specific estimated magnitudes for the prehistoric earthquakes (see Table 3.2) at the locations of the sand blows near the CPT locations in this study were

used to back-calculate the minimum peak ground accelerations that could cause sand blows for these prehistoric earthquakes.

Table 3.5 Peak ground acceleration for source sand layer.

Location	Maximum Acceleration (g)											
	M=5				M=6				M=7.5			
	ΔDR [8]	5% [5]	ΔDR [8]	10% [5]	ΔDR [8]	5% [5]	ΔDR [8]	10% [5]	ΔDR [8]	5% [5]	ΔDR [8]	10% [5]
SAM-CPT-1	0.23	0.46	0.20	0.39	0.18	0.29	0.16	0.24	0.12	0.16	0.10	0.14
SAM-CPT-2	0.16	0.30	0.15	0.30	0.13	0.19	0.12	0.18	0.08	0.11	0.08	0.10
SAM-CPT-3	0.20	0.35	0.19	0.34	0.16	0.22	0.15	0.21	0.10	0.12	0.10	0.12
GAP-CPT-1	0.19	0.43	0.17	0.37	0.15	0.27	0.14	0.23	0.10	0.15	0.09	0.13
GAP-CPT-2	0.20	0.34	0.18	0.30	0.16	0.21	0.15	0.19	0.11	0.12	0.10	0.11
GAP-CPT-3	0.16	0.31	0.15	0.29	0.13	0.20	0.13	0.18	0.09	0.11	0.08	0.10

At the Sampit site, SAM-SCPT-1 is in the vicinity of the sand blow at SAM-04 that is associated with Episode B occurring 1021±30 years.B.P. At the Gapway site, GAP-SCPT-1 is in the vicinity of the sand blow at GAP-04 and GAP-SCPT-2 and GAP-SCPT-3 are in the vicinity of the sand blows at GAP-03 and GAP-02, respectively. The sand blow at GAP-03 is associated with Episode E, 3548±66 years.B.P. and the sand blow at GAP-02 is associated with Episode F' and F, occurring 5038±166 years.B.P. for a Northeast and Charleston source, respectively.

The range of accelerations (preliminary) for these three episodes is shown in Table 3.6. Following the same trend as the data shown in Table 3.5, the newer method leads to lower accelerations than the previous approach for the CPT data set used herein. Research is still on-going to apply the newer methods to the CPT and SPT data set used by Hu et al. 2002b and Leon at al. 2005.

Table 3.6 Estimated peak ground accelerations of prehistoric earthquake episodes in the SCCP.

Estimated Peak Ground Accelerations (g)							
Episode	**Age, Years B.P.**	**Source**	**Associated Sand blow**	**Hu et al., 2002b**	**Leon et al., 2005**	**This Study (Preliminary Range)**	
						Idriss& Boulanger 2008	**Youd& Idriss 1997**
A	546±17	Charleston	SAM-02	0.16 to 0.18	0.14	…	
B	1021±30	Charleston	SAM-04	0.16 to 0.18	0.14 to 0.15	0.10 to 0.18	0.14 to 0.29
C	1648±74	Northeast	SAM-05	0.21 to 0.28	0.20 to 0.29	…	
C'	1683±70	Charleston	SAM-05	0.16 to 0.17	0.14 to 0.15	…	
D	1996±212	South	…	0.23 to 0.24	0.21 to 0.26	…	
E	3548±66	Charleston	GAP-02	0.31 to 0.42	0.30 to 0.53	0.10 to 0.14	0.12 to 0.25
F	5038±166	Northeast	GAP-03	0.23 to 0.24	0.22 to 0.24	0.15 to 0.20	0.19 to 0.34
F'	5038±166	Charleston	GAP-03	…	…	0.11 to 0.18	0.13 to 0.27

3.5 CONCLUSION

The prehistoric earthquake peak ground accelerations at the Sampit and Gapway sites in the South Carolina Coastal Plain were reassessed using cone penetration data corrected for the effect of time-dependent mechanisms ("aging") together with the revised relations for cyclic resistance ratio of Idriss and Boulanger. The newer method leads to lower accelerations to initiate liquefaction than the previous approach. The difference is significant for lower magnitude earthquakes. The newer method resulted in accelerations that are about 50% less than from the previous method for M=5; whereas, the accelerations are about 23% less for M=7.5.

CHAPTER 4

MAGNITUDES OF PREHISTORIC EARTHQUAKES AT THE HOLLYWOOD, SOUTH CAROLINA SITE[2]

[2] Gheibi, E., and Gassman, S. L. (2015). Geotechnical Special Publication, Vol.256. Page: 1246-1256, Paper, DOI: 10.1061/9780784479087.112. Reprinted here with permission of publisher.

ABSTRACT

Pleistocene soil deposits show an increase in liquefaction resistance compared to younger deposits; thus, semi-empirical procedures for evaluating liquefaction potential that are derived from databases of young Holocene soils may not be applicable to aged soils. In this study, the minimum earthquake magnitude and peak ground acceleration required to initiate liquefaction were computed for soils estimated to be about 120,000 to 130,000 years old at the Hollywood site located in the South Carolina Coastal Plain. Discovered sand blows at this site are associated with earthquakes that date back to 11,000 years before present. In-situ geotechnical data, including SPT and CPT with pore water pressure measurements, were used with empirical methods that account for the age of the soil deposit to back analyse the minimum earthquake magnitude and peak ground acceleration at the time of the prehistoric earthquakes. When the age of the earthquake was not considered, the magnitude ranged from 7 to 7.2 and the corresponding acceleration ranged from 0.23 to 0.35g. The earthquake magnitude at the time of earthquake was found to be lower when accounting for age; for the most recent prehistoric earthquake with the age of 546±17, the magnitude was reduced and ranged from 5.7 to 6.7 with corresponding acceleration ranging from 0.17 to 0.30g.

4.1 INTRODUCTION

The South Carolina Coastal Plain (SCCP) experiences infrequent earthquakes and paleoliquefaction analysis plays an important role in studying the paleoseismicity of this region. As an example, over 160 paleoliquefaction features have been discovered at a site near Hollywood, South Carolina (Obermeier et al. 1987) that have been associated with earthquakes dating from 500 to 11,000 years B.P. (Talwani and Cox 1985 and Weems et

al. 1986). From studies of these paleoliquefaction features, at least seven, large, prehistoric earthquakes have occurred within the last 6000 years in the SCCP with an average occurrence rate, based on the three most recent events, of about 500 years (Talwani and Schaeffer 2001).

To estimate the minimum values of magnitudes (M) and peak ground accelerations (a_{max}) needed for liquefaction to occur from these prehistoric earthquakes, Hu et al. 2002a and 2002b, used site-specific geotechnical data (penetration resistance and shear wave velocity) in the vicinity of paleoliquefaction features studied by Talwani and Schaeffer 2001 at two sites (Gapway and Sampit) near Georgetown, South Carolina and two sites near the Ten Mile Hill Air Force Base north of Charleston, South Carolina. The back-calculations were based on empirical correlations using Seed's Simplified Method (Seed and Idriss 1971) as reported in Youd and Idriss 1997 that are extensively used to determine liquefaction resistance of sand deposits from in-situ soil indices (e.g. $(N_1)_{60}$ from the standard penetration test (SPT) and q_{c1} from the cone penetration test (CPT)). Similarly, Martin and Clough 1994 used the Seed et al. 1984 method, as well as the Ishihara 1985 method, to back-calculate the peak ground accelerations at the Hollywood site.

The correlations between in-situ geotechnical data and cyclic resistance ratio used in these studies are primarily based on studies of recent earthquakes in Japan, China and the west coast region of the U.S. where the soil deposits are of Holocene age (<10,000 years old). Therefore, Leon et al. 2005 developed a method to account for the effect of time-dependent mechanisms ("aging") on the back-calculated magnitudes and peak ground accelerations for the sand deposits in the SCCP that are older than 100,000 years

and obtained an approximately 0.9 unit reduction in magnitude and 15% reduction in peak ground acceleration. Neglecting the effect of aging resulted in a 60% underestimation of CRR (Leon et al. 2006).

Furthermore, since the time of the earlier back-calculations, Idriss and Boulanger 2008 have reexamined Seed's original method and have proposed new relations for the stress reduction factor (r_d), earthquake magnitude scaling factor for cyclic stress ratios (MSF), overburden correction factor for cyclic stress ratios (K_σ), and the overburden normalization factor for penetration resistances (C_N). Gheibi and Gassman 2014 and Gheibi et al. 2013 reviewed the prehistoric earthquake magnitudes and effect of aging on soil resistance against liquefaction at Hollywood and Fort Dorchester sites, respectively. In general, Gheibi and Gassman 2014 also found that using the newer method reduces the acceleration values about 50% for M=5 and 23% for M=7.5 for the Gapway and Sampit sites when compared to using Seed's original method.

Therefore, the purpose of this paper is to back-calculate the minimum magnitude and acceleration required to initiate liquefaction and form the paleoliquefaction features associated with prehistoric earthquakes at the Hollywood site using the newer semi-empirical method of Idriss and Boulanger 2008 and time-dependent approach of Leon et al. 2005. The results will be compared to earlier back-calculations by Martin and Clough 1994.

4.2 SITE STUDIED

The Hollywood site is located 0.8 km northeast of the town of Hollywood, South Carolina. Obermeier et al. 1987 reported finding 162 liquefaction features along the side walls of two flood control channels excavated at the site. Many of the observed features

are sand blows as large as 8 feet diameter from prehistoric earthquakes and some are minor fissures related to the Charleston earthquake of 1886. Talwani and Cox 1985 and Weems et al. 1986 have used radiocarbon dates of the trapped organic material in and around sand blows to estimate the times of formation of the sand blows. Based on calibrated ages described in Talwani and Schaeffer 2001, times of sand blow formation range from 500 to 11,000 years B.P. and have been associated with four episodes: Episode A occurring 546±17 years B.P., Episode B 1021±30 years B.P., Episode E 3548±66 years B.P. and Episode F 5038±166 years B.P.

The in-situ data used in this study were obtained along an east-west exploration alignment that is parallel to one of the flood control channels and lies along the flank of a Pleistocene beach deposit with soils estimated to be about 120,000 to 130,000 years old (Weems et al. 1986). The alignment includes three CPTs (HWD-CPT-4, HWD-CPT-5 and HWD-CPT-6) and one SPT with energy measurements (HWD-SPTE-1) that were performed as part of a larger study to investigate the effect of aging on the liquefaction potential of SCCP soils (e.g. Hasek 2016, Williamson and Gassman 2014, and Hayati et al. 2008). Figure 4.1shows the CPT tip resistance and the SPT blow count profiles obtained at the site. Note that HWD-SPTE-1 is located near HWD-CPT-4. The water table depth was in the range of 1.7 to 2.3 m below the ground surface from 2007 to 2010. Laboratory index tests were performed on the SPT split spoon samples to characterize the soil and obtain the fines content.

The soil classification chart of Robertson 1990, was used to obtain the soil profiles shown in Figure 4.2. Samples from the SPT split spoon, near HWD-CPT-4, were used to classify the soil according to USCS. The general soil profile along the testing

alignment consists of about 2.30 m of silty sand with average CPT tip resistance as shown in Figure 4.1 of about 15 MPa (maximum of 18 to 24 MPa) and blow counts between 4 and 17. The underlying layer is the source sand layer and consists of 1.4 to 2 m of clean sand to silty sand with an average tip resistance value of 6 MPa and average blow count of 6. This layer is underlain by a mixture of clayey silt to sandy silt and silty sand.

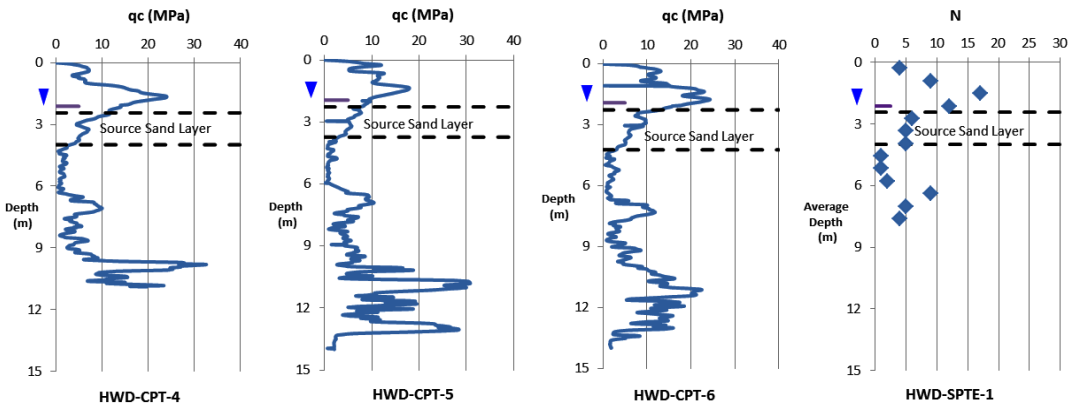

Figure 4.1 CPT and SPT profiles at the Hollywood sites.

The source sand layer identified in Figure 4.2 is the layer most prone to liquefaction. This layer was identified using the interpretation of SPT blow counts, CPT tip resistance, excess pore water pressure, fines content and soil type. The fines content is in the range of 8 to 13% and excess pore pressures did not develop during the CPT push at any of the test locations. The equivalent clean sand tip resistance, $(q_{c1N})_{cs}$, and SPT blow counts, $(N_1)_{60}$, are less than 160 and 30 in the source sand which are the boundaries for liquefiable/nonliquefiable soils per Robertson and Wride 1998, and Youd and Idriss 1997.

Earlier studies by Martin 1990, included eleven CPTs, eight SPTs and twelve auger borings. The soil profile was described to consist of about 2.6 m of clean, fine dense sand underlain by 2.3 m of clean, fine loose sand which was identified as the source of liquefied materials (Martin and Clough 1994) and is in general agreement with the study herein. All fines were non-plastic silts.

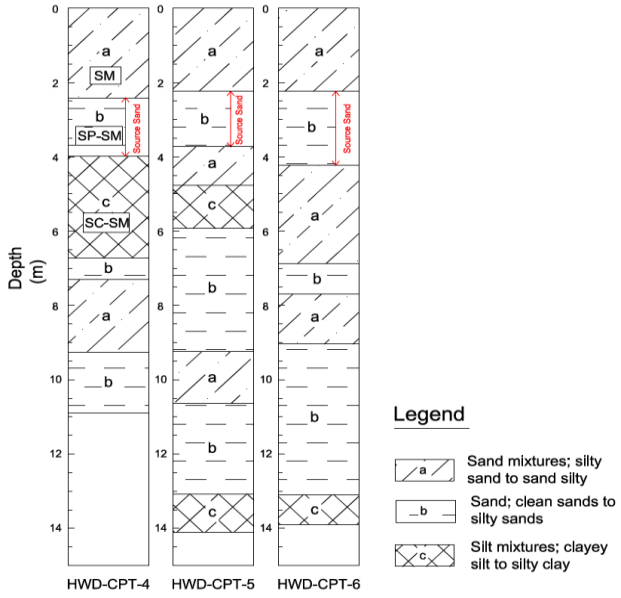

Figure 4.2 Soil profile at Hollywood.

4.3 FRAMEWORK FOR AGE AND DISTURBANCE CORRECTION

The methodology of Leon et al. 2005, Was used to correct the cone penetration tip resistance, q_{c1}, and SPT blow count, $(N_1)_{60}$, for 1) aging of the soil and 2) disturbance due to post-liquefaction consolidation (primary) and densification (or loosening). The method is based on the idea that the empirical correlations for liquefaction evaluation applicable for young or freshly deposited soils can be used for the older soil deposits as long as the currently measured penetration resistances are modified to account for the effect of aging.

By correcting the currently recorded in situ geotechnical data for aging, the corresponding data immediately after the earthquake for the sites that liquefied are determined and termed "post-earthquake". These data are further corrected for disturbance from the earthquake to obtain the "pre-earthquake" data.

The method accounts for disturbance due to the liquefaction event and post-liquefaction aging using two different approaches. Approach 1 is based on the relations offered by Mesri et al. 1990, for both the age and disturbance correction and Approach 2 is based on work by Kulhawy and Mayne 1990, for the age correction and Seed et al. 1988 for the disturbance correction. As suggested by Ellis and De Alba 1999, and Stark et al. 2002, Leon et al. 2005, considered the change in relative density (ΔD_R) to be 5% and 10% between the pre- ($q_{c1\ (pre)}$ and $(N_1)_{60\ (pre)}$) and post- ($q_{c1\ (post)}$ and $(N_1)_{60\ (post)}$) earthquake state.

The average $q_{c1\ (pre)}$ and $q_{c1\ (post)}$ values of tip resistance found using this method for the ages associated with earthquake Episodes A, B, E and F from Talwani and Schaeffer 2001, are summarized in Table 4.1. As shown, $q_{c1\ (post)}$ is less than $q_{c1\ (pre)}$ for Approach 1; whereas, $q_{c1\ (post)}$ is greater than or equal to $q_{c1\ (pre)}$ for Approach 2. In both cases the average values of tip resistance corrected for both age and disturbance are less than current measurements.

The average $(N_1)_{60\ (pre)}$ and $(N_1)_{60\ (post)}$ values found using the blow count data from HWD-SPTE-1 are summarized in Table 4.2. In addition, blow counts obtained through correlations to the CPT data obtained at HWD-CPT-4, -5 and -6 using Lunne et al. 1997 are also shown. The blow counts obtained in the field at HWD-SPTE-1 differ

from those obtained through correlation at HWD-CPT-4, the CPT closest to the SPTE test, by 7 units.

Table 4.1 Average values of age-corrected tip resistance for source sand layer.

Episode	Age, years B.P.	$q_{c1\,(post)}$ (MPa) / $q_{c1\,(pre)}$ (MPa)														
		HWD-CPT-4					HWD-CPT-5					HWD-CPT-6				
			1		2			1		2			1		2	
		$q_{c1\,(current)}$ (MPa)	ΔDR 5%	ΔDR 10%	ΔDR 5%	ΔDR 10%	$q_{c1\,(current)}$ (MPa)	ΔDR 5%	ΔDR 10%	ΔDR 5%	ΔDR 10%	$q_{c1\,(current)}$ (MPa)	ΔDR 5%	ΔDR 10%	ΔDR 5%	ΔDR 10%
A	546±17	10	4/7	3/4	8/8	8/7	9	3/6	3/4	7/7	7/7	10	4/7	3/5	8/8	8/8
B	1021±30		3/6	3/4	8/8	8/7		3/6	2/4	7/7	7/7		4/7	3/4	8/8	8/8
E	3548±66		3/5	2/3	8/7	8/7		3/5	2/3	7/7	7/7		3/6	2/4	8/8	8/8
F	5038±166		3/5	2/3	8/7	8/7		3/5	2/3	7/7	7/7		3/6	2/3	8/8	8/8

Table 4.2 Average values of age-corrected blow counts for source sand layer.

Episode	Age, years B.P.	$(N_1)_{60\,(post)}$ / $(N_1)_{60\,(pre)}$																			
		HWD-SPTE-1					HWD-CPT-4					HWD-CPT-5					HWD-CPT-6				
			1		2			1		2			1		2			1		2	
		$(N_1)_{60\,(current)}$	ΔDR 5 %	ΔDR 10 %	ΔDR 5 %	ΔDR 10 %	$(N_1)_{60\,(current)}$	ΔDR 5 %	ΔDR 10 %	ΔDR 5 %	ΔDR 10 %	$(N_1)_{60\,(current)}$	ΔDR 5 %	ΔDR 10 %	ΔDR 5 %	ΔDR 10 %	$(N_1)_{60\,(current)}$	ΔDR 5 %	ΔDR 10 %	ΔDR 5 %	ΔDR 10 %
A	546±17	11	4/7	3/5	8/6	8/5	18	7/12	5/8	14/11	14/9	17	6/11	5/7	13/11	13/8	19	7/13	6/8	15/12	15/10
B	1021±30		4/7	3/4	8/6	8/5		6/11	5/7	14/11	14/9		6/11	4/7	13/11	13/8		7/12	5/8	15/12	15/10
E	3548±66		3/6	2/4	8/6	8/5		5/10	4/6	14/11	14/9		5/9	4/6	13/10	13/8		6/11	4/6	15/12	15/10
F	5038±166		3/6	2/3	8/6	8/4		5/10	4/6	14/11	14/9		5/9	4/5	13/10	13/8		6/10	4/6	15/12	15/10

4.3.1 Back-Calculation of the Earthquake Magnitude

The earthquake magnitude was back-calculated using the Energy Stress method (Hu et al. 2002b) which relates the seismic intensity at the site in terms of magnitude, M, in Richter, hypocentral distance, R_h, in km, and liquefaction susceptibility represented by $(N_1)_{60}$ in the following equation:

$$M = \frac{2}{3}\log[1.445R^2(N_1)_{60}^{6.06}] \quad (4.1)$$

This relationship is assumed to be applicable for world-wide tectonic conditions, recognizing that the magnitude could be constrained further knowing localized information such as stress drop, focal depth, the degree of liquefaction susceptibility on the extent of liquefaction, and the attenuation of bedrock shaking (Obermeier and Pond 1999). Uncertainties regarding back-calculation of earthquake magnitudes and peak ground accelerations are presented in Olson et al. 2005.

Two possible earthquake sources: 1) the NE trending Wood Stock Fault (WF) and 2) NW trending Sawmill Branch Fault (SBF) identified by Dura-Gomez and Talwani 2009, were considered to obtain the epicentral and hypocentral distances. Epicentral distances from WF and SBF are considered to be 25 km for Hollywood and hypocentral distances, rounded to the nearest km are one more km than the epicentral distances.

4.3.2 Back Analysis of Peak Ground Acceleration

The peak ground acceleration at the surface, a_{max}, was found using the following equation for the cyclic stress ratio for a given earthquake ($CSR_{M,\sigma'_{vc}}$) given by Idriss and Boulanger 2008:

$$CSR_{M,\sigma'_{vc}} = CRR_{M=7.5,\sigma'_{vc}=1} * MSF * K_\sigma = 0.65 * r_d * \left(\frac{\sigma_{v0} * a_{max}}{\sigma'_{v0} * g}\right) \quad (4.2)$$

where σ_{v0} is the vertical stress and σ'_{v0} is the vertical effective stress at depth z, and r_d is the reduction factor that considers the flexibility of soil column. A coefficient of 0.65 is

applied to consider the significant cycles during the earthquake. The magnitude scaling factor (MSF) is used for earthquakes with magnitudes other than 7.5. The proposed relations of MSF, r_d, K_σ and C_N of Idriss and Boulanger 2008 were used in this study. K_σ is the overburden correction factor which has effect on SPT blow counts $(N_1)_{60}$, and normalized cone penetrometer resistance $(q_{c1N})_{cs}$ for calculation of CRR and is achieved using the following equation:

$$K_\sigma = 1 - C_\sigma \ln\left(\frac{\sigma'_{v0}}{P_a}\right) \leq 1.1;\ C_\sigma = \frac{1}{37.3 - 8.27(q_{C1N})^{0.264}} \leq 0.3,\ q_{C1N} \leq 211 \quad (4.3)$$

q_{c1N} is the normalized value of q_{c1} (q_{c1N}=q_{c1}/Pa) to obtain a dimensionless value of penetration resistances in sand to an equivalent σ'_{v0} of one atmosphere. q_{c1} is the corrected value of tip penetration resistance for overburden pressure and is defined by Equation 4.4.

$$q_{c1} = q_c * C_N, C_N = \left(\frac{P_a}{\sigma'_{v0}}\right)^\beta \leq 1.7,\ \ \beta = 1.338 - 0.249(q_{C1N})^{0.264}, 21 \leq q_{c1N} \leq 254 \quad (4.4)$$

An iterative procedure is needed to determine the C_N and q_{c1} because C_N depends on q_{c1} and q_{c1} depends on C_N. In this research 100 times of iteration is done to achieve q_{c1N}. Note that following the Idriss and Boulanger 2008, procedure, q_{c1Ncs} is applied instead of q_{c1N} in Equation 4.3 and 4.4.

Idriss and Boulanger 2008, also re-evaluated the CPT-based liquefaction correlation using an expanded case history database of liquefaction/no liquefaction sites

and adjusted the relation to reflect the number of equivalent cycles that had occurred up to the time when liquefaction was triggered for cases where liquefaction occurs early in shaking. The relation between CRR and $(q_{c1N})_{cs}$ is given by:

$$CRR_{M=7.5,\sigma'_{vc}=1} = exp\left\{\frac{(q_{c1N})_{cs}}{540} + \left(\frac{(q_{c1N})_{cs}}{67}\right)^2 - \left(\frac{(q_{c1N})_{cs}}{80}\right)^3 + \left(\frac{(q_{c1N})_{cs}}{114}\right)^4 - 3\right\} \quad (4.5)$$

$(q_{c1N})_{cs}$ is the equivalent clean-sand value of the corrected tip resistance, computed by:

$$(q_{c1N})_{cs} = q_{c1N} + \Delta q_{c1N}\,, \quad \Delta q_{c1N} = \left(5.4 + \frac{q_{C1N}}{16}\right) * \exp\left\{1.63 + \frac{9.7}{FC + 0.01} - \left(\frac{15.7}{FC + 0.01}\right)^2\right\} \quad (4.6)$$

FC is the fines content percentage which was about 10% at the Hollywood site. The $(q_{c1N})_{cs}$ values that correspond to the $q_{c1(pre)}$ values in Table 4.1 are shown in Table 4.3.

Table 4.3 Average values of $(q_{c1N})_{cs\ (pre)}$ corresponding to $q_{c1(pre)}$.

Episode	Age, years B.P.	HWD-CPT-4					HWD-CPT-5					HWD-CPT-6				
		$(q_{c1N})_{cs\ (current)}$	Average $(q_{c1N})_{cs\ (pre)}$				$(q_{c1N})_{cs\ (current)}$	Average $(q_{c1N})_{cs\ (pre)}$				$(q_{c1N})_{cs\ (current)}$	Average $(q_{c1N})_{cs\ (pre)}$			
			1		2			1		2			1		2	
			ΔDR 5%	ΔDR 10%	ΔDR 5%	ΔDR 10%		ΔDR 5%	ΔDR 10%	ΔDR 5%	ΔDR 10%		ΔDR 5%	ΔDR 10%	ΔDR 5%	ΔDR 10%
A	546±17	110	78	52	88	86	102	73	48	82	80	121	86	58	97	95
B	1021±30		74	48	87	85		68	45	81	79		81	53	96	94
E	3548±66		65	42	86	84		60	39	79	78		72	46	94	92
F	5038±166		63	40	85	83		58	37	79	77		69	44	93	92

4.4 RESULTS

4.4.1 Earthquake Magnitude

The minimum estimated magnitudes obtained from the Energy Stress method are shown in Table 4.4. Using the current in-situ soil properties ($(N_1)_{60\ current}$ in Table 4.2) the

results range from 6.3 (using HWD-SPTE-1) to an average of 7.1 (using HWD-CPT-4, -5 and -6). When the soil properties are corrected ($(N_1)_{60\ pre}$ in Table 4.2) for age and disturbance of each earthquake episode, the magnitude is reduced. The reduction ranges from 0.5 to 1.3 units for Episode A and is greater for older earthquakes (e.g. reduction of 0.7 to 1.8 units for Episode F). Note that the magnitudes obtained from the Energy Stress Method (Equation 4.1) using the SPT data (HWD-SPTE-1) are 0.5 to 1 units less than when obtaining $(N_1)_{60}$ from the CPT data (HWD-CPT-4, -5 and -6) via the Lunne et al. 1997, correlation.

Table 4.4 Earthquake magnitudes.

Episode	Age, years B.P.	HWD-SPTE-1		HWD-CPT-4		HWD-CPT-5		HWD-CPT-6	
		Current	Aged	Current	Aged	Current	Aged	Current	Aged
A	546±17	6.3	5.1 to 5.7	7.1	5.8 to 6.5	7	5.7 to 6.4	7.2	6 to 6.7
B	1021±30		5 to 5.6		5.7 to 6.4		5.5 to 6.3		5.8 to 6.5
E	3548±66		4.8 to 5.5		5.4 to 6.3		5.3 to 6.2		5.6 to 6.5
F	5038±166		4.7 to 5.5		5.3 to 6.3		5.2 to 6.2		5.5 to 6.5

4.4.2 Peak Ground Acceleration

Using the age-corrected $(q_{c1N})_{cs(pre)}$ values from Table 4.3, the $CRR_{M=7.5}$ values found from Equation 4.2, representing those at the time of the earthquake at each episode for HWD-CPT-4, -5, and -6, are presented in Table 4.5.

Table 4.5 Average values of $CRR_{M=7.5}$.

Episode	Age, years B.P.	CRR $_{M=7.5}$ (Average of Approach 1 and 2)					
		HWD-CPT-4		HWD-CPT-5		HWD-CPT-6	
		ΔDR 5%	ΔDR 10%	ΔDR 5%	ΔDR 10%	ΔDR 5%	ΔDR 10%
A	546±17	0.12	0.11	0.11	0.10	0.14	0.12
B	1021±30	0.12	0.11	0.11	0.09	0.13	0.11
E	3548±66	0.12	0.10	0.10	0.09	0.12	0.11
F	5038±166	0.11	0.10	0.10	0.09	0.12	0.11

The peak ground acceleration, a_{max}, found using Equation 4.2 and the CRR values in Table 4.5 are summarized for earthquake magnitudes M=5, M=6 and M=7 in Table 4.6. Stronger earthquakes need less acceleration for the soil to be liquefied; e.g., for Episode A, the peak ground accelerations range from 0.25 to 0.34g for M=5 which are greater than the range of 0.15 to 0.21g for M=7.

Table 4.6 Peak ground acceleration for source sand layer.

Episode, years B.P.	Location	Peak Ground Acceleration (g)					
		M=5		M=6		M=7	
		ΔDR 5%	ΔDR 10%	ΔDR 5%	ΔDR 10%	ΔDR 5%	ΔDR 10%
A 546±17	HWD-CPT-4	0.32	0.27	0.26	0.22	0.20	0.17
	HWD-CPT-5	0.29	0.25	0.23	0.20	0.18	0.15
	HWD-CPT-6	0.34	0.29	0.28	0.23	0.21	0.18
B 1021±30	HWD-CPT-4	0.31	0.26	0.25	0.21	0.19	0.16
	HWD-CPT-5	0.28	0.24	0.22	0.19	0.17	0.15
	HWD-CPT-6	0.33	0.28	0.27	0.22	0.20	0.17
E 3548±66	HWD-CPT-4	0.29	0.25	0.24	0.20	0.18	0.15
	HWD-CPT-5	0.26	0.23	0.21	0.19	0.16	0.14
	HWD-CPT-6	0.31	0.26	0.25	0.21	0.19	0.16
F 5038±166	HWD-CPT-4	0.29	0.25	0.23	0.20	0.18	0.15
	HWD-CPT-5	0.26	0.23	0.21	0.18	0.16	0.14
	HWD-CPT-6	0.30	0.26	0.24	0.21	0.18	0.16

Also, for a given earthquake magnitude, the peak ground accelerations decrease as the soil age increases. For instance, when M=5, acceleration in Episode A for the HWD-CPT-4 is in the range of 0.27 to 0.32g while, with increase in the soil age in Episode F, acceleration ranges from 0.25g to 0.29g. For the cases when relative density changes more during the earthquake (i.e. more disturbance is assumed to occur when ΔDR=10% compared to ΔDR=5%) around 15% less acceleration is needed for the soil to be liquefied.

Note that the Youd and Idriss 1997, method that was used in the Leon et al. 2005, results in higher values of acceleration. The increase is greater for lower magnitudes. As

was shown for the Gapway and Sampit sites in the SCCP (Gheibi and Gassman 2014), the accelerations found from the Idriss and Boulanger 2008, method are about 50% for M=5 and 23% for M=7.5 lower than found using Youd and Idriss 1997.

It is also important to note that when correcting for both age and disturbance (using $q_{c1\ (pre)}$ and $(N_1)_{60\ (pre)}$ per Leon et al. 2005) the results for acceleration are up to 0.04g higher (based on HWD-5 data and Episodes A and B) than when a correction is made for age only (using $q_{c1\ (post)}$ and $(N_1)_{60\ (post)}$); the results for magnitude are up to 0.6 units higher (range from 5.1 to 6.6 for Episode A and from 5.0 to 6.6 for Episode B). The Energy Intensity equation (Pond and Martin 1997) used in the Energy Stress method (Hu et al. 2002b) and the Simplified Method stress boundary curves are based on field data measured after earthquakes and thus using these methods may inherently account for disturbance. However, it is unknown if time dependent mechanisms were present at these sites prior to liquefaction.

The minimum earthquake magnitude and peak ground acceleration at the time of earthquake were calculated for each episode and the range of values for all test locations are summarized in Table 4.7. As shown, an increase in the soil age leads to a decrease in the required magnitude and peak ground acceleration for liquefaction initiation at time of earthquake. For instance, the range of earthquake magnitude is 5.7 to 6.7 with the corresponding acceleration range of 0.17 to 0.3 g when the soil age is 546 years B.P.; whereas, the earthquake magnitude and accelerations are in the range of 5.2 to 6.5 and 0.16 to 0.29 when the soil age is 5038 years B.P.

The magnitudes and peak ground accelerations for the range of parameters examined in this study are compared to those previously found by Martin and Clough

1994, in Table 4.7. Assuming the whole source sand layer to be liquefied, Martin and Clough 1994, back calculated the peak ground acceleration at the Hollywood site to be 0.3g based on the Seed et al. 1984, method and 0.2g from the Ishihara 1985, method. They combined the Seed and Ishihara procedures and found a_{max} equal to 0.25g for M=7.5. In this study, when M=7.5 and the current in-situ data are used, the acceleration ranges from 0.21 to 0.3g which is in a good agreement with the accelerations from Martin and Clough 1994. For a magnitude in the range of 7 to 7.2, as was found from the Energy Stress method in this work, the corresponding acceleration ranges from 0.23 to 0.35g which is slightly greater than the accelerations for M=7.5.

Table 4.7 Estimated peak ground accelerations.

Episode, years B.P.	This study				Martin and Clough 1994			
	Age Corrected		Current		Current			
						a_{max} (g)		
	M	a_{max} (g)	M	a_{max} (g)	M	Seed et al (1984)	Ishihara (1985)	Martin Clough (1994)
A (546±17)	5.7-6.7	0.17-0.30	7 -7.2	0.23-0.35	7.5	0.3	0.2	0.25
B (1021±30)	5.5-6.5	0.17-0.30						
E (3548±66)	5.3-6.5	0.17-0.29						
F (5038±166)	5.2-6.5	0.16-0.29						

4.5 CONCLUSIONS

The earthquake magnitudes and peak ground accelerations associated with four episodes of prehistoric earthquakes at the Hollywood site in the South Carolina Coastal Plain were back analysed using in-situ geotechnical data and time-dependent procedures to correct for the age of the earthquake. For the most recent episode (546±17 years B.P.), the magnitude ranged from 5.7 to 6.7 and for the oldest earthquake (5038±166 years B.P.) was found to decrease to the range of 5.2 to 6.5. The corresponding accelerations ranged from 0.16 to 0.30g. When the age of the earthquake was not considered, the

magnitude was greater and ranged from 7 to 7.2 with corresponding peak ground accelerations of 0.23 to 0.35g which is in good agreement with earlier studies that did not consider age.

CHAPTER 5

APPLICATION OF GEOTECHNICAL DATA TO DETERMINE A CHARLESTON-AREA PREHISTORIC EARTHQUAKE MAGNITUDE

ABSTRACT

A sand blow from a paleo-earthquake was identified at Fort Dorchester, South Carolina in 2007. Geotechnical field investigations indicate the thickness of the source sand layer ranges from 1.2 to 3.1 m and the depth below the ground surface to the top of the layer ranges from 2.3 to 3.9 m. The layer is predominantly angular to subangular silty quartz sand with a fines content of 4 to 22 % and the predominant mean grain diameter of 0.18 to 0.26 mm. The geotechnical data were used with paleoliquefaction evaluation methods and three independent relations to account for soil aging to estimate the minimum magnitude and peak ground acceleration of the prehistoric earthquake. For a range of magnitude from 5.1 to 6.2, acceleration is constrained from about 0.19 to 0.40 g. When the size of the fault is considered, the magnitude is 5.6 and the acceleration ranges from 0.21 to 0.36 g.

5.1 INTRODUCTION

Paleo-seismology is being used increasingly in seismic hazard analysis. In the eastern United States, the indirect effects of prehistoric earthquakes occur as seismically-induced liquefaction features such as sand blows that are embedded in shallow, soft sediments. By dating trapped organic material in and around sand blows, it is possible to reconstruct the chronology of past earthquakes associated with liquefaction and their recurrence rates (Talwani and Schaeffer 2001; Tuttle et al. 2002).

In the South Carolina Coastal Plain (SCCP), studies over the past two decades have revealed at least seven, large, prehistoric earthquakes occurring within the last 6000 years with an average occurrence rate, based on the three most recent events, of about 500 years (Talwani and Schaeffer 2001). Using site-specific geotechnical data

(penetration resistance and shear wave velocity) at four locations in the vicinity of paleoliquefaction features in the SCCP, Hu et al. 2002a,b back-calculated the minimum magnitude and peak ground accelerations of prehistoric earthquakes. The back-calculations were based on empirical formulas developed for Holocene soils. However, the sand blows studied in the SCCP occurred in soils that are up to 250,000 years in age. When a correction was made for the age of the soils, the estimate of the minimum magnitudes of the prehistoric earthquakes associated with liquefaction features were reduced by approximately 0.9 units (Leon et al. 2005) and the associated cyclic resistance ratios (CRR) were reduced by 60% (Leon et al. 2006).

Recently, a sand blow was discovered at the Colonial Dorchester State Historical Park (Talwani, et al. 2011). The 1886 Charleston earthquake caused significant structural damage to the walls of the fort; however, field evidence indicates that liquefaction did not occur during the 1886 earthquake. Thus, the recently discovered sand blow is evidence of liquefaction that occurred during a prehistoric earthquake that pre-dates the Charleston 1886 earthquake. The site provides additional information for determining the age-related liquefaction potential of SCCP soils and the investigation of an older paleo-liquefaction feature. The purpose herein is to estimate the minimum earthquake magnitude and peak ground acceleration at a site where paleoliquefaction is known to have occurred and at which the minimum age of the sand blow is known. This is accomplished by using geotechnical field and laboratory data that have been collected at the Fort Dorchester site and by using newer methods of analysis that have a time-dependent function.

5.2 SITE DESCRIPTION

The Fort Dorchester site is located approximately eight kilometers southeast of Summerville, South Carolina and overlooks the Ashley River as shown in Figure 5.1. The Fort is situated on flat ground, and the ground slopes moderately to the west and gently to the south towards the Ashley River, slopes gently to the east, and is flat to the north. The foundation level of the fort proper sits on a bluff that is about 7.5 m higher than the Ashley River and is underlain by the Ten Mile Hill beds that were deposited during the early to middle Pleistocene (200 ka) as fluvial-estuarine deposits (Weems and Lemon 1984). Following the Charleston 1886 earthquake, significant structural damage was noted in the fort walls by Dutton 1888. Damage to the fort includes numerous fractures - the most prominent being in the north wall (up to 7 cm offset) and the south wall (up to 10 cm offset) - with left lateral offsets for both walls. The strike slip movements were associated with the 1886 Charleston earthquake (Talwani et al. 2011).

In 2007, Talwani et al. 2011 dug an E-W trench on the north side of the fort and discovered a sand blow along a ~N30°W line joining the crack in the southern wall with that in the northern wall. By comparing the location of the offset walls and the discovered sand blow with subsurface geological, seismic reflection, and seismicity data, the sand blow was interpreted to be associated with a splay of the Sawmill Branch fault. The splay is located below Fort Dorchester where a left lateral motion was observed. Talwani et al. 2011 used the water table level, geomorphological profile and absence of a sharp boundary between the sand blow and surrounding clay to estimate the age of the earthquake that created the sand blow to have occurred 3,500 years B.P. or earlier.

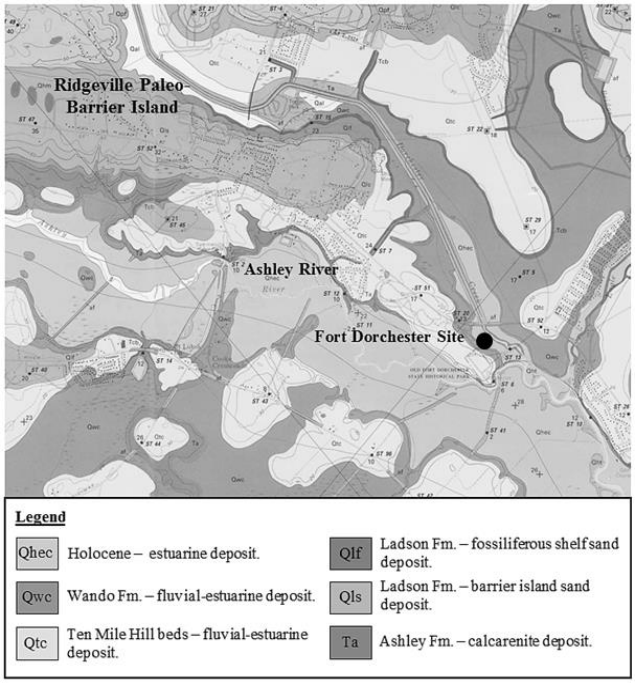

Figure 5.1 Geology of the Fort Dorchester area (adapted from Weems and Lemon, 1984).

5.3 GEOTECHNICAL FIELD AND LABORATORY DATA

The geotechnical properties of the soils were determined at the locations shown in Figure 5.2. Site exploration included four cone penetration tests (CPT-FD-1, -2, -3, and -7A) with pore pressure measurements, one piezometer (PZ-FD-1 installed at CPT-FD-7A), and a shallow trench at the sand blow. The trench was excavated to view the soil fabric of the sand blow and to obtain samples for carbon dating (Talwani et al. 2011). In addition, three vibracore soil cores (VC-1, VC-2, and VC-3) were obtained by the South Carolina Geological Survey (Doar 2007) to depths up to 7 m below ground surface. Laboratory index tests were performed on soils from each of the vibracores. The tests included grain size distribution (ASTM D422-63(2007)e2), Atterberg limits (ASTM D4318-10e1 (2010)), specific gravity (ASTM D854-14 (2014)) and soil classification (ASTM D2487-11 (2011) and D2488-09a (2009)).

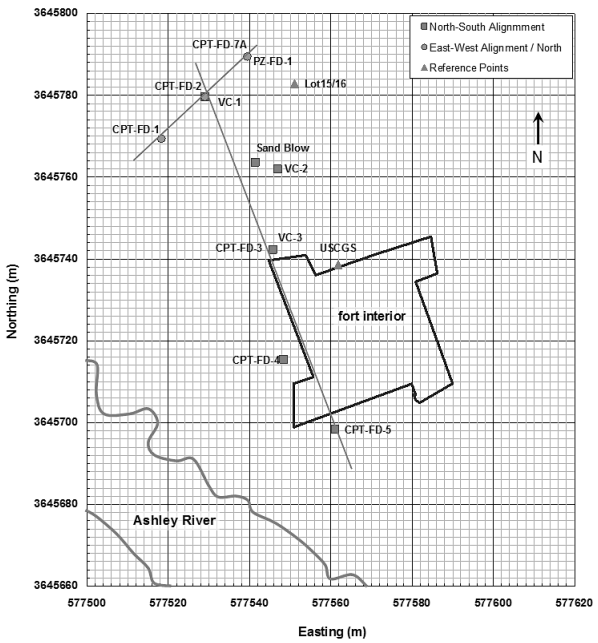

Figure 5.2 Locations of field tests and profile alignments.

The exploration alignments are oriented east-west and north-south as shown in Figure 5.2 with the respective profiles shown in Figures 5.3 and 5.4. The profiles delineate the soil strata and water table elevations as they were interpreted from the CPT tip and sleeve stresses and the vibracore logs. In the vicinity of the sand blow, the soil profile includes approximately 1.5 m of sandy clay and silty clay overlying the source sand that is about 3.0 m thick. This is underlain by approximately 1.3 m of silty and clayey sand followed by about 1.5 m of sandy silt and then by about 1.4 m of silty and clayey sand. The present-day water table measured at PZ-FD-1, which is furthest from the river, ranges from 5.2 to 5.5 m below the ground surface.

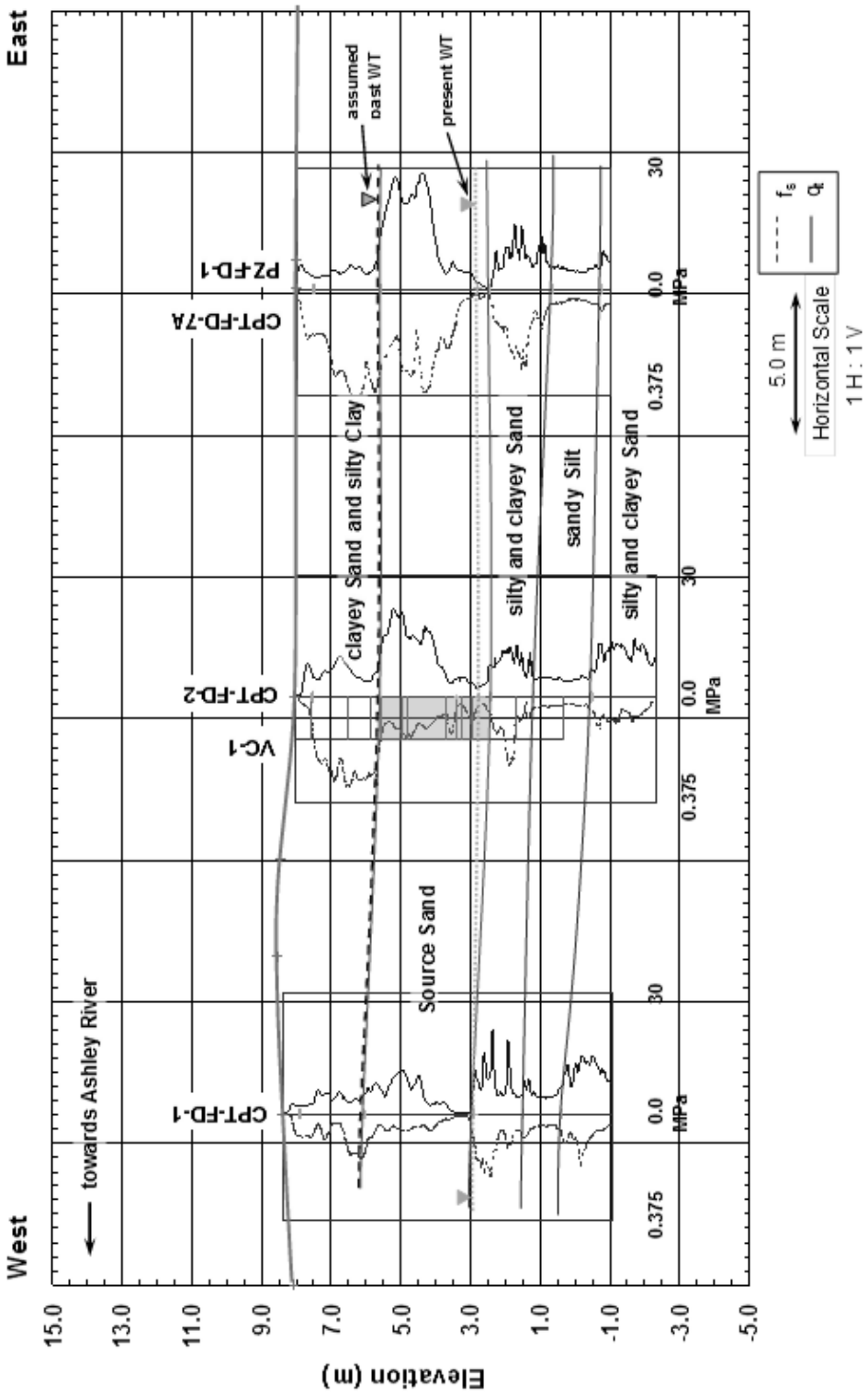

Figure 5.3 Subsurface profile of the northern East-West alignment.

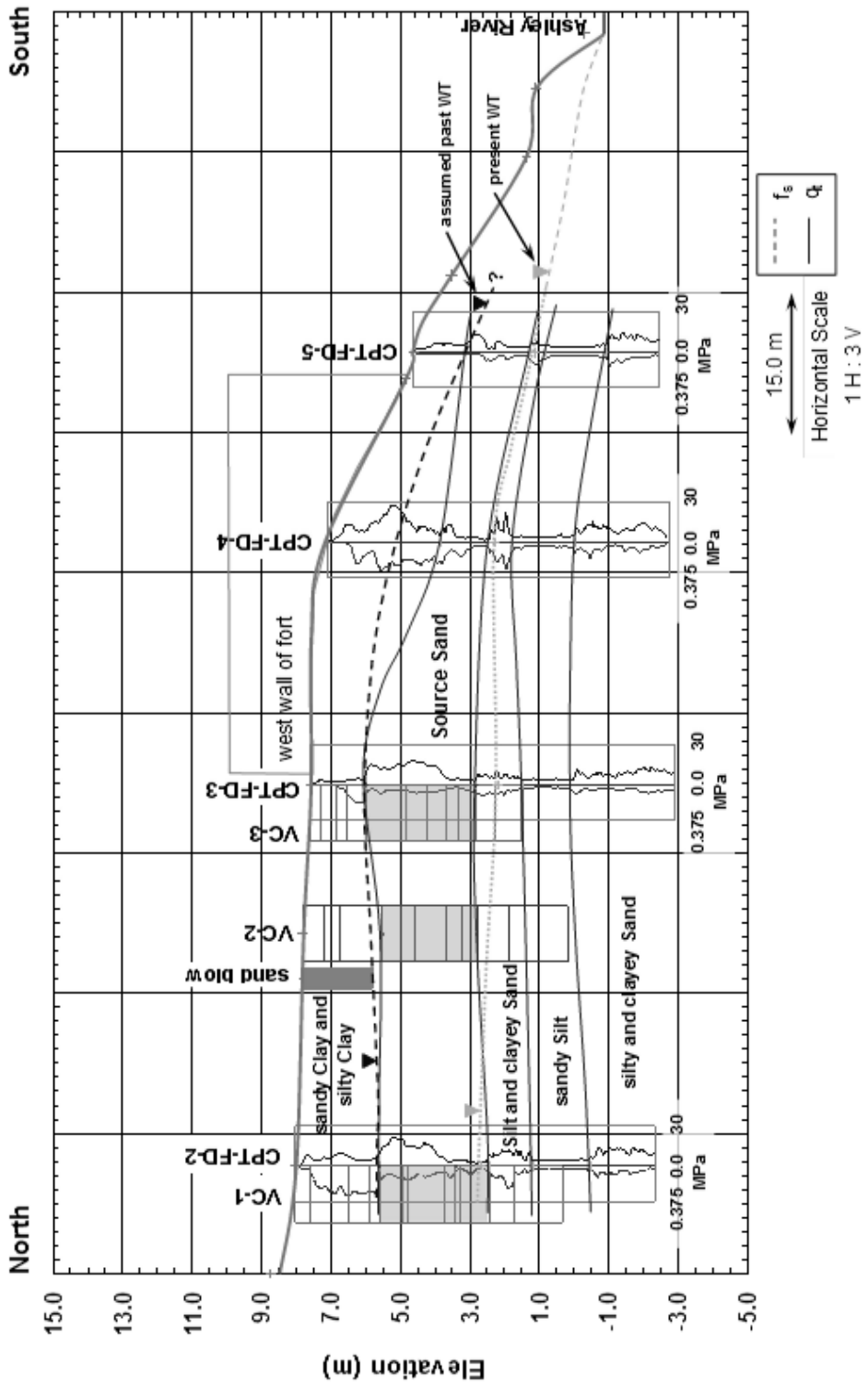

Figure 5.4 Subsurface profile of the North-South alignment.

The source sand layer was identified using the results from cone penetration tests at CPT-FD-2 and CPT-FD-3, the field logs from co-located vibracores VC-1 and VC-3 and laboratory index testing on the retrieved vibracore soil samples. Similar sand layers were also encountered in VC-2 and the CPT-FD-1, -4, -5 and -7 profiles and were used to interpret the source sand layer depth and thickness on the east-west and north-south alignments as shown in Figures 5.3 and 5.4. The source sand layer depth, elevation and thickness, and the present-day water table depth for each of the test locations are summarized in Table 5.1.

Table 5.1 Source sand layer depth, elevation, thickness, and water table depth.

Location No.	Source Sand Depth Range (m)	Ground Surface Elevation (m) above Mean Sea Level	Thickness of Source Sand (m)	Present Water Table Depth (m)
CPT-FD-1	2.3 to 5.5	8.40	3.2	5.5
CPT-FD-2	2.4 to 5.6	8.04	3.2	5.3
CPT-FD-3	1.6 to 4.8	7.59	3.2	5.4
CPT-FD-4	3.3 to 4.6	7.09	1.3	4.8
CPT-FD-5	1.5 to 3.4	4.63	1.9	3.5
CPT-FD-7A	2.4 to 5.5	8.00	3.1	5.2
VC-1	2.4 to 4.5	8.04	3.1	--
VC-2	2.3 to 5.0	7.80	3.2	--
VC-3	1.6 to 4.8	7.59	3.2	--
Sand blow	2.3 to 5.0	7.80	2.7	--

The physical characteristics of the source sand layer were obtained through laboratory testing of the vibracore samples and are summarized in Table 5.2. Figure 5.5 shows the distribution of these characteristics with depth. The soils of the source layer

range from reddish-brown mottled to tan to light gray predominantly silty sands with minor occurrences of poorly-sorted sands and clayey sands. The fines content (< #200 sieve) ranges from 4 to 22% with 70% of the samples containing 10 to 20% fines, the majority of the mean grain diameter, D_{50}, values range from 0.18 to 0.26 mm, and the soils are rapidly dilatant per ASTM D2488-09a (2009). The soils consist almost entirely of angular to subangular quartz with small to trace quantities of mica, feldspar, and opaque minerals. In the dry state, the source sand has a low strength, is friable, and when wetted exhibits a high degree of slaking. Due to core quality, the dry unit weights in Table 5.2 are approximate and the majority of values range from about 13 to 15 kN/m3. None of the samples show an indication of carbonates, but there is an indication of phosphates in soils underlying the source sand.

As shown in Figure 5.5, the source sand average fines contents for VC-1, VC-2, and VC-3 are 14%, 19%, and 13 %, respectively. The average D50 of the source sand at VC-1, VC-2, and VC-3 are 0.20 mm, 0.19 mm, and 0.21 mm, respectively. In addition to other index properties, the physical and chemical properties of the source sand indicate liquefaction-susceptibility due to a low unit weight, a lack of cementitious components, and little to no cohesion. The fines in the source sand have a liquid limit that ranges from 18 to 32 and a plasticity index from 0 to 5, which indicates the fines in the source sand have low-plasticity. The source sand is classified as SM, SP or SC-SM according to the Unified Soil Classification System. Based on criteria determined in studies by Bray and Sancio 2006, Boulanger and Idriss 2006, and Andrews and Martin 2000 concerning the effect of plastic and non-plastic fine-grained soils on liquefaction, the plasticity index, liquid limit, and moisture content indicate the source sand is susceptible to liquefaction.

Table 5.2 Source sand index test results.

Vibracore No.	Depth (m)	G_s	γ_d (kN/m^3)	D_{50} (mm)	< #200 (%)	LL	PI	USCS Soil Type
VC-1	2.82	2.70	13.8	0.17	21.6	26	5	SC-SM
VC-1	3.87	2.70	13.9	0.22	8.0	-	-	SP-SM
VC-1	4.39	2.69	-	0.48	15.3	-	-	SC-SM
VC-1	4.63	2.68	-	0.21	12.9	-	-	SC-SM
VC-2	2.37	2.68	14.4	0.23	16.1	22	0	SM
VC-2	2.90	2.69	14.3	0.17	18.3	22	0	SM
VC-2	3.36	2.70	13.5	0.16	21.6	32	4	SC-SM
VC-2	3.58	2.66	19.7	0.17	19.7	-	-	SM
VC-2	4.05	2.65	15.1	0.25	17.1	-	-	SM
VC-2	4.36	2.65	13.0	0.68	19.3	-	-	SM
VC-3	1.73	2.72	-	0.22	15.9	22	0	SM
VC-3	1.95	2.70	13.2	0.19	19.0	24	3	SM
VC-3	2.32	2.69	14.0	0.20	4.1	-	-	SP
VC-3	2.84	2.68	14.2	0.21	9.7	-	-	SP
VC-3	3.82	2.76	15.0	0.24	10.1	-	-	SP
VC-3	4.13	2.68	-	0.18	19.3	-	-	SP
VC-3	4.59	2.65	17.4	0.26	11.0	18	1	SM

G_S is the specific gravity
γ_d is dry unit weight
D_{50} is value of the particle diameter at 50% in the cumulative distribution
LL is the liquid limit
PI is the plasticity index

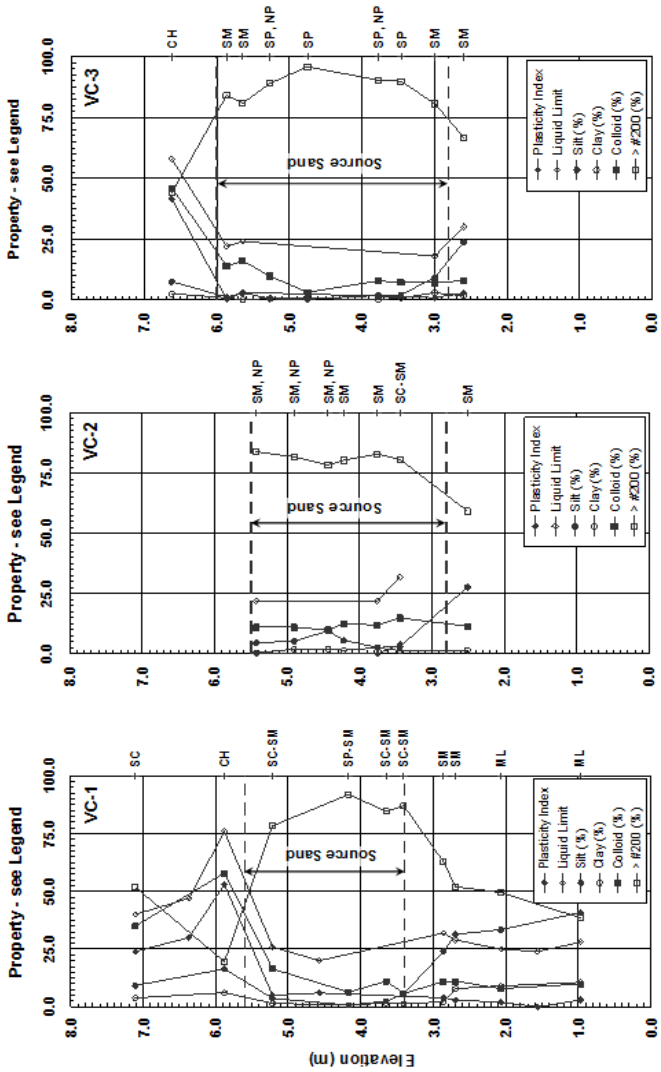

Figure 5.5 Index properties of soils from vibracores.

For CPT-FD-1, -2, -3 and -7A (the test locations encompassing the sand blow), the empirically observed upper limit for liquefaction of $(q_{c1N})_{cs}$ = 211 (Idriss and Boulanger 2008) (where $(q_{c1N})_{cs}$ is the clean sand equivalent of the normalized cone tip resistance) was used to identify the depth and thickness of the portion of the source sand layer that is susceptible to liquefaction at present. Note that the soil behavior type index from CPT data, I_c, was also less than 2.6 (Robertson and Wride 1998) within the specified liquefiable depth. The average cone tip resistance, q_c, normalized cone tip

resistance, q_{c1N}, sleeve stress, f_s, and friction ratio, F_r, within the portion of the source sand layer susceptible to liquefaction are presented in Table 5.3. The average corrected, normalized blow counts, $(N_1)_{60}$, derived from Lunne et al. 1997, are also shown. For the four test locations, the average q_c ranges from 5 to 8 MPa and the corresponding q_{c1N} ranges from 75 to 103. The average f_s range from 45 to 122 kPa and the average F_r ranges from 1.03 to 2.25. The derived $(N_1)_{60}$ ranges from 16 to 20.

The source sand is about 200,000 years old (McCartan et al. 1984; Weems and Lemon 1984) and is part of the Ten Mile Hill beds that were deposited during the early to middle Pleistocene as fluvial/lagoonal and possibly beach deposits as noted from inspection of the vibracores.

Table 5.3 CPT results for the source sand layer susceptible to liquefaction.

CPT No.	Liquefaction Susceptible Layer		q_c (MPa)	q_{c1N}	f_s (kPa)	F_r [(1)] (%)	(N_{60}) [(2)]	$(N_1)_{60}$
	Depth (m)	Thickness (m)						
FD-1	2.3 to 5.4	3.1	5 (0.3 to 11)	87 (21 to 151)	45 (8 to 153)	1.5 (0.46 to 7)	11 (2 to 19)	16 (3 to 27)
FD-2	3.3 to 5.56	2.25	8 (2 to 16)	103 (31 to 205)	73 (25 to 134)	1.21 (0.56 to 3.82)	15 (5 to 28)	20 (7 to 36)
FD-3	3.6 to 4.8	1.2	6 (3 to 14)	86 (50 to 192)	50 (26 to 87)	1.03 (0.51 to 2.25)	11 (8 to 24)	17 (11 to 34)
FD-7A	3.9 to 5.25	1.35	5.5 (2 to 17)	75 (23 to 214)	122 (21 to 288)	2.25 (0.7 to 5.7)	12 (4 to 33)	16 (6 to 41)

[(1)]Derived from $F_r = \frac{F_s}{(q_t - \sigma_{v0})} * 100\%$

[(2)]Derived from CPT-SPT correlation (Lunne et al. 1997); $\frac{q_c/P_a}{N_{60}} = 8.5(1 - \frac{I_c}{4.6})$

Note: q_c is the "measured cone resistance";
q_{c1N} is the "normalized cone resistance": $q_{c1N} = q_{c1}/P_a$; $q_{c1} = C_N q_c$

5.4 METHODOLOGY

The field tests provide the in situ soil properties that are used to estimate the minimum magnitude and peak ground acceleration of the prehistoric earthquake that created the newly-discovered sand blow. The current measurements of the source sand properties (q_{c1}, $(N_1)_{60}$ and CRR) were corrected for time dependent mechanisms (i.e. "aging") prior to back-calculating the earthquake magnitude and peak ground acceleration (see Olson et al. 2005 for a summary of methods to back-calculate earthquake magnitudes and peak ground accelerations and uncertainties associated with those methods). In this way, the empirical correlations for liquefaction evaluation (e.g. the cyclic stress method originally developed by Seed and Idriss 1971) applicable for young or freshly deposited soils can be used for the older soil deposits (see Leon et al. 2005, 2006).

5.4.1 Accounting for Soil Aging

While aging is known to change the geotechnical properties of soils over time (Baxter and Mitchell 2004; Mitchell and Solymar 1984; Schmertmann 1991), the site-specific mechanisms and their significance at the Fort Dorchester site is uncertain. Therefore, three different independent methods were used to account for aging: 1) the methodology of Leon et al. 2005 using aging relations offered by Mesri et al. 1990, 2) the methodology of Leon et al. 2005 using aging relations by Kulhawy and Mayne 1990, and 3) the methodology of Hayati and Andrus 2009. In the Leon et al. 2005 methodology (with Mesri et al. 1990 or Kulhawy and Mayne 1990), the aging correction is applied to the current measurements of penetration resistance (q_{c1} or $(N_1)_{60}$) to find the post-liquefaction penetration resistance; whereas, in the Hayati and Andrus 2009

methodology, the aging correction is applied to the current CRR (which is a function of the current penetration resistance). Each of these three methods is used separately to back-calculate the earthquake magnitudes and peak ground accelerations. Similar results from different methods yield greater confidence.

The relation offered by Mesri et al. 1990 is based on an observed increase in penetration resistance after ground densification by blasting, vibrocompaction, and dynamic compaction in clean sands and is a function of time, *t*, the change in relative density, ΔD_R, and the ratio of the secondary compression index to the compression index, C_α/C_c. For the work herein, the post-earthquake tip resistance, $q_{c1\ (post)}$ and blow count, $(N_1)_{60\ (post)}$ are obtained using the current penetration resistance and this relation $[q_{c1}/q_{c1(post)}=(N_1)_{60}/(N_1)_{60(post)}=(t/t_R)^{C_D C\alpha/Cc}]$ where $t_R= 0.082$ yrs, $C_\alpha/C_c=0.02$ and $C_D=5.5$ to 7.0 per Leon et al. 2005.

The Kulhawy and Mayne 1990 relation is based on collected SPT blow count and relative density data as a function of soil particle size for aged fine to medium overconsolidated sands from four geologic periods. A correction factor, $C_A=1.2+0.5\log(t/100)$, was proposed to describe the influence of aging (*t*) on the $(N_1)_{60}/D_r^2$ ratio and is used herein to relate the current penetration resistance to the post-earthquake values of penetration resistance, $[q_{c1}/q_{c1(post)}=(N_1)_{60}/(N_1)_{60(post)}= C_A]$.

Note that in previous recent studies using the Leon et al. 2005 method (Gheibi and Gassman 2014 and Gheibi and Gassman 2015) the disturbance correction proposed by Leon et al. 2005 was used to account for post-liquefaction re-consolidation (primary) and densification (or loosening) to obtain "pre-earthquake" data. The disturbance correction (i.e. the difference between the post-earthquake (after post-liquefaction re-

consolidation (primary)) and pre-earthquake (before the earthquake) resistance values) is not used herein since the Energy Intensity equation (Pond and Martin 1997) and the empirical relations between CRR and in situ measurements are almost exclusively based on field data measurements after earthquakes, not prior to earthquakes and thus inherently account for disturbance.

The methodology of Hayati and Andrus 2009 uses an updated liquefaction resistance correction factor, $K_{DR,}$ given in Equation 5.1, where *t* is the time since initial deposition or critical disturbance in years, to find CRR_k (the deposit resistance-corrected CRR) from Equation 5.2. K_{DR} is based on data from over 30 sites in five countries and is used to account for the influence of age, cementation and stress history on CRR.

Two methods were used to account for aging: the methodology of Leon et al. 2005 and the methodology of Hayati and Andrus 2009. The methodology of Leon et al. 2005 was used to modify the current measurements of cone penetration tip resistance, blow count, and cyclic resistance ratio for the effect of aging. The Hayati and Andrus 2009 methodology was used to back-calculate the CRR at the time of earthquake.

$$\mathrm{K_{DR}} = 0.13.\log(\mathrm{t}) + 0.83 \qquad (5.1)$$

$$\mathrm{CRR_K} = \mathrm{CRR}.\,\mathrm{K_{DR}} \qquad (5.2)$$

To calculate CRR_K, the $(N_1)_{60}$ in Table 5.3 were first modified for the effect of fines content to obtain $(N_1)_{60cs}$ and then used with the following equation from Idriss and Boulanger 2008 to calculate the CRR:

$$CRR_{M=7.5,\sigma'_{vc}=1} = \exp\left\{\frac{(N_1)_{60cs}}{14.1} + \left(\frac{(N_1)_{60cs}}{126}\right)^2 - \left(\frac{(N_1)_{60cs}}{23.6}\right)^3 + \left(\frac{(N_1)_{60cs}}{25.4}\right)^4 - 2.8\right\} \quad (5.3)$$

where $CRR_{M=7.5,\sigma'vc=1}$ is the equivalent CRR for the reference values of $M=7.5$ (σ'_{vc} $=1atm$) and $(N_1)_{60cs}$ is the equivalent clean-sand number of blow counts. This CRR is then used with Equations 5.1 and 5.2 to find CRR_K. The Hayati and Andrus 2009 method was also used to back-calculate $(N_1)_{60\ (post)}$, by solving Equation 5.3 for $(N_1)_{60cs}$ ($= (N1)_{60\ (post)}$) when $CRR_{M=7.5,\sigma'vc=1} = CRR_K$.

The source sand at the Fort Dorchester site is about 200,000 years old, and times of 3500, 6000 and 10,000 years B.P. were selected to represent possible ages of formation of the sand blow. These times were selected based on the work of Talwani et al 2011, with an age of 10,000 years being an upper bound, and used to obtain the corrected values of the source sand properties representative of the time of the earthquake for each of the three methods.

5.4.2 Evaluation of Peak Ground Acceleration

An estimate of the peak ground acceleration at the surface, a_{max}, was found using the following equation for the cyclic stress ratio for a given earthquake ($CSR_{M,\sigma'vc}$) given by Idriss and Boulanger 2008:

$$CSR_{M,\sigma'_{vc}} = CRR_{M=7.5,\sigma'_{vc}=1} * MSF * K_\sigma = 0.65 * r_d * \left(\frac{\sigma_{v0} * a_{max}}{\sigma'_{v0} * g}\right) \quad (5.4)$$

where σ_{vo} is the vertical stress and σ'_{vo} is the vertical effective stress at depth z, MSF is the magnitude scaling factor used to consider earthquakes with magnitudes other than 7.5,

and r_d is the reduction factor that considers the flexibility of soil column. A coefficient of 0.65 is applied to approximate an average cyclic stress during earthquake shaking. K_σ is the overburden correction factor which is a function of the in situ penetration resistance ($(N_1)_{60}$, or $(q_{c1N})_{cs}$). The proposed relations of K_σ, MSF and r_d of Idriss and Boulanger 2008 were used in this study.

To back-calculate a_{max} using Equation 5.4, $CRR_{M=7.5,\sigma'vc=1}$, was found using the Idriss and Boulanger 2008 relation between $CRR_{M=7.5,\sigma'vc=1}$ and cone penetration test results. Note that previous work by Leon et al. 2005 used the relation of Youd and Idriss 1997. The Idriss and Boulanger 2008 relation was updated to include an expanded case history database of liquefaction/no liquefaction sites and adjusted to reflect the number of equivalent cycles that had occurred up to the time when liquefaction was triggered for cases where liquefaction occurs early in shaking. The relation was also modified to account for the effect of non-plastic fines on the liquefaction resistance, thus is a function of $(q_{c1N})_{cs}$, and is given as follows:

$$\mathrm{CRR}_{\mathrm{M=7.5},\sigma'_{\mathrm{vc}}=1} = \exp\left\{\frac{(\mathrm{q_{c1N}})_{cs}}{540} + \left(\frac{(\mathrm{q_{c1N}})_{cs}}{67}\right)^2 - \left(\frac{(\mathrm{q_{c1N}})_{cs}}{80}\right)^3 + \left(\frac{(\mathrm{q_{c1N}})_{cs}}{114}\right)^4 - 3\right\} \qquad (5.5)$$

Note that for the calculations of vertical effective stress, a high stand water table was assumed at the time of the prehistoric earthquake as shown in Figures 5.3 and 5.4. This water level corresponds to the top of the source sand layer assuming complete submergence would have been necessary for the occurrence of liquefaction (see Talwani et al. 2011 for discussion of prehistoric water table level at the site).

5.4.3 Evaluation of Magnitude

Olson et al. 2005 suggest using a regional magnitude bound relationship and the distance from the energy center to the most distal site of liquefaction to estimate magnitude; however, for the discovered sand blow herein that has been associated with a splay of the Sawmill Branch fault (Talwani et al. 2011), the most distal site of liquefaction is unknown. Therefore, an estimate of the minimum earthquake magnitude was found using the following relationship between the seismic intensity at the site in terms of magnitude (M) and hypocentral distance (R_h) in km with the liquefaction susceptibility represented by $(N_1)_{60}$:

$$M = \frac{2}{3} * \log\left[1.445 * {R_h}^2 * (N_1)_{60}^{6.06}\right] \quad (5.6)$$

The relation was derived by Hu et al. 2002b based on the energy-stress method of Obermeier and Pond 1999. The seismicity associated with the fault (see Figure 5.2 in Talwani et al. 2011) suggests a hypocentral distance ranging from four to ten kilometers. $(N_1)_{60}$ values were obtained via the Lunne et al. 1997 correlation to CPT data. The energy-stress method of Obermeier and Pond 1999 is assumed to be applicable for world-wide tectonic conditions, but it was also recognized the magnitude could be constrained further knowing localized information such as stress drop, focal depth, the degree of liquefaction susceptibility on the extent of liquefaction, and the attenuation of bedrock shaking.

Work by Wells and Coppersmith 1994, based on a study of over 148 earthquakes, was also used to estimate the earthquake magnitude given the rupture length and rupture

area of a slip-type fault such as that found near Fort Dorchester. The earthquake magnitude (M) is related to the subsurface rupture length (RLD):

$$M = 4.38 + 1.49.\log(RLD) \quad (5.7)$$

and the fault rupture area (RA):

$$M = 4.07 + 0.98.\log(RA) \quad (5.8)$$

Note there is no difference between intraplate settings (compressional) or plate boundary (compressional and or extensional) settings in these parameters. Wells and Coppersmith 1994 state: "Separating the data according to extensional and compressional tectonic environments neither provides statistically different results nor improves the statistical significance of the regressions."

5.5 RESULTS

5.5.1 Age-Corrected In-Situ Data

The average $q_{c1\ (post)}$ and $(N_1)_{60\ (post)}$ for the estimated sand blow ages of 3500, 6000 and 10,000 years found using the data (q_{c1N} and $(N_1)_{60}$) in Table 5.3 and the Leon et al. 2005 methodology (Mesri et al. 1990 and Kulhawy and Mayne 1990 relations) at the four CPT locations are summarized in Table 5.4. The results show that the age-corrected values of tip resistance are less than current measurements, thus showing the increase in soil resistance with time. Furthermore, the age-corrected q_{c1} and $(N_1)_{60}$ using Mesri et al. 1990 are more than 50% lower than the corresponding values from Kulhawy and Mayne

1990. Also, there is a negligible effect on the values of $q_{c1(post)}$ and $(N_1)_{60(post)}$ for the age of the sand blow ranging from 3500 to 10,000 years.

Table 5.4 Post-earthquake values of q_{c1} and $(N_1)_{60}$ and CRR for the source sand layer.

CPT No.	Sand blow Age (yrs)	Correction for Age (Post-Earthquake)							
		Mesri et al. (1990)			Kulhawy and Mayne (1990)			Hayati and Andrus (2009)	
		q_{c1} (MPa)	$(N_1)_{60}$	CRR_a^{*} (CPT)	q_{c1} (MPa)	$(N_1)_{60}$	CRR_a^{*} (CPT)	CRR_k^{+} (SPT)	CRR_k° (CPT)
FD-1	3500	2	4	0.07	7	13	0.15	0.18	0.16
	6000	2	4	0.07	7	13	0.15	0.17	0.15
	10000	2	4	0.07	7	13	0.15	0.17	0.15
FD-2	3500	3	5	0.07	8	15	0.16	0.17	0.15
	6000	3	5	0.07	8	15	0.16	0.18	0.15
	10000	2	5	0.07	8	15	0.15	0.18	0.14
FD-3	3500	2	4	0.07	7	13	0.13	0.19	0.13
	6000	2	4	0.07	7	13	0.13	0.18	0.13
	10000	2	4	0.07	7	13	0.13	0.19	0.12
FD-7A	3500	2	4	0.06	6	13	0.12	0.14	0.11
	6000	2	4	0.06	6	13	0.12	0.14	0.11
	10000	2	4	0.06	6	12	0.12	0.14	0.10

* Cyclic resistance ratio obtained from CPT results and Leon et al. (2005) methodology.
+ Cyclic resistance ratio obtained from SPT results and Hayati and Andrus (2009) methodology.
° Cyclic resistance ratio obtained from CPT results and Hayati and Andrus (2009) methodology.

The post-earthquake CRR values are also shown in Table 4. $CRR_{a\ (CPT)}$ was obtained using Equation 5.5 with the post-earthquake (age-corrected) values of tip resistance obtained from both the Mesri et al. 1990 and Kulhawy and Mayne 1990 age relations. $CRR_{k\ (CPT)}$ was obtained using Equation 5.5 with the current measured values of tip resistance and then corrected for age using Equation 2. Similarly $CRR_{k\ (SPT)}$ was obtained using Equation 5.3 with the current measured SPT values and then corrected for age using Equation 5.2. As shown, the post-earthquake CRR values calculated using CPT

tip resistance and the Hayati and Andrus 2009 age relation ($CRR_{k\ (CPT)}$) from Equation 5.2 are in a good agreement with those obtained using Kulhawy and Mayne 1990 ($CRR_{a\ (CPT)}$), but are not in agreement with those obtained using Mesri et al. 1990.

5.5.2 Accelerations

The a_{max} found using Equation 5.4 and the CRR values in Table 5.4 for each of the three aging relations are summarized for earthquake magnitudes M=5, M=5.6, M=6 and M=7 in Table 5.5. For the larger earthquake magnitudes, as expected, less acceleration is required for liquefaction initiation. For example, using the Kulhawy and Mayne 1990 age relation for FD-1 results in a peak ground acceleration of 0.23g for M=7 compared to 0.38g for M=5. Also, for a given earthquake magnitude at each CPT location, acceleration values obtained using the aging relations offered by Hayati and Andrus 2009 and Kulhawy and Mayne 1990 are in a good agreement and are about twice those obtained from the Mesri et al. 1990 relation. Similar to the trends shown for CRR in Table 5.4, a_{max} decreases as the age of the sand blow increases. However, for the selected range of sand blow ages (3500 to 10,000 years B.P.), the decrease is small (0.01g).

Note that the Youd and Idriss 1997 method that was used in Leon et al. 2005 results in higher values of acceleration than the Idriss and Boulanger 2008 method used herein. The increase is greater for lower magnitudes. As was shown for the Gapway and Sampit sites in the SCCP (Gheibi and Gassman 2014), the accelerations found from the Idriss and Boulanger 2008 method are about 50% lower for M=5 and 23% lower for M=7.5 than found using Youd and Idriss 1997.

Table 5.5. Peak ground acceleration for source sand layer.

Location	Sand blow Age (yrs)	Peak Ground Acceleration (g)											
		M=5			M=5.6			M=6			M=7		
		Mesri et al. (1990)	Kulhawy and Mayne (1990)	Hayati and Andrus (2009)	Mesri et al. (1990)	Kulhawy and Mayne (1990)	Hayati and Andrus (2009)	Mesri et al. (1990)	Kulhawy and Mayne (1990)	Hayati and Andrus (2009)	Mesri et al. (1990)	Kulhawy and Mayne (1990)	Hayati and Andrus (2009)
FD-1	3500	0.18	0.38	0.40	0.16	0.34	0.36	0.15	0.31	0.33	0.11	0.23	0.25
	6000	0.18	0.38	0.40	0.16	0.34	0.36	0.14	0.30	0.32	0.11	0.23	0.24
	10000	0.17	0.37	0.40	0.16	0.33	0.36	0.14	0.30	0.32	0.11	0.23	0.24
FD-2	3500	0.15	0.38	0.36	0.14	0.34	0.32	0.12	0.31	0.29	0.09	0.23	0.22
	6000	0.15	0.38	0.35	0.14	0.34	0.32	0.12	0.30	0.28	0.09	0.23	0.21
	10000	0.15	0.37	0.34	0.13	0.33	0.31	0.12	0.30	0.28	0.09	0.22	0.21
FD-3	3500	0.13	0.26	0.25	0.12	0.24	0.23	0.10	0.21	0.20	0.08	0.16	0.15
	6000	0.13	0.26	0.25	0.12	0.24	0.22	0.10	0.21	0.20	0.08	0.16	0.15
	10000	0.12	0.26	0.24	0.11	0.23	0.22	0.10	0.21	0.19	0.08	0.16	0.15
FD-7	3500	0.14	0.27	0.24	0.13	0.24	0.22	0.11	0.22	0.19	0.09	0.16	0.15
	6000	0.14	0.27	0.24	0.13	0.24	0.21	0.11	0.21	0.19	0.08	0.16	0.14
	10000	0.14	0.26	0.23	0.12	0.24	0.21	0.11	0.21	0.19	0.08	0.16	0.14

5.5.3 Earthquake Magnitude

The estimated minimum magnitudes obtained from the Energy Stress method are shown in Table 5.6 for a range of hypocentral distances from 4 km to 10 km. The magnitudes for the Energy Stress Method (Equation 6) range from 4.0 to 4.8, 5.5 to 6.2, and 5.1 to 6.1 using the Mesri et al. 1990, Kulhawy and Mayne 1990, and Hayati and Andrus 2009 relations for age, respectively. These values were found using the age corrected $(N_1)_{60(post)}$ in Table 5.4 for a sand blow age of 3500 years. For a sand blow age of 6000 or 10,000 years, the magnitudes reduce by up to 0.1 and 0.2 units, respectively. In general, the magnitudes found using the Mesri et al. 1990 relation for age are about 1 to 1.6 units lower than those found using the Kulhawy and Mayne 1990 and Hayati and Andrus 2009 methods which are in good agreement (Hayati and Andrus 2009 results are up to 0.5 units lower than Kulhawy and Mayne 1990).

Table 5.6 Earthquake Magnitude (M) for the age of 3500 years B.P.

Location	Energy Stress Method											
	Mesri et al. (1990)				Kulhawy and Mayne (1990)				Hayati and Andrus (2009)			
	Rh=4 km	Rh=6 km	Rh=8 km	Rh=10 km	Rh=4 km	Rh=6 km	Rh=8 km	Rh=10 km	Rh=4 km	Rh=6 km	Rh=8 km	Rh=10 km
FD-1	4.3	4.5	4.7	4.8	5.6	5.9	6.0	6.2	5.6	5.8	6.0	6.1
FD-2	4.1	4.3	4.5	4.6	5.7	5.9	6.1	6.2	5.2	5.4	5.6	5.7
FD-3	4.2	4.4	4.6	4.7	5.6	5.9	6.0	6.2	5.4	5.6	5.8	5.9
FD-7A	4.0	4.2	4.4	4.5	5.5	5.7	5.9	6.0	5.1	5.3	5.5	5.6

Note for the Energy Stress Method: 1) the age of the sand blow (a difference of 2500 or 6500 yrs) has a negligible effect (0.l to 0.2 unit) on the back-calculated magnitude and 2) the R_h (a difference of 6 km for depths of 4 km to 10 km) causes a maximum 0.6 units change. Also, consideration must be given to the fact that analyses performed herein use $(N_1)_{60}$ values that have been derived from CPT data via Lunne et al. 1997.

Talwani et al. 2011 found the earthquake to have occurred on a splay of the Sawmill Branch fault with a seismological depth range of ~6 km *i.e.*, a maximum rupture area of ~36 km^2". Thus, the Wells and Coppersmith 1994 method using the rupture length and rupture area estimated to be 6 km and 36 km^2 respectively, correlates to an estimated magnitude of 5.6. This result is independent of the in-situ soil properties and disconnected from the aging factor.

For a range of magnitudes from M=5.1 to M=6.2 (based on the good agreement with Kulhawy and Mayne 1990 and Hayati and Andrus 2009 in Tables 5.5 and 5.6), it appears that a_{max} is constrained from about 0.19 to 0.40 g. Furthermore, using the estimated earthquake magnitude of 5.6 determined from Wells and Coppersmith 1994, a_{max} ranges from 0.21 to 0.36 g.

5.6 SUMMARY AND CONCLUSIONS

Field investigations using cone penetration tests with pore pressure measurements, vibracore logs, a shallow trench, and a piezometer have been performed at the Fort Dorchester site. The cone penetration test results and the vibracore logs were used to delineate the soil stratigraphy and identify the soils that are most susceptible to liquefaction. The thickness of the liquefiable sand layer was found to range from 1.2 to 3.1 m with the top of the layer located 2.3 to 3.9 m below the ground surface. Consistent with the findings at four paleoliquefaction sites in the SCCP from Hu et al. 2002a, b, the geotechnical engineering properties of the liquefiable sand at the Fort Dorchester site indicate that it was susceptible to prehistoric liquefaction with a water table at the top of the source sand layer.

The accelerations found per Idriss and Boulanger 2008 using the in situ geotechnical data with the Mesri et al. 1990 relation for age are about one-half of the values determined using the Kulhawy and Mayne 1990 or Hayati and Andrus 2009 relations for age. The magnitudes determined using the Energy Stress Method and the three relations for age yield a range from 4.0 to 6.2; however, a range of 5.1 to 6.2 is more likely given the agreement with the results found using the Kulhawy and Mayne 1990 and Hayati and Andrus 2009 relations. When the size of the fault is considered via Wells and Coppersmith 1994, an approach independent of the in-situ soil properties, the maximum magnitude is 5.6 and the corresponding peak ground acceleration ranges from 0.21 to 0.36 g.

CHAPTER 6

USING REGRESSION MODEL TO PREDICT CYCLIC RESISTANCE RATIO AT SOUTH CAROLINA COASTAL PLAIN (SCCP)[3]

[3] Gheibi, E., Gassman, S. L., Tavakoli, A. (2014). Advanced Analytics (distributer), Paper, DOI: 10.13140/2.1.4893.4081. Reprinted here with permission of publisher.

ABSTRACT

Seismically-induced liquefaction is one of the most hazardous geotechnical phenomena from earthquakes that can cause loss of life and devastating damages to infrastructures. In 1964, a 7.5 Richter magnitude earthquake in Nigata, Japan destroyed numerous buildings and structures and initiated studies to understand soil liquefaction. One major outcome of these studies was the development of correlations that are used to determine liquefaction resistance of soil deposits from in-situ soil indices. These relations are based on Holocene soils (<10,000 years old) while the sand deposits encountered in the South Carolina Coastal Plain (SCCP) are older than 100,000 years. In-situ and geotechnical laboratory data that have been obtained in the vicinity of sand blows which date back to 6000 years ago at Fort Dorchester, Sampit, Gapway, Hollywood and Four Hole Swamp sites in the SCCP have been used with methodology that considers the effect of aging on the liquefaction potential of sands to back analyze the cyclic resistance ratio at the time of the prehistoric earthquake. For this paper, descriptive statistics, including frequency distribution for categorical variables and summary statistics for continuous variables, was carried out using this data. Statistical analyses using regression models were performed for selected variables on the calculated values of cyclic resistance ratio (dependent variables). SAS ® 9.4 was used to analyze the data. The main finding is the significant correlation between equivalent clean sand tip resistance and the cyclic resistance ratio at the time of earthquake.

6.1 INTRODUCTION

The South Carolina Coastal Plain (SCCP) experiences infrequent earthquakes and paleoliquefaction analysis plays an important role in studying the paleoseismicity of this

region. Studies performed by Talwani and Schaeffer 2001, show that at least seven, large, prehistoric earthquakes have occurred within the last 6000 years in the SCCP with an average occurrence rate, based on the three most recent events, of about 500 years. Hu et al. 2002a and 2002b, used site-specific geotechnical data (penetration resistance and shear wave velocity) and back analysed the earthquake magnitude, M, and peak ground acceleration, a_{max}, at four sites in the South Carolina Coastal Plain. Back analyses were based on the empirical correlations presented in Youd and Idriss 1997. These relations are based on the studies of recent earthquakes in Japan, China and the west coast region of the U.S. where the soil deposits are of Holocene age (<10,000 years old). Leon et al. 2005, developed a methodology that considered the effect of age in soil deposits and back calculated magnitudes, cyclic resistance ratio, CRR, and peak ground accelerations for the sand deposits in the SCCP that are older than 100,000 years. Neglecting the effect of aging resulted in a 60% underestimation of CRR (Leon et al. 2006).

Gheibi and Gassman 2014, used the Idriss and Boulanger 2008, methodology to back calculate the magnitude, maximum acceleration, and CRR at the Sampit and Gapway sites and showed that using the newer method reduces the acceleration values about 50% for M=5 and 23% for M=7.5 for the Gapway and Sampit sites when compared to using Seed's original method.

Empirical liquefaction potential assessment correlations are developed based on analyzing experimental studies and case studies. Running statistical analyses on the smaller liquefaction data sets leads to extend meaningful correlations that can be used as a larger data base to predict liquefaction at the sites where complete sets of data are not available. Therefore, the purpose of this paper is to perform regression analysis on the

current measurements of field test data (CPT tip resistance values) to predict the cyclic resistance ratio of the soil at the time of prehistoric earthquake.

6.2 SITE STUDIED

Given the importance of evaluating liquefaction potential in the SCCP, in-situ and geotechnical laboratory tests have performed in the vicinity of sand blows which date back to 6000 years ago at the five sites of Fort Dorchester, Sampit, Gapway, Hollywood and Four Hole Swamp. Cone Penetration Tests, CPT, and Standard Penetration Tests, SPT, were carried out at three to four test locations at each site. Figure 6.1 indicates the location of these five sites.

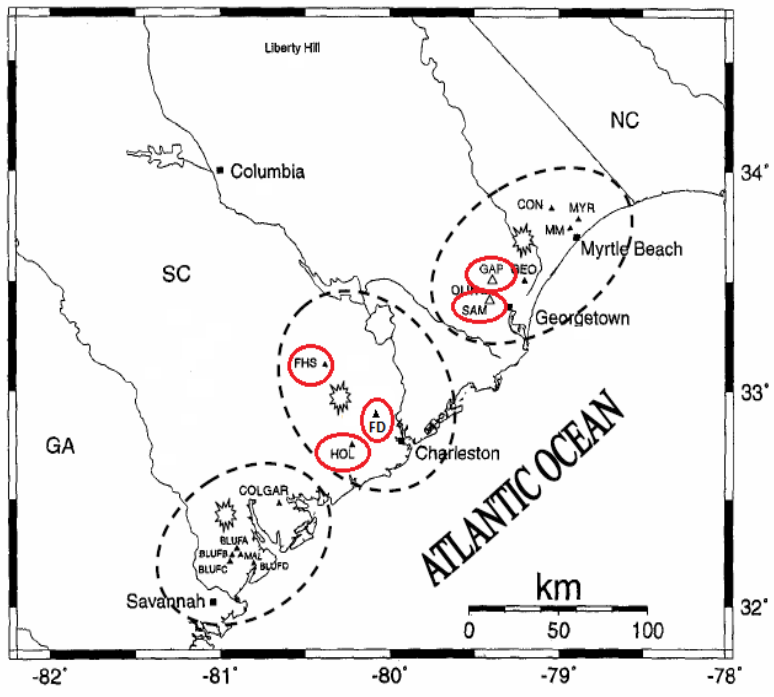

Figure 6.1 Locations of paleoliquefaction features in South Carolina Coastal Plain.

The in-situ data used in this study were obtained from CPT and SPT performed at the site. The geotechnical laboratory tests were also performed on the samples obtained from SPT split spoon sampler to characterize the soil and obtain the fines content. The soil profile was obtained using the field and laboratory test results.

The source sand layer is the layer most prone to liquefaction and was determined using the interpretation of SPT blow counts, CPT tip resistance and laboratory test results. Two scenarios were considered for the depth of source sand layer at Four Hole Swamp. In the first case (A) the source sand layer was assumed to be deeper than the other case (B). In this study, CPT tip resistance data were analysed to calculate the CRR. Table 6.1 indicates the average value of cone penetration tip resistance in the source sand layer at each test location.

Talwani and Schaeffer 2001 found the paleoliquefaction features in freshly cut drainage ditches and described the calibrated ages for the sand blow formations range from 500 to 11,000 years before present and have been associated with liquefaction episodes in SCCP. Ages of sand deposits based on these episodes at all test locations are categorized to four scenarios and are presented in Table 6.2.

6.3 METHODOLOGY

The methodology of Leon et al., 2005, was used to obtain the cyclic resistance ratio at the time of earthquake. In this method, empirical correlations for liquefaction evaluation which are applicable for young or freshly deposited soils can be used for the older soil deposits if the age corrected parameters (cone penetration tip resistance, q_{c1}, at the time of earthquake) are applied.

Table 6.1 Average values of current tip resistance in the source sand layer.

Test Location	q_c (Mpa)
FD-1	5
FD-2	11.2
FD-3	11.3
FD-7	12.8
SAM-1	6.8
SAM-2	6
SAM-3	7.7
GAP-1	3.8
GAP-2	6.6
GAP-3	2.4
HWD-4	6.4
HWD-5	5.5
HWD-6	6.9
FHS-1 (A)	3.6
FHS-2 (A)	6.6
FHS-3 (A)	4.9
FHS-1 (B)	5.7
FHS-2 (B)	9.9
FHS-3 (B)	6.8

Post and pre-earthquake values of tip resistance ($q_{c1\ (post)}$, $q_{c1\ (pre)}$) for the discussed ages and episodes are obtained using two different approaches. Approach 1 is based on the relations offered by Mesri et al. 1990, for both the age and disturbance correction and Approach 2 is based on work by Kulhawy and Mayne 1990, for the age correction and Seed, 1988, for the disturbance correction. Change in relative density of the soil (ΔD_R) is considered to be 5% and 10% between the pre- ($q_{c1\ (pre)}$) and post- ($q_{c1\ (post)}$) earthquake state.

Pre-earthquake values of tip resistance at depth of soil are corrected for the effect of fines content in soil using Equation 6.1 and then are applied in Equation 6.2 to obtain CRR using the Idriss and Boulanger 2008, approach.

Table 6.2 Age of sand blows at each test location (adapted from Talwani and Schaeffer 2001).

Test Location	t (years before present)			
	First Scenario	Second Scenario	Third Scenario	Forth Scenario
FD-1	3,500	5,000	–	–
FD-2	3,500	5,000	–	–
FD-3	3,500	5,000	–	–
FD-7	3,500	5,000	–	–
SAM-1	1,021	–	–	–
SAM-2	450,000	–	–	–
SAM-3	450,000	–	–	–
GAP-1	5,038	–	–	–
GAP-2	5,038	–	–	–
GAP-3	5,038	–	–	–
HWD-4	546	1,021	3,548	5,038
HWD-5	546	1,021	3,548	5,038
HWD-6	546	1,021	3,548	5,038
FHS-1	1,660	–	–	–
FHS-2	1,660	–	–	–
FHS-3	1,660	–	–	–

$$(q_{c1N})_{cs} = q_{c1N} + \Delta q_{c1N}, \quad \Delta q_{c1N} = \left(5.4 + \frac{q_{C1N}}{16}\right) * \exp\left\{1.63 + \frac{9.7}{FC + 0.01} - \left(\frac{15.7}{FC + 0.01}\right)^2\right. \quad (6.1)$$

$$CRR_{M=7.5,\sigma'_{vc}=1} = exp\left\{\frac{(q_{c1N})_{cs}}{540} + \left(\frac{(q_{c1N})_{cs}}{67}\right)^2 - \left(\frac{(q_{c1N})_{cs}}{80}\right)^3 + \left(\frac{(q_{c1N})_{cs}}{114}\right)^4 - 3\right\} \quad (6.2)$$

where FC is the percent of fines content in soil, q_{C1N} is the normalized value of tip resistance and $(q_{C1N})_{CS}$ is the equivalent clean sand value of tip resistance.

6.4 DATA ANALYSIS

Statistical analyses were used to organize and summarize the data to support the research methodology. Proc MEANS and FREQ were used to describe the data. Proc CORR and REG were used to examine the linear relationship of predicted variables (age of earthquake and fines of content) with outcomes (cyclic resistance ratio at the time of earthquake with two approaches (Approach 1 and 2) and different percentage of change

in relative density (5 and 10). Pearson correlation, parameter estimates, and R-Square were used to determine the significant and strength effect among independent variable with outcomes.

6.5 RESULTS

Table 6.3a shows the frequency distribution for the age of earthquake and Table 6.3b for the fines content. Fifty percent of obtained soil samples in the SCCP have fines content in the range of 5-12%. The percentage of age of earthquake for each category is between 9% to 15 %. The precision reported herein does not represent the experimental uncertainty.

Table 6.3 Frequency distribution of a. Age and b. Fines content.

a. Age of Earthquake				
Age	**Frequency**	**Percent**	**Cumulative Frequency**	**Cumulative Percent**
546	191	8.89	191	8.89
1021	365	16.98	556	25.87
1660	292	13.59	848	39.46
3500	249	11.59	1097	51.05
3548	191	8.89	1288	59.93
5000	249	11.59	1537	71.52
5038	279	12.98	1816	84.50
450000	333	15.50	2149	100.00

b. Fines Content Categories				
Fines Content Categories	**Frequency**	**Percent**	**Cumulative Frequency**	**Cumulative Percent**
0-5	462	21.50	462	21.50
5-12	1077	50.12	1539	71.61
12-35	607	28.25	2146	99.86
Greater than 35	3	0.14	2149	100.00

Table 6.4 shows the mean, standard deviation, and MIN and MAX of variables. The results show the overall mean of fines content for the obtained soil samples from all the test locations is 9.2. The mean of the current cyclic resistance ratio is 0.17 and is greater than the corresponding values at the time of earthquake for both approaches which is because of the increase in soil resistance against liquefaction with time.

Table 6.4 N, mean, standard deviation, minimum, and maximum for variables.

Variables	N	Mean	Std Dev	Min	Max
Fines content	2149	9.2	4.61	2	38
Equivalent clean sand tip resistance	2149	105	36.5	18	222
Current cyclic resistance ratio	2107	0.17	0.09	0.05	0.57
Cyclic resistance ratio at the time of earthquake, Approach 1, 5%	2149	0.09	0.03	0.05	0.31
Cyclic resistance ratio at the time of earthquake, Approach 1, 10%	2149	0.07	0.01	0.05	0.15
Cyclic resistance ratio at the time of earthquake, Approach 2, 5%	2149	0.12	0.05	0.05	0.51
Cyclic resistance ratio at the time of earthquake, Approach 2, 10%	2149	0.12	0.05	0.05	0.47

Table 6.5 presents the mean, standard deviation, and minimum and maximum of variables by fines content. Results show that for a given range of fines content, Approach 1 leads to lower values of CRR compared to the Approach 2. The mean of equivalent clean sand tip resistance are 95, 114, 99, 131 for 0-5, 5-12, 12-35, and greater than 35 of fines content levels; respectively. The mean of the cyclic resistance ratio at the time of the earthquake were different with levels of fines of content.

Table 6.6 indicates Pearson correlation among variables. For each variable, three numbers are shown: the first row indicates bivariate correlation, the second row is P-value and the last row shows the number of observations. The results show the positive linear relationship between $(q_{c1N})_{cs}$ and CRR at the time of earthquake for all cases is greater than 0.75 which is considered to be strong.

Table 6.5 N, means, standard deviation, minimum, and maximum for variables by fines content levels.

Fines Content	Label	N	Mean	Std Dev	Min	Max
0-5	-Equivalent clean sand tip resistance	462	95	33.77	18	174
	-Current cyclic resistance ratio	462	0.15	0.07	0.05	0.45
	-Cyclic resistance ratio at the time of earthquake, Approach 1, 5%	462	0.07	0.02	0.05	0.16
	-Cyclic resistance ratio at the time of earthquake, Approach 1, 10%	462	0.06	0.01	0.05	0.10
	-Cyclic resistance ratio at the time of earthquake, Approach 2, 5%	462	0.11	0.03	0.05	0.22
	-Cyclic resistance ratio at the time of earthquake, Approach 2, 10%	462	0.10	0.03	0.05	0.21
5-12	-Equivalent clean sand tip resistance	1077	114	38.18	26	222
	-Current cyclic resistance ratio	1037	0.18	0.09	0.06	0.57
	-Cyclic resistance ratio at the time of earthquake, Approach 1, 5%	1077	0.10	0.04	0.05	0.31
	-Cyclic resistance ratio at the time of earthquake, Approach 1, 10%	1077	0.07	0.02	0.05	0.15
	-Cyclic resistance ratio at the time of earthquake, Approach 2, 5%	1077	0.13	0.06	0.06	0.51
	-Cyclic resistance ratio at the time of earthquake, Approach 2, 10%	1077	0.13	0.05	0.06	0.47
12-35	-Equivalent clean sand tip resistance	607	99	31.73	39	193
	-Current cyclic resistance ratio	605	0.16	0.09	0.07	0.56
	-Cyclic resistance ratio at the time of earthquake, Approach 1, 5%	607	0.09	0.02	0.06	0.19
	-Cyclic resistance ratio at the time of earthquake, Approach 1, 10%	607	0.07	0.01	0.06	0.12
	-Cyclic resistance ratio at the time of earthquake, Approach 2, 5%	607	0.12	0.04	0.06	0.29
	-Cyclic resistance ratio at the time of earthquake, Approach 2, 10%	607	0.11	0.04	0.06	0.28
Greater than 35	-Equivalent clean sand tip resistance	3	131	28.52	105	162
	-Current cyclic resistance ratio	3	0.23	0.10	0.15	0.34
	-Cyclic resistance ratio at the time of earthquake, Approach 1, 5%	3	0.13	0.03	0.11	0.16
	-Cyclic resistance ratio at the time of earthquake, Approach 1, 10%	3	0.10	0.01	0.09	0.11
	-Cyclic resistance ratio at the time of earthquake, Approach 2, 5%	3	0.16	0.04	0.12	0.21
	-Cyclic resistance ratio at the time of earthquake, Approach 2, 10%	3	0.16	0.04	0.12	0.20

Table 6.7 presents the results from the multiple regression models for equivalent clean sand tip resistance on cyclic resistance ratio at the time of earthquake for Approaches 1 and 2 and different percentages of change in relative density. Each model includes the age of the earthquake and the fines content as predictors. The results indicate there is significant relation between the predictors and outcome variable (CRR at time of earthquake). Parameter estimate in Table 6.7 is the slope between the predictors and outcome and shows how the CRR at time of earthquake will change by one unit of increase in the predictors.

Table 6.6 Pearson Correlation.

Pearson Correlation Coefficients Prob > |r| under H0: Rho=0 Number of Observations							
	FC	**qc1Ncs**	**CRRc**	**CRR15**	**CRR110**	**CRR25**	**CRR210**
FC Fines content	1.00000	0.19871 <.0001 2149	0.17426 <.0001 2107	0.43048 <.0001 2149	0.54077 <.0001 2149	0.25273 <.0001 2149	0.24724 <.0001 2149
qc1Ncs Equivalent clean sand tip resistance		1.00000	0.92467 <.0001 2107	0.77656 <.0001 2149	0.74988 <.0001 2149	0.94260 <.0001 2149	0.95095 <.0001 2149
CRRc Current cyclic resistance ratio			1.00000	0.72320 <.0001 2107	0.68974 <.0001 2107	0.96634 <.0001 2107	0.96726 <.0001 2107
CRR15 Cyclic resistance ratio at the time of earthquake, Approach 1, 5%				1.00000	0.98807 <.0001 2149	0.86005 <.0001 2149	0.85102 <.0001 2149
CRR110 Cyclic resistance ratio at the time of earthquake, Approach 1, 10%					1.00000	0.82872 <.0001 2149	0.82067 <.0001 2149
CRR25 Cyclic resistance ratio at the time of earthquake, Approach 2, 5%						1.00000	0.99947 <.0001 2149
CRR210 Cyclic resistance ratio at the time of earthquake, Approach 2, 10%							1.00

The slopes are different for Approach 1 with different percentages; however, the slopes are similar for Approach 2 with different percentages. 84 % variability of cyclic resistance is explained by equivalent clean sand tip resistance, age of earthquake, and fines content in Approach 1 for both 5 and 10 %. The results also reveal that 91 % variability of cyclic resistance is explained by equivalent clean sand tip resistance, age of earthquake, and fines content with Approach 2 for both 5 and 10 %.

Research is still on going to find the correlation between equivalent clean sand values of tip resistance and the cyclic resistance ratio at the time of earthquake.

Table 6.7 Multiple regression models for equivalent clean sand tip resistance on cyclic resistance ratio at the time of earthquake for Approach 1 and 2 and different percentages of change in relative density.

Variable	DF	Parameter Estimate	Standard Error	t Value	Pr > |t|	Standardized Estimate	Squared Semi-partial Corr Type II	Squared Partial Corr Type II
Intercept	1	0.02405	0.00101	23.87	<.0001	0	.	.
Age of earthquake	1	-8.88454E-8	1.943581E-9	-45.71	<.0001	-0.45038	0.15669	0.49346
Fines content	1	0.00047404	0.00006966	6.80	<.0001	0.06840	0.00347	0.02113
Equivalent clean sand tip resistance	1	0.00066376	0.00000777	85.39	<.0001	0.75785	0.54672	0.77267

R^2 = .84 Approach 1, 5%

Variable	DF	Parameter Estimate	Standard Error	t Value	Pr > |t|	Standardized Estimate	Squared Semi-partial Corr Type II	Squared Partial Corr Type II
Intercept	1	0.03582	0.00046647	76.79	<.0001	0	.	.
Age of earthquake	1	-3.59756E-8	8.99826E-10	-39.98	<.0001	-0.39193	0.11866	0.42700
Fines content	1	0.00070031	0.00003225	21.71	<.0001	0.21718	0.03500	0.18021
Equivalent clean sand tip resistance	1	0.00028620	0.00000360	79.52	<.0001	0.70227	0.46946	0.74672

R^2 = .84 Approach 1, 10%

Variable	DF	Parameter Estimate	Standard Error	t Value	Pr > |t|	Standardized Estimate	Squared Semi-partial Corr Type II	Squared Partial Corr Type II
Intercept	1	-0.01151	0.00123	-9.33	<.0001	0	.	.
Age of earthquake	1	-1.99549E-8	2.377846E-9	-8.39	<.0001	-0.06637	0.00340	0.03179
Fines content	1	0.00037841	0.00008523	4.44	<.0001	0.03583	0.00095264	0.00911
Equivalent clean sand tip resistance	1	0.00125	0.00000951	131.19	<.0001	0.93472	0.83168	0.88918

R^2 = .90 Approach 2, 5%

Variable	DF	Parameter Estimate	Standard Error	t Value	Pr > |t|	Standardized Estimate	Squared Semi-partial Corr Type II	Squared Partial Corr Type II
Intercept	1	-0.00884	0.00109	-8.10	<.0001	0	.	.
Age of earthquake	1	-1.3358E-8	2.107121E-9	-6.34	<.0001	-0.04684	0.00169	0.01839
Fines content	1	0.00037957	0.00007552	5.03	<.0001	0.03789	0.00107	0.01164
Equivalent clean sand tip resistance	1	0.00119	0.00000843	141.66	<.0001	0.94289	0.84628	0.90343

R^2 = .91 Approach 2, 10%

6.6 CONCLUSIONS

PROC REG in SAS was used to examine the relationship between equivalent clean sand tip resistance and cyclic resistance ratio at the time of earthquake with two approaches and two percentages of change in relative density. Each model included the age of the earthquake and the fines content. The results showed the bivariate correlations between equivalent clean sand tip resistance and cyclic resistance ratio at the time of earthquake using Approach 1 for 5 and 10% were 0.78 and 0.75, respectively. Bivariate correlations for Approach 2 were 0.94 and 0.95 for 5 and 10% of change in relative density. The results also revealed that an increase in predictor variable values (fines content, age of earthquake and equivalent clean sand tip resistance) produced different changes in CRR at the time of the earthquake for both 5 and 10% in Approach 1; whereas similar changes were produced for CRR for 5 and 10% in Approach 2. Variability of cyclic resistance ratio were explained 84% and 91% by equivalent clean sand tip resistance, age of earthquake, and fines content in Approaches 1 and 2, respectively.

SAS SYNTAX

```
proc format;
value fcgf 1=" 0-5"
                2=" 5-12"
                3="12-35"
          4="greater than 35";
data one;
set  crr.crr14;

if 0<fc =<5 then fcg=1;
else if 5<fc =<12 then fcg=2;
else if 12<fc =<35 then fcg=3;
else if 35<fc<100 then fcg=4;

lABEL
site =" Site"
age = " age of earthquake"
FC  =" fines content"
FCg  =" fines content categories"
qc1ncs  =" equivalent clean sand tip resistance"
CRRc ="current cyclic resistance ratio"
CRR15 ="cyclic resistance ratio at the time of earthquake, method 1, 5%"
CRR110 ="cyclic resistance ratio at the time of earthquake, method 1, 10%"
CRR25 ="cyclic resistance ratio at the time of earthquake, method 2, 5%"
CRR210 ="cyclic resistance ratio at the time of earthquake, method 2, 10%"
;
format fcg fcgf.;
run;

ods rtf;
ods listing close;
proc freq data =ONE;
tables site age fcg;
title ' Frequency tables/';
run;

proc means data=one maxdec=2;
    var fc -- crr210;
    TITLE1 'Mean';
run;
proc means data=one maxdec=2;
   class fcg;
    var qc1ncs -- crr210;
    TITLE1 'Mean';
     run;
```

```
proc CORR Data=one ;
    var fc -- crr210;
    TITLE1 'CORREALTION';
run;
ods rtf close;
ods listing;
quit;
run;
ods rtf;
ods listing close;

%macro reg  (d,i,t);
proc reg data=one;
     model &d = &i / stb pcorr2 scorr2;
title ' Regression model' &t;
  %mend reg;
 %reg (crr15,age fc qc1ncs, cyclic resistance ratio at the time of earthquake method 1 5%
);
%reg (crr110,age fc qc1ncs, cyclic resistance ratio at the time of earthquake method 1
10% );
%reg (crr25,age fc qc1ncs, cyclic resistance ratio at the time of earthquake method 2 5%
);
%reg (crr210,age fc qc1ncs, cyclic resistance ratio at the time of earthquake method 2
10% );
run;
ods rtf close;
ods listing;
quit;
run;
```

CHAPTER 7

APPLICATION OF GMPES TO ESTIMATE THE A_{MAX}-M OF PREHISTORIC EARTHQUAKES FOR THE CHARLESTON AREA [4]

[4] Results for Hollywood site are published in : Gheibi, E., Gassman, S.L. (2016). Engineering Geology, DOI: 10.1016/j.enggeo.2016.09.016. Reprinted here with permission of publisher.
Results for Fort Dorchester site are submitted in : Gheibi, E., Gassman, S.L. Hasek, M., Talwani, P. (2017). Bulletin of Earthquake Engineering.

ABSTRACT

In this study, the minimum earthquake magnitude and peak ground acceleration required to initiate liquefaction at the time of prehistoric earthquakes that date back to 11,000 years before present at the Hollywood, Fort Dorchester, Sampit, and Gapway sites located in the South Carolina Coastal Plain were computed. In-situ geotechnical data, including cone penetration data with pore water pressure measurements, were used with empirical methods that account for the age of the soil deposit to back analyse the minimum peak ground acceleration. Results were then combined with the corresponding values obtained using Ground Motion Prediction Equations (GMPEs) to obtain a proper estimation of minimum a_{max}-M of the prehistoric earthquakes at these sites. For instance, at the Hollywood site, when the age of the earthquake was not considered, the minimum magnitude ranged from 5.8 to 6.5 and the corresponding peak ground acceleration ranged from 0.31 to 0.39g. When the age of the earthquake was considered, the earthquake magnitude was found to be 0.2 to 0.3 units lower depending on earthquake age and the GMPE model. For the most recent prehistoric earthquake with the age of 546±17, the minimum M and a_{max} ranged from 5.6 to 6.3 and from 0.26 to 0.34g, respectively.

7.1 INTRODUCTION

The South Carolina Coastal Plain (SCCP) experiences infrequent earthquakes, thus paleoliquefaction analysis plays an important role in studying the paleoseismicity of this region. As an example, over 160 paleoliquefaction features have been discovered at a site near Hollywood, South Carolina (Obermeier et al. 1987) that have been associated with earthquakes dating from 500 to 11,000 years B.P. (Talwani and Cox 1985 and Weems et al. 1986). Furthermore, sand blows have been discovered at the Sampit and

Gapway sites, and have been associated with earthquake episodes that occurred about 546±17 and 1021±30 years ago at the Sampit site and 3548±66 and 5038±166 years ago at the Gapway site (Talwani and Schaeffer 2001). From studies of the paleoliquefaction features found in the SCCP, at least seven, large, prehistoric earthquakes have occurred within the last 6000 years in the SCCP with an average occurrence rate, based on the three most recent events, of about 500 years (Talwani and Schaeffer 2001).

More recently, a sand blow was discovered at the Colonial Dorchester State Historical Park (Talwani et al. 2011). At this site, the 1886 Charleston earthquake caused significant structural damage to the walls of the fort; however, field evidence indicates that liquefaction did not occur during the 1886 earthquake. Thus, the recently discovered sand blow is evidence of liquefaction that occurred during a prehistoric earthquake that pre-dates the Charleston 1886 earthquake. The site provides additional information for determining the age-related liquefaction potential of SCCP soils and the investigation of an older paleo-liquefaction feature.

Initial studies to investigate the paleoseismicity at the Hollywood site were performed by Martin 1990 and Martin and Clough 1994. Using geotechnical data (CPT, SPT and auger borings), they back calculated the peak ground acceleration, a_{max}, to be 0.3g based on the Seed et al. 1984 method and 0.2g from the Ishihara 1985 method. They combined the Seed et al. 1984 and Ishihara 1985 procedures and found a_{max} equal to 0.25g for earthquake magnitude, M, equal to 7.5. They did not consider the effect of the soil deposit age on the results. More recent studies by Gheibi and Gassman 2015 as discussed in Chapter 4, used methods developed by Hu et al. 2002a, 2002b and Leon et al. 2005 with site-specific geotechnical data (e.g. $(N_1)_{60}$ from the standard penetration test

(SPT) and q_{c1} from the cone penetration test (CPT)) in the vicinity of paleoliquefaction features studied by Talwani and Schaeffer 2001 to estimate the minimum values of magnitudes and peak ground accelerations associated with earthquakes that occurred at the Hollywood site. Time dependent studies by Mesri et al. 1990 and Kulhawy and Mayne 1990 were used to account for the soil age. The earthquake magnitude at the time of earthquake was found to be lower when accounting for age. For example at the Hollywood site, for the most recent prehistoric earthquake with the age of 546±17 years B.P., the magnitude ranged from 5.7 to 6.7 with corresponding acceleration ranging from 0.17 to 0.30g.

Given the uncertainties associated with back-analysis (e.g. factors related to liquefaction susceptibility, factors related to field observations and ground failure mechanisms, factors related to seismicity, and validity of in-situ testing techniques), Olson et al. 2005 recommended a regional approach using acceleration attenuation models in combination with cyclic stress methods to minimize the uncertainties associated with back-calculation of the peak ground acceleration and earthquake magnitude. They recommended first performing back-calculations using liquefaction evaluation procedures at individual sites to estimate a likely combination of a_{max} and M, then integrating the back-calculations at individual sites into a regional assessment to better assess the magnitude of the paleo-earthquake. This procedure overcomes some uncertainties related to time-depending mechanisms (aging) and changes in density resulting from liquefaction discussed by Olson et al. 2001. Use of this approach was illustrated by Green et al. 2005 for the Vincennes Earthquake that occurred around 6100 years B.P. in the Wabash Valley. Mechanical and chemical effects of aging were

interpreted to be small for the soils within the study area, thus an aging correction factor was not applied to the measured penetration resistance data.

The purpose of this study is to re-examine the geotechnical data collected at the Hollywood, Fort Dorchester, Sampit, and Gapway sites and back-calculate the minimum magnitude and acceleration required to initiate prehistoric liquefaction using regionally proper attenuation models (GMPEs) in combination with cyclic stress methods that account for time-dependent mechanisms to form a regional assessment of minimum a_{max}-M in the SCCP. Attenuation models from Toro et al. 1997, Tavakoli and Pezeshk 2005, Atkinson 2008' and Pezeshk et al. 2011 are used with the semi-empirical cyclic stress method of Idriss and Boulanger 2008 and the time dependent approaches of Kulhawy and Mayne 1990 and Hayati and Andrus 2009. The results will be compared to earlier back-calculations by Martin and Clough 1994 and Gheibi and Gassman 2015 for the Hollywood site and to the results in Chapter 5 for the Fort Dorchester site. The Sampit and Gapway results will be compared to earlier work by Gheibi and Gassman 2014 and Leon et al. 2005.

7.2 SITES STUDIED

Descriptions of the Hollywood, Fort Dorchester, Sampit, and Gapway sites are explored in previous chapters. Readers are referred to Section 4.2 for a description of the Hollywood site, Section 5.2 for the Fort Dorchester site and Section 3.2 for the Sampit and Gapway sites.

7.3 FRAMEWORK FOR AGE CORRECTION

As proposed by Leon et al. 2005 the empirical correlations for liquefaction evaluation (i.e. Seed's Simplified method, as reported in Youd and Idriss 1997) that were

developed based on freshly deposited or young (Holocene) soils can be used for older soil deposits as long as the currently measured penetration resistances are modified to account for the effect of time dependent processes (i.e. "aging"). For the study herein, two methods were used to account for aging by correcting the current cone penetration tip resistance to a representative post-earthquake penetration resistance value; the methodology of Kulhawy and Mayne 1990 (one of two methods proposed by Leon et al. 2005; the other being Mesri et al. 1990) and the methodology of Hayati and Andrus 2009. The post-earthquake value of penetration resistance, rather than the pre-earthquake penetration resistance (as proposed by Leon et al. 2005 and used in Gheibi and Gassman 2014 and Gheibi and Gassman 2015), is used herein because the Energy Intensity equation (Pond and Martin 1997) and the empirical relations between CRR and in situ measurements are almost exclusively based on field data measurements after earthquakes, not prior to earthquakes, and thus inherently account for disturbance (Olson et al. 2005).

The Kulhawy and Mayne 1990 method is based on collected SPT blow count data and relative density data as a function of soil particle size, D_{50}, for aged fine to medium overconsolidated sands from four geologic periods. A correction factor, C_A, was proposed to describe the influence of aging (t) on the $(N_1)_{60}/D_r^2$ ratio. This correction factor was extended to CPT data by Leon et al. 2005 and used herein to correlate the current penetration tip resistance to the post-earthquake values of penetration resistance, $q_{c1\ (post)}$.

The methodology of Hayati and Andrus 2009 uses an updated liquefaction resistance correction factor, $K_{DR,}$ given in Equation 7.1, where t is the time since initial

deposition or critical disturbance in years, to find CRR_k (the deposit resistance-corrected CRR) from Equation 7.2. K_{DR} is based on data from over 30 sites in five countries and is used to account for the influence of age, cementation and stress history on CRR.

$$K_{DR} = 0.13.\log(t) + 0.83 \quad (7.1)$$

$$CRR_K = CRR.K_{DR} \quad (7.2)$$

where *t* is the time since initial deposition or critical disturbance in years, to find CRR_k (the deposit resistance-corrected CRR). Age of prehistoric earthquakes used to back-calculate CPT tip resistance and CRR are associated with discovered sand blows at each site. Prehistoric earthquakes at the Hollywood, Sampit, and Gapway sites were inferred to be in the Charleston seismic source zone (Talwani and Schaeffer 2001); whereas, at the Fort Dorchester site, the earthquake has been associated with a splay of the Sawmill Branch fault zone in the Middleton Place Summerville seismic zone (Talwani et al. 2011).

The average q_{c1} values of tip resistance found using Kulhawy and Mayne 1990 and Hayati and Andrus 2009 methods for the ages associated with age of earthquakes (i.e., $q_{c1(post)}$) are summarized in Table 7.1 for the CPT soundings. As shown, in both cases the average values of tip resistance corrected for age are less than when no correction is considered. The average CRR values that have been corrected for age (i.e, $CRR_{(post)}$) using Kulhawy and Mayne 1990 and Hayati and Andrus 2009 are in a good agreement.

Table 7.1 Average values of q_{c1} and CRR for the source sand layer that have been corrected for age.

Test Locations	No Age Correction		Age Corrected (Y.B.P)																		
			Charleston Source												Sawmill Branch fault						
			546±17			1021±30			3548±66			5038±166			3500			6000		
			K&M (1990)		H&A (2009)	K&M (1990)		H&A (2009)	K&M (1990)		H&A (2009)	K&M (1990)		H&A (2009)	K&M (1990)		H&A (2009)	K&M (1990)		H&A (2009)
	q_{c1} (MPa)	CRR	q_{c1} (MPa)	CRR	CRR	q_{c1} (MPa)	CRR	CRR	q_{c1} (MPa)	CRR	CRR	q_{c1} (MPa)	CRR	CRR	q_{c1} (MPa)	CRR	CRR	q_{c1} (MPa)	CRR	CRR
HWD-4	10	0.18	8	0.15	0.15	8	0.15	0.14	8	0.14	0.14	8	0.14	0.14	-	-	-	-	-	-
HWD-5	9	0.17	7	0.13	0.13	7	0.13	0.13	7	0.13	0.12	7	0.13	0.12	-	-	-	-	-	-
HWD-6	10	0.21	8	0.17	0.16	8	0.16	0.16	8	0.16	0.15	8	0.16	0.15	-	-	-	-	-	-
FD-1	9	0.19	-	-	-	-	-	-	-	-	-	-	-	-	7	0.15	0.16	7	0.15	0.15
FD-2	11	0.15	-	-	-	-	-	-	-	-	-	-	-	-	8	0.16	0.15	8	0.16	0.15
FD-3	9	0.15	-	-	-	-	-	-	-	-	-	-	-	-	7	0.13	0.13	7	0.13	0.13
FD-7	8	0.14	-	-	-	-	-	-	-	-	-	-	-	-	6	0.12	0.11	6	0.12	0.11
SAM-1	10	0.16	8	0.12	0.12	8	0.12	0.12	-	-	-	-	-	-	-	-	-	-	-	-
SAM-2	9	0.14	7	0.11	0.11	7	0.11	0.11	-	-	-	-	-	-	-	-	-	-	-	-
SAM-3	10	0.23	8	0.16	0.18	8	0.16	0.18	-	-	-	-	-	-	-	-	-	-	-	-
GAP-1	6	0.11	-	-	-	-	-	-	5	0.09	0.08	5	0.09	0.08	-	-	-	-	-	-
GAP-2	11	0.13	-	-	-	-	-	-	9	0.14	0.1	9	0.14	0.09	-	-	-	-	-	-
GAP-3	4	0.08	-	-	-	-	-	-	3	0.07	0.05	3	0.07	0.05	-	-	-	-	-	-

K&M stands for Kulhawy and Mayne 1990 and H&A stands for Hayati and Andrus 2009.

7.4 PALEOLIQUEFACTION BACK-ANALYSIS PROCEDURE

Techniques proposed by Olson et al. 2005 and Green et al. 2005 were used in this study to reduce the uncertainties associated with back-analysis. Back-calculation was conducted using liquefaction procedures at each test location to determine the minimum required peak ground acceleration for different earthquake magnitudes. The obtained values of M and a_{max} were then combined with regional attenuation relationships to determine the proper combinations of a_{max}-M.

7.4.1 Back Analysis of Peak Ground Acceleration

The peak ground acceleration at the surface was found using the following equation as a function of the earthquake magnitude and the cyclic stress ratio for a given earthquake ($CSR_{M=7.5,\sigma'_{vc=1}}$) given by Idriss and Boulanger 2008:

$$a_{max} = CSR_{M=7.5,\sigma'_{vc}=1} * MSF * K_{\sigma} * \left(\frac{\sigma'_{v0} * g}{0.65 * r_d * \sigma_{v0}}\right) \quad (7.3)$$

where σ_{v0} is the vertical stress and σ'_{v0} is the vertical effective stress at depth z, and r_d is the reduction factor that considers the flexibility of soil column. The magnitude scaling factor (MSF) is used for earthquakes with magnitudes other than 7.5. K_{σ} is the overburden correction factor which has effect on the normalized cone penetrometer resistance for calculation of CRR. The proposed relations of MSF, r_d, K_{σ} and C_N of Idriss and Boulanger 2008 were used in this study.

For a factor of safety against liquefaction (FS_{liq}) of one, CSR is equal to CRR and $CSR_{M=7.5,\sigma'_{vc=1}}$ is obtained for Equation 7.3 using the relation between CRR and $(q_{c1N})_{cs}$ given by Idriss and Boulanger 2008:

$$CRR_{M=7.5,\sigma'_{vc}=1} = exp\left\{\frac{(q_{c1N})_{cs}}{540} + \left(\frac{(q_{c1N})_{cs}}{67}\right)^2 - \left(\frac{(q_{c1N})_{cs}}{80}\right)^3 + \left(\frac{(q_{c1N})_{cs}}{114}\right)^4 - 3\right\} \quad (7.4)$$

where $(q_{c1N})_{cs}$ is a function of q_{c1N}, the normalized value of q_{c1} by Pa, and the fines content, FC, as defined by Idriss and Boulanger 2008.

The peak ground acceleration obtained by Equation 7.3 is a function of earthquake magnitude. An example of an a_{max}-M combination for a hypothetical site is

shown in Figure 7.1. The factor of safety for the combinations blow the line (shaded part) is more than one and so the a_{max}-M combinations above the line are proper for liquefaction initiation.

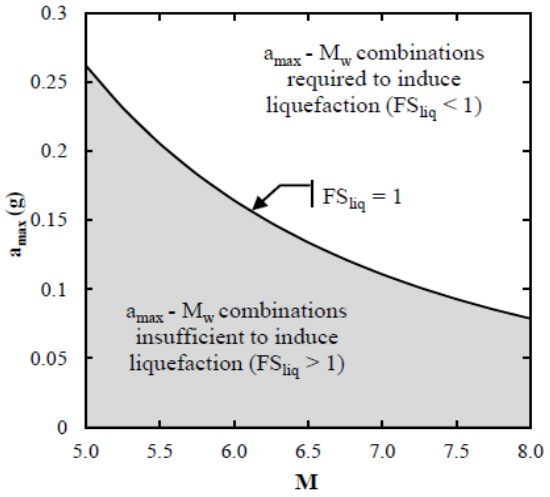

Figure 7.1 An example of a_{max}-M combination to trigger liquefaction (adapted from Green et al. 2005).

7.4.2 Regional Ground Motion Prediction Equations (GMPEs)

Liquefaction evaluation procedures provide a wide range of a_{max}-M combinations for liquefaction initiation (see Figure 7.1). Ground Motion Prediction Equations define maximum acceleration as a function of earthquake magnitude and site-to-source distance, R. As there are many combinations sufficient to induce liquefaction, the results of both methods are combined to find the intersection of the results to provide a reasonable combination of a_{max}-M. Green et al. 2005 explained this concept in a schematic design in Figure 7.2. As shown, the dashed line presents the a_{max}-M combination obtained using GMPE for a hypothetical site. The point of intersection is the minimum estimation of earthquake magnitude and peak ground acceleration for liquefaction initiation.

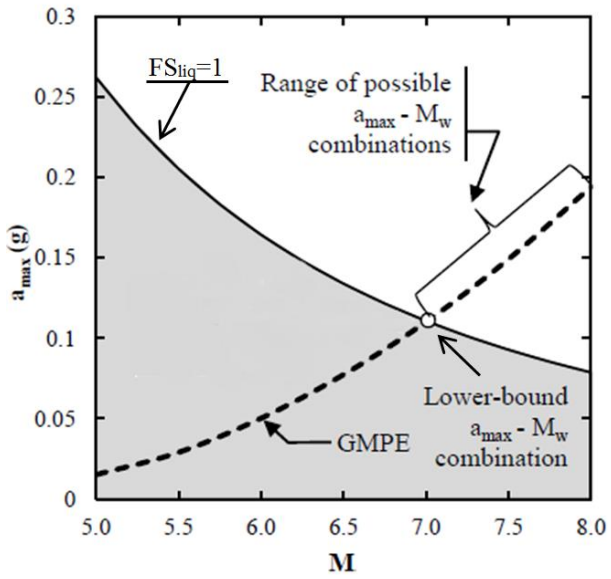

Figure 7.2 Combined GMPE and liquefaction evaluation methods (adapted from Green et al. 2005).

Four ground motion prediction equations were selected using the 2014 Update of the United States National Seismic Hazard Maps (Petersen et al. 2014). Toro et al. 1997 (T02), Tavakoli and Pezeshk 2005 (TP05), Pezeshk et al. 2011 (P11) and Atkinson 2008' (A08') that are regionally proper for the central and eastern US (CEUS) were used in this study (see Table 7.2) to estimate maximum acceleration at the bedrock. Atkinson 2008' refers to Atkinson 2008 as updated in Atkinson and Boore 2011.

Small-strain stiffness, damping variation, and soil layer thickness for each soil layer and site topography are the local site conditions that influence site amplification (Idriss 1990). For the study herein the amplification factors per Aboye et al. 2015 were used to modify the results obtained from GMPEs to obtain the minimum peak ground acceleration at the surface. Site amplification factors found by Aboye et al. 2015, were obtained using 1-D ground response analysis and are most applicable for the Charleston area (flat area) assuming not to consider the actual topography of the bed rock. The soil

layer thickness in the Charleston area is assumed to be about 600 to 1200 m. Aboye et al. 2015 noted that the shear wave velocity data at each depth used to find the site amplification factors were not generated assuming a correlation between layers. Accurate estimation of amplification factors requires information about correlation between layers and larger number of generated shear wave velocity data (Aboye et al. 2015). They also noted that the depth to soft and hard rock has significant effect on ground response analysis and further work is needed to consider the effect of depth variation to the soft and hard rock.

Table 7.2 Ground motion prediction models used for back-calculations (adapted from USGS update 2014 (Petersen et al. 2014)).

Model	**Abbreviation**	**Site-to-Source distance**	**Type**
Toro et al. (1997)	T02	1 to 500 km	Single Corner
Tavakoli and Pezeshk (2005)	TP05	1 to 1000 km	Hybrid
Atkinson (2008')	A08'	1 to 500 km	Reference Empirical
Pezeshk et al. (2011)	P11	1 to 1000 km	Hybrid

Site-to-source distance is the closest distance to the rupture at each site and was found by considering the epicentral and hypocentral distances at each site. For the Charleston Source, Dura-Gomez 2009 estimated the site-to-source distance at the Hollywood site to be about 25 km whereas at Sampit and Gapway sites, the site-to-source distance was estimated to range from 100 to 140 km (Talwani and Schaeffer 2001). For the Sawmill Branch fault, Talwani et al. 2011 suggested the site-to-source distance at the Fort Dorchester site to range from 4 to 10 km.

7.5 RESULTS

7.5.1 Peak Ground Acceleration

The age-corrected values of tip resistance and CRR in Table 7.1 were used in the procedure described in Section 7.4.1 to obtain the peak ground acceleration values for magnitudes ranging from 5 to 8. The results are shown in Table 7.3 and were found for each site by taking the average of a_{max} found from all age corrected q_{c1} readings within the source sand layer. As shown in Table 7.3, regardless of the approach used to account for the age of the earthquake, the age-corrected peak ground acceleration values are smaller than when a correction for the age of the earthquake is not made. Furthermore, as shown in Figures 7.3, 7.4, 7.5, and 7.6 for each test location at Hollywood, Fort Dorchester, Sampit, and Gapway sites, respectively, peak ground acceleration values are slightly higher for younger sand blow ages. As an example, when the age of sand blow is about 546 years B.P., the peak ground acceleration found using Kulhawy and Mayne 1990 at HWD-6 is about 0.39g; whereas it is 0.36g for the sand blow age of about 5038 years B.P. Also, the peak ground acceleration decreases as the earthquake magnitude increases. For example at the Fort Dorchester site (see Figure 7.4a), for the sand blow age of 3500 years B.P. using the Kulhawy and Mayne 1990 age relation for FD-1, a peak ground acceleration of 0.23g was obtained for M=7; whereas, 0.38g was found for M=5.

Also as shown in Figures 7.3 to 7.6, peak ground accelerations found using Kulhawy and Mayne 1990 and Hayati and Andrus 2009 are in a good agreement. The highest difference was found for SAM-3 and GAP-2. At these sites, the peak ground acceleration found using Kulhawy and Mayne 1990 and Hayati and Andrus 2009 are up to 0.07 and 0.09g different for M=5.

Table 7.3 Values of a_{max} found for source sand layer.

Magnitude	Test Locations	No Age Correction	Age Corrected (Y.B.P)											
			Charleston Source								Sawmill Branch fault			
			546±17		1021±30		3548±66		5038±166		3500		6000	
			K&M	H&A	K&M	H&A	K&M	H&A	K&M	H&A	K&M	H&A	K&M	H&A
5	HWD-4	0.43	0.36	0.39	0.35	0.38	0.34	0.38	0.34	0.38	-	-	-	-
	HWD-5	0.40	0.31	0.34	0.31	0.33	0.30	0.31	0.30	0.30	-	-	-	-
	HWD-6	0.49	0.39	0.41	0.38	0.40	0.37	0.38	0.36	0.37	-	-	-	-
	FD-1	0.49	-	-	-	-	-	-	-	-	0.38	0.4	0.38	0.4
	FD-2	0.36	-	-	-	-	-	-	-	-	0.38	0.36	0.38	0.35
	FD-3	0.30	-	-	-	-	-	-	-	-	0.26	0.25	0.26	0.25
	FD-7	0.31	-	-	-	-	-	-	-	-	0.27	0.24	0.27	0.24
	SAM-1	0.34	0.26	0.29	0.26	0.28	-	-	-	-	-	-	-	-
	SAM-2	0.28	0.23	0.24	0.22	0.23	-	-	-	-	-	-	-	-
	SAM-3	0.45	0.31	0.38	0.31	0.38	-	-	-	-	-	-	-	-
	GAP-1	0.25	-	-	-	-	0.21	0.20	0.20	0.19	-	-	-	-
	GAP-2	0.29	-	-	-	-	0.31	0.22	0.30	0.22	-	-	-	-
	GAP-3	0.19	-	-	-	-	0.17	0.15	0.17	0.14	-	-	-	-
6	HWD-4	0.35	0.29	0.31	0.29	0.31	0.28	0.31	0.28	0.30	-	-	-	-
	HWD-5	0.32	0.25	0.27	0.25	0.26	0.24	0.25	0.24	0.25	-	-	-	-
	HWD-6	0.40	0.31	0.33	0.31	0.32	0.30	0.31	0.30	0.30	-	-	-	-
	FD-1	0.40	-	-	-	-	-	-	-	-	0.31	0.33	0.30	0.32
	FD-2	029	-	-	-	-	-	-	-	-	0.31	0.29	0.30	0.28
	FD-3	0.24	-	-	-	-	-	-	-	-	0.21	0.20	0.21	0.20
	FD-7	0.25	-	-	-	-	-	-	-	-	0.22	0.19	0.21	0.19
	SAM-1	0.27	0.21	0.23	0.21	0.22	-	-	-	-	-	-	-	-
	SAM-2	0.23	0.18	0.19	0.18	0.19	-	-	-	-	-	-	-	-
	SAM-3	0.35	0.25	0.30	0.24	0.30	-	-	-	-	-	-	-	-
	GAP-1	0.21	-	-	-	-	0.17	0.16	0.17	0.16	-	-	-	-
	GAP-2	0.24	-	-	-	-	0.25	0.18	0.25	0.18	-	-	-	-
	GAP-3	0.15	-	-	-	-	0.14	0.12	0.14	0.12	-	-	-	-
7	HWD-4	0.27	0.22	0.24	0.22	0.23	0.21	0.23	0.21	0.23	-	-	-	-
	HWD-5	0.24	0.19	0.21	0.19	0.20	0.19	0.19	0.18	0.19	-	-	-	-
	HWD-6	0.30	0.24	0.25	0.23	0.25	0.23	0.23	0.22	0.23	-	-	-	-
	FD-1	0.30	-	-	-	-	-	-	-	-	0.23	0.25	0.23	0.24
	FD-2	0.22	-	-	-	-	-	-	-	-	0.23	0.22	0.23	0.21
	FD-3	0.18	-	-	-	-	-	-	-	-	0.16	0.15	0.16	0.15
	FD-7	0.19	-	-	-	-	-	-	-	-	0.16	0.15	0.16	0.14
	SAM-1	0.20	0.16	0.17	0.15	0.17	-	-	-	-	-	-	-	-
	SAM-2	0.17	0.14	0.14	0.13	0.14	-	-	-	-	-	-	-	-
	SAM-3	0.26	0.18	0.22	0.18	0.22	-	-	-	-	-	-	-	-

Magnitude	Test Locations	No Age Correction	Age Corrected (Y.B.P)											
			Charleston Source								Sawmill Branch fault			
			546±17		1021±30		3548±66		5038±166		3500		6000	
			K&M	H&A	K&M	H&A	K&M	H&A	K&M	H&A	K&M	H&A	K&M	H&A
	GAP-1	0.16	-	-	-	-	0.13	0.12	0.13	0.12	-	-	-	-
	GAP-2	0.18	-	-	-	-	0.19	0.14	0.19	0.14	-	-	-	-
	GAP-3	0.12	-	-	-	-	0.10	0.09	0.10	0.09	-	-	-	-
7.5	HWD-4	0.23	0.19	0.21	0.19	0.20	0.18	0.20	0.18	0.20	-	-	-	-
	HWD-5	0.21	0.17	0.18	0.17	0.17	0.16	0.17	0.16	0.16	-	-	-	-
	HWD-6	0.26	0.21	0.22	0.20	0.21	0.20	0.20	0.19	0.20	-	-	-	-
	FD-1	0.26	-	-	-	-	-	-	-	-	0.20	0.21	0.20	0.21
	FD-2	0.19	-	-	-	-	-	-	-	-	0.20	0.19	0.20	0.18
	FD-3	0.16	-	-	-	-	-	-	-	-	0.14	0.13	0.14	0.13
	FD-7	0.16	-	-	-	-	-	-	-	-	0.14	0.13	0.14	0.12
	SAM-1	0.18	0.14	0.15	0.13	0.14	-	-	-	-	-	-	-	-
	SAM-2	0.15	0.12	0.13	0.12	0.12	-	-	-	-	-	-	-	-
	SAM-3	0.23	0.16	0.19	0.15	0.19	-	-	-	-	-	-	-	-
	GAP-1	0.14	-	-	-	-	0.11	0.11	0.11	0.11	-	-	-	-
	GAP-2	0.16	-	-	-	-	0.17	0.12	0.17	0.12	-	-	-	-
	GAP-3	0.10	-	-	-	-	0.09	0.08	0.09	0.08	-	-	-	-
8	HWD-4	0.20	0.17	0.18	0.17	0.18	0.16	0.18	0.16	0.18	-	-	-	-
	HWD-5	0.19	0.15	0.16	0.14	0.15	0.14	0.14	0.14	0.14	-	-	-	-
	HWD-6	0.23	0.18	0.19	0.18	0.19	0.17	0.18	0.17	0.17	-	-	-	-
	FD-1	0.23	-	-	-	-	-	-	-	-	0.18	0.19	0.18	0.18
	FD-2	0.16	-	-	-	-	-	-	-	-	0.17	0.16	0.17	0.16
	FD-3	0.14	-	-	-	-	-	-	-	-	0.12	0.11	0.12	0.11
	FD-7	0.14	-	-	-	-	-	-	-	-	0.12	0.11	0.12	0.11
	SAM-1	0.15	0.12	0.13	0.12	0.13	-	-	-	-	-	-	-	-
	SAM-2	0.13	0.10	0.11	0.10	0.11	-	-	-	-	-	-	-	-
	SAM-3	0.20	0.14	0.17	0.13	0.16	-	-	-	-	-	-	-	-
	GAP-1	0.12	-	-	-	-	0.10	0.09	0.10	0.09	-	-	-	-
	GAP-2	0.14	-	-	-	-	0.15	0.11	0.15	0.11	-	-	-	-
	GAP-3	0.09	-	-	-	-	0.08	0.07	0.08	0.07	-	-	-	-

K&M stands for Kulhawy and Mayne 1990 and H&A stands for Hayati and Andrus 2009.

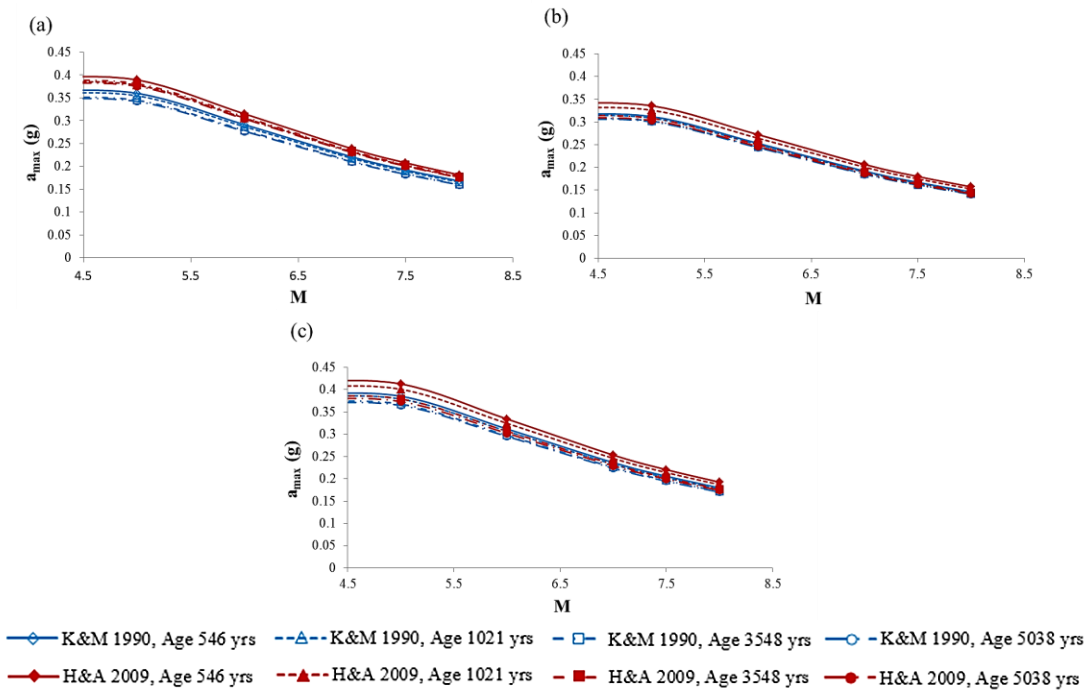

Figure 7.3 Relation between a_{max} and M for each test location at Hollywood site: (a) HWD-4, (b) HWD-5, and (c) HWD-6.

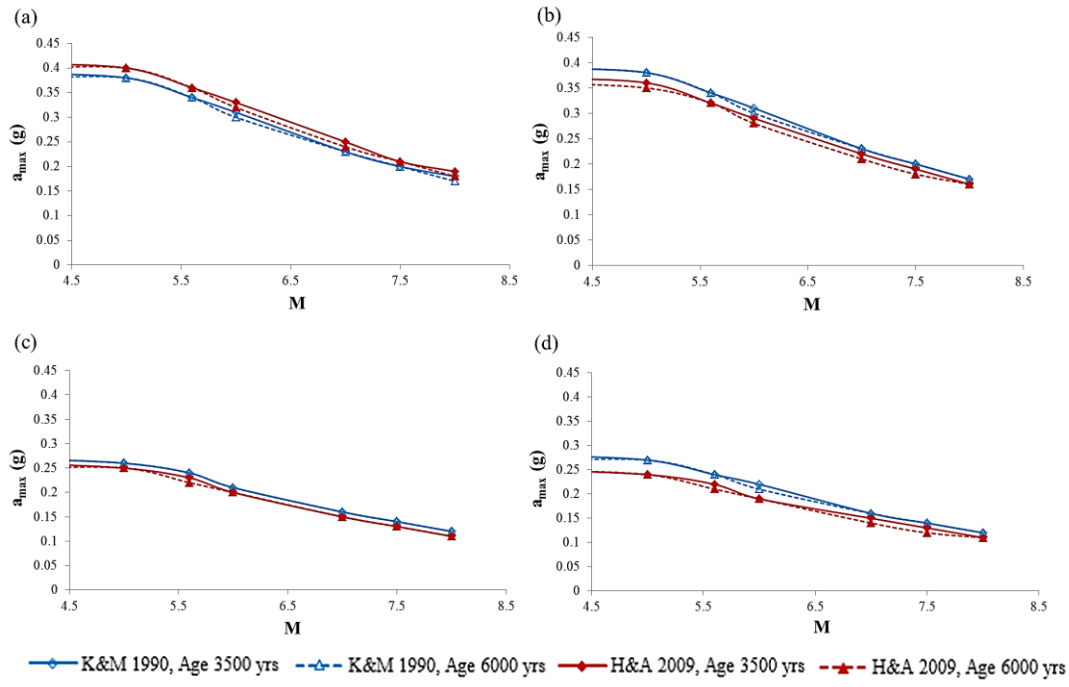

Figure 7.4 Relation between a_{max} and M for each test location at Fort Dorchester site: (a) FD-1, (b) FD-2, (c) FD-3, and (d) FD-7.

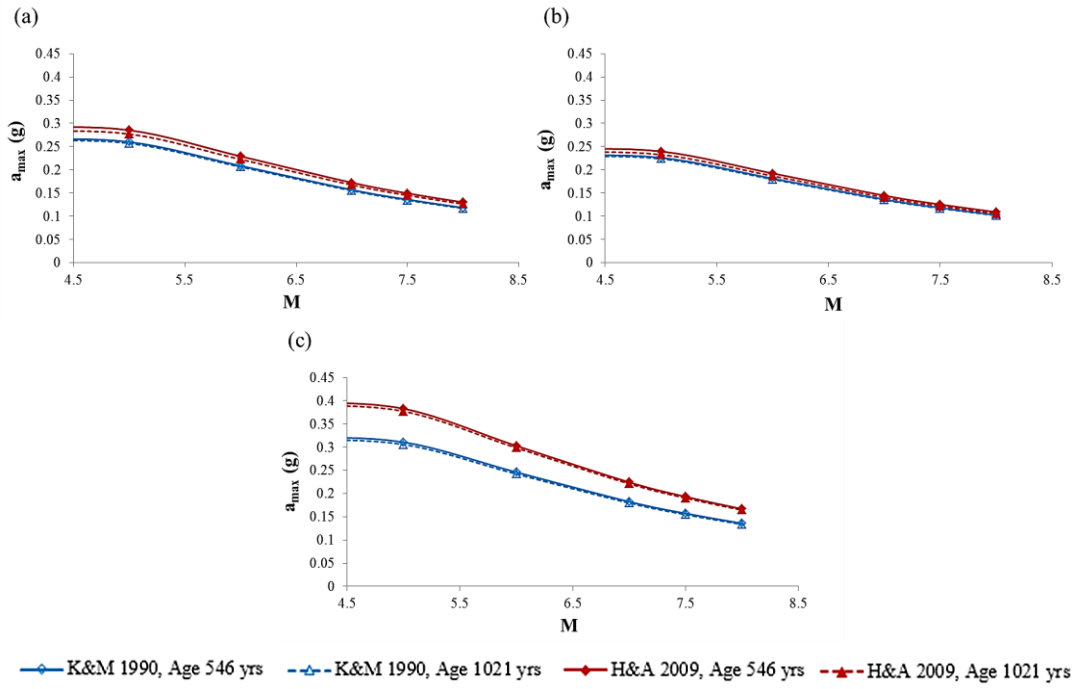

Figure 7.5 Relation between a_{max} and M for each test location at Sampit site: (a) SAM-1, (b) SAM-2, and (c) SAM-3.

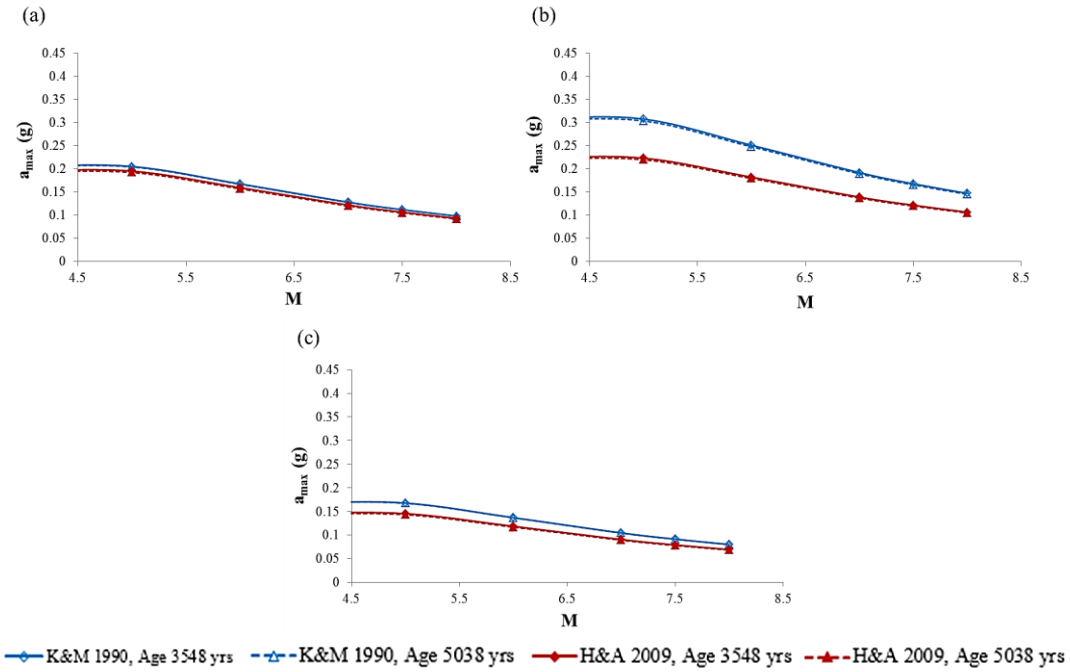

Figure 7.6 Relation between a_{max} and M for each test location at Gapway site: (a) GAP-1, (b) GAP-2, and (c) GAP-3.

7.5.2 Earthquake Magnitude

The age-corrected values of tip resistance and CRR in Table 7.1 were used to estimate the peak ground acceleration at the time of earthquake as a function of earthquake magnitude (see Figures 7.3 to 7.6) using the cyclic stress method as described in Section 7.5.1. Four regionally proper GMPEs discussed in section 7.4.2 were also used to find the intersection point with the acceleration values found from the cyclic stress method to estimate the minimum peak ground acceleration and earthquake magnitude. This is shown in Figures 7.7, 7.8, 7.9, and 7.10 and tabulated in Tables 7.4, 7.5, 7.6, and 7.7 for the Hollywood, Fort Dorchester, Sampit and Gapway sites, respectively. Results at each site were obtained using GMPEs for the range of site-to-source distance discussed in section 7.4.2 combined with the acceleration values for each sand blow age found using both the Kulhawy and Mayne 1990 and Hayati and Andrus 2009 approaches. At Fort Dorchester, the minimum a_{max}-M was obtained for only a sand blow age of 3500 years because, even though the age of the sand blow is unknown and could be as old as 10,000 years B.P., for the results found using GMPEs, the age of the sand blow (a difference of 2500 yrs) had a negligible effect on the back-calculated magnitude (0.l to 0.2 units).

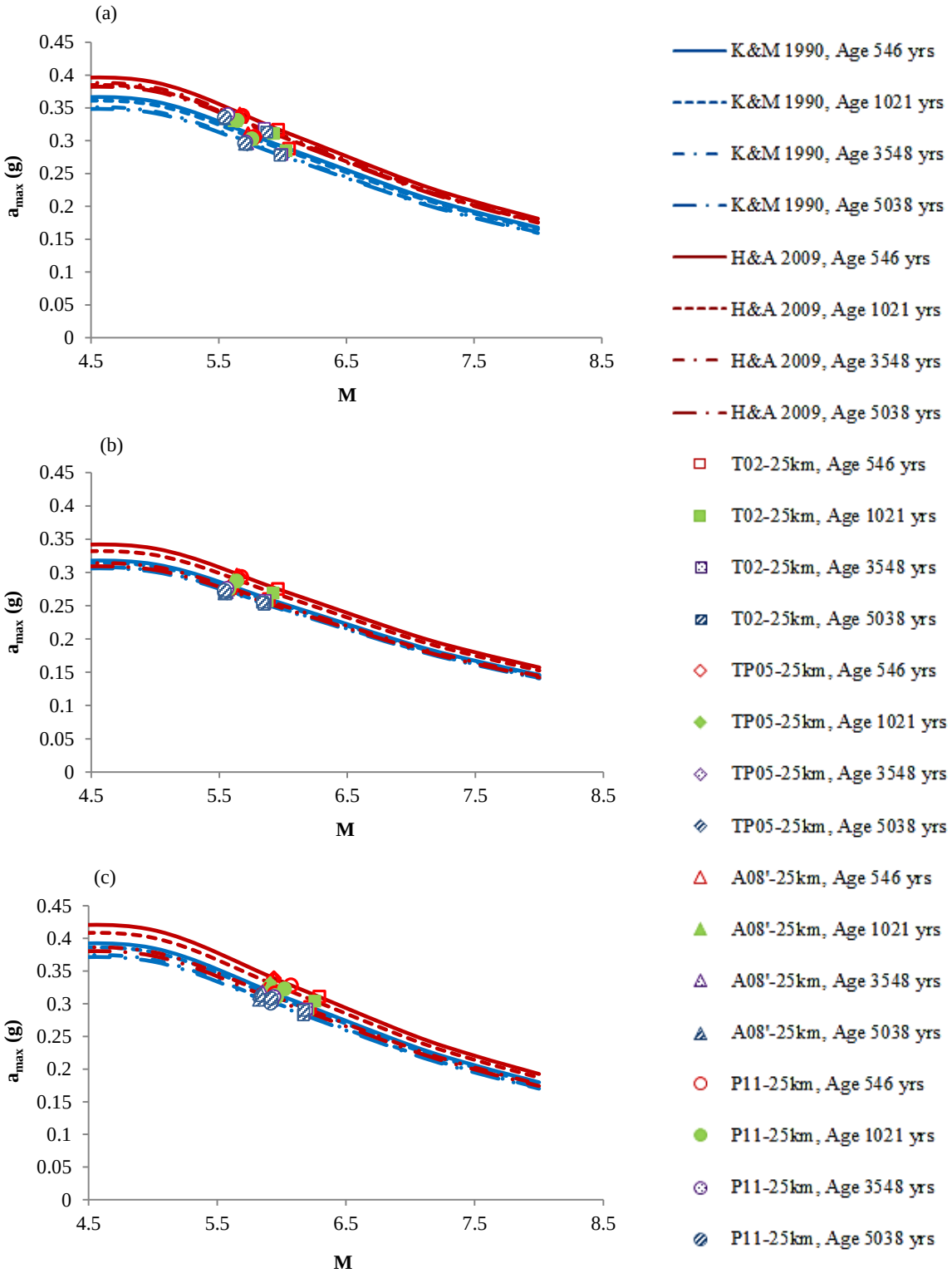

Figure 7.7 Combination of the cyclic stress method and GMPEs to find the minimum a_{max} and M for each test location at the Hollywood site: (a) HWD-4, (b) HWD-5, and (c) HWD-6.

Table 7.4 Minimum a_{max}-M for each test location at the Hollywood site, found using the combined methods of cyclic stress and GMPEs for different earthquake episodes.

Test Location	Model	Earthquake Magnitudes	No Age Correction	Age Corrected (Y.B.P)							
				546±17		1021±30		3548±66		5038±166	
				K&M	H&A	K&M	H&A	K&M	H&A	K&M	H&A
HWD-4	T02	M	6.1	6.1	6.0	6.0	5.9	6.0	5.9	6.0	5.9
		a_{max}	0.34	0.29	0.32	0.29	0.31	0.28	0.32	0.28	0.31
	TP05	M	5.9	5.8	5.7	5.8	5.7	5.7	5.6	5.7	5.6
		a_{max}	0.36	0.31	0.34	0.30	0.33	0.30	0.34	0.30	0.33
	A08'	M	5.8	5.7	5.7	5.8	5.6	5.7	5.6	5.7	5.6
		a_{max}	0.37	0.31	0.34	0.30	0.33	0.30	0.34	0.30	0.34
	P11	M	5.9	5.8	5.7	5.8	5.6	5.7	5.6	5.7	5.5
		a_{max}	0.36	0.31	0.34	0.30	0.33	0.30	0.34	0.30	0.34
HWD-5	T02	M	6.2	5.9	6.0	5.9	5.9	5.9	5.9	5.9	5.8
		a_{max}	0.31	0.26	0.28	0.26	0.27	0.25	0.26	0.25	0.26
	TP05	M	5.8	5.6	5.7	5.6	5.6	5.6	5.6	5.6	5.6
		a_{max}	0.33	0.28	0.29	0.28	0.29	0.27	0.28	0.27	0.27
	A08'	M	5.8	5.6	5.6	5.6	5.6	5.6	5.6	5.5	5.5
		a_{max}	0.34	0.28	0.30	0.28	0.29	0.27	0.28	0.27	0.27
	P11	M	5.9	5.6	5.7	5.6	5.6	5.5	5.6	5.5	5.5
		a_{max}	0.33	0.28	0.29	0.28	0.29	0.27	0.28	0.27	0.27
HWD-6	T02	M	6.5	6.2	6.3	6.2	6.3	6.2	6.2	6.2	6.2
		a_{max}	0.35	0.30	0.31	0.29	0.30	0.29	0.29	0.28	0.29
	TP05	M	6.1	5.9	5.9	5.9	5.9	5.8	5.9	5.8	5.8
		a_{max}	0.39	0.32	0.34	0.32	0.33	0.31	0.32	0.31	0.31
	A08'	M	6.1	5.9	5.9	5.9	5.9	5.8	5.9	5.8	5.8
		a_{max}	0.39	0.32	0.34	0.32	0.33	0.31	0.32	0.31	0.31
	P11	M	6.3	5.9	6.1	6.0	6.0	5.9	5.9	5.9	5.9
		a_{max}	0.37	0.32	0.33	0.31	0.32	0.30	0.31	0.30	0.31

K&M stands for Kulhawy and Mayne 1990 and H&A stands for Hayati and Andrus 2009.

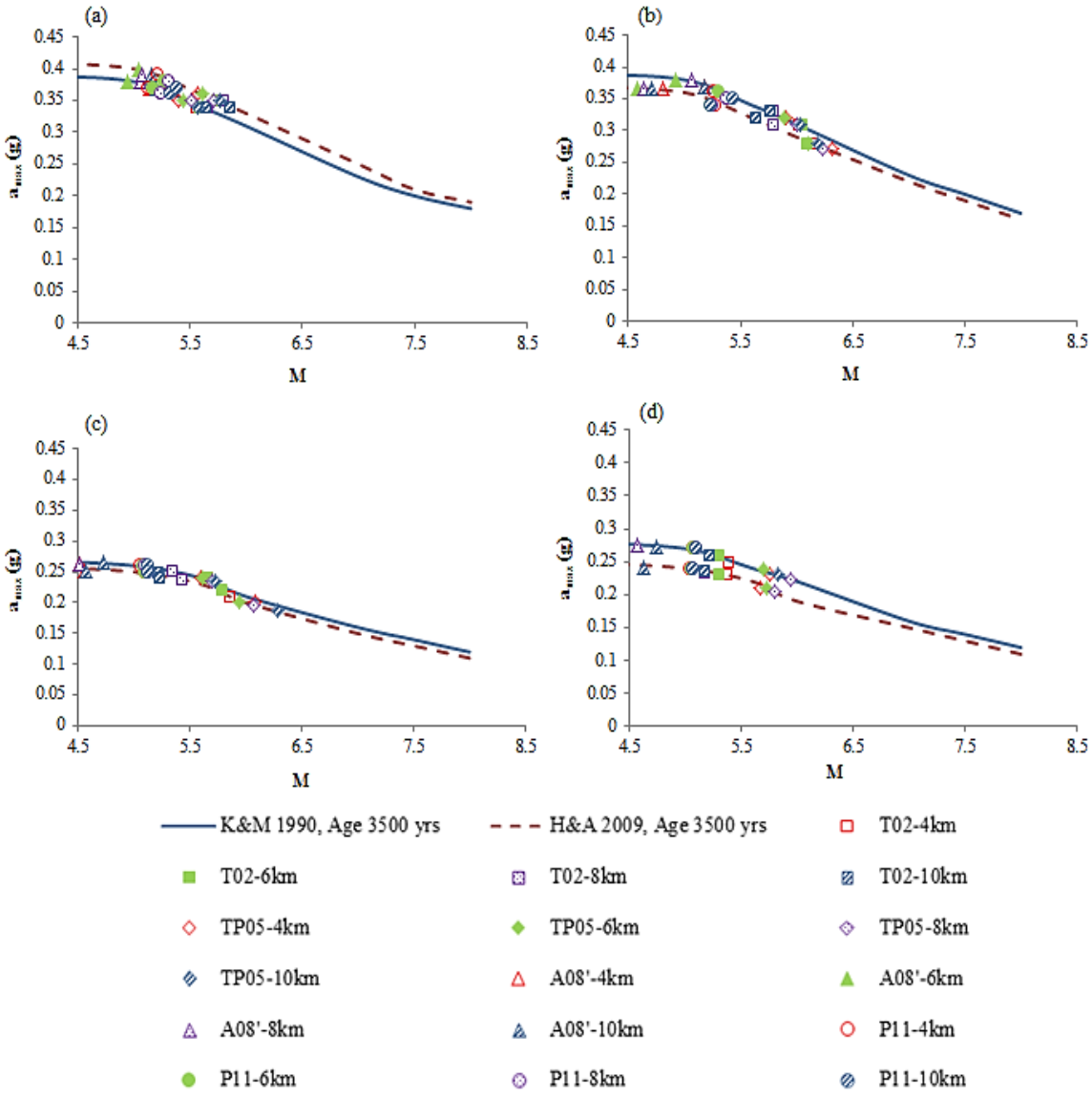

Figure 7.8 Combination of the cyclic stress method and GMPEs to find the minimum a_{max} and M for each test location at the Fort Dorchester site: (a) FD-1, (b) FD-2, (c) FD-3, and (d) FD-7.

Table 7.5 Minimum a_{max}-M for each test location at the Fort Dorchester site, found using the combined methods of cyclic stress and GMPEs for different earthquake episodes.

Test Location	Model	Earthquake Magnitudes	No Age Correction				Age Corrected (Y.B.P.)							
							3500							
			Site-to-Source Distance				Site-to-Source Distance							
			4 km	6 km	8 km	10 km	4 km		6 km		8 km		10 km	
							K&M	H&A	K&M	H&A	K&M	H&A	K&M	H&A
FD-1	T02	M	6.1	6.2	6.1	5.9	5.6	5.7	5.6	5.7	5.6	5.8	5.6	5.9
		a_{max}	0.39	0.38	0.39	0.41	0.34	0.35	0.34	0.35	0.34	0.35	0.34	0.34
	TP05	M	5.9	5.9	6.0	6.1	5.4	5.6	5.4	5.6	5.5	5.7	5.6	5.8
		a_{max}	0.42	0.41	0.40	0.39	0.35	0.36	0.35	0.36	0.35	0.35	0.34	0.35
	A08'	M	5.7	5.4	5.5	5.7	5.2	5.3	4.9	5.1	5.1	5.1	5.2	5.2
		a_{max}	0.44	0.46	0.45	0.44	0.37	0.38	0.38	0.40	0.38	0.39	0.37	0.39
	P11	M	5.4	5.5	5.6	5.7	5.1	5.2	5.2	5.3	5.2	5.3	5.3	5.4
		a_{max}	0.46	0.46	0.45	0.44	0.37	0.39	0.37	0.38	0.36	0.38	0.36	0.37
FD-2	T02	M	5.7	5.6	5.6	5.5	6.0	6.1	6.1	6.1	5.8	5.8	5.8	5.6
		a_{max}	0.31	0.32	0.32	0.33	0.31	0.28	0.31	0.28	0.33	0.31	0.33	0.32
	TP05	M	6.1	6.1	6.0	6.1	5.9	6.3	5.9	6.1	6.0	6.2	6.0	6.2
		a_{max}	0.29	0.28	0.29	0.28	0.32	0.27	0.32	0.28	0.31	0.27	0.31	0.28
	A08'	M	4.7	4.5	4.6	4.8	5.2	4.8	4.9	4.6	5.1	4.6	5.2	4.7
		a_{max}	0.36	0.36	0.36	0.36	0.37	0.36	0.38	0.36	0.38	0.36	0.37	0.36
	P11	M	5.2	5.2	5.2	5.2	5.3	5.3	5.3	5.2	5.4	5.2	5.4	5.2
		a_{max}	0.34	0.35	0.35	0.35	0.36	0.34	0.36	0.34	0.35	0.34	0.35	0.34
FD-3	T02	M	5.4	5.3	5.2	5.2	5.7	5.9	5.7	5.8	5.3	5.4	5.2	5.2
		a_{max}	0.28	0.29	0.29	0.29	0.24	0.21	0.24	0.22	0.25	0.24	0.25	0.24
	TP05	M	5.8	5.8	5.9	5.9	5.6	6.1	5.6	5.9	5.7	6.1	5.7	6.3
		a_{max}	0.26	0.26	0.25	0.24	0.24	0.20	0.24	0.20	0.23	0.20	0.23	0.19
	A08'	M	4.3	4.5	4.7	4.9	4.5	4.6	4.3	4.3	4.5	4.4	4.7	4.6
		a_{max}	0.31	0.31	0.30	0.30	0.26	0.25	0.27	0.26	0.26	0.26	0.26	0.25
	P11	M	5.1	5.1	5.1	5.1	5.1	5.1	5.1	5.1	5.1	5.1	5.1	5.1
		a_{max}	0.30	0.29	0.29	0.29	0.26	0.25	0.26	0.25	0.26	0.25	0.26	0.25
FD-7	T02	M	5.3	5.2	5.3	5.3	5.4	5.4	5.3	5.3	5.2	5.2	5.2	5.2
		a_{max}	0.30	0.30	0.30	0.30	0.25	0.23	0.26	0.23	0.26	0.23	0.26	0.23
	TP05	M	5.8	5.5	5.7	5.5	5.8	5.7	5.7	5.7	5.9	5.8	5.8	5.9
		a_{max}	0.27	0.28	0.28	0.28	0.23	0.21	0.24	0.21	0.22	0.21	0.23	0.20
	A08'	M	4.4	4.6	4.8	4.9	4.3	4.3	4.4	4.3	4.6	4.5	4.7	4.6
		a_{max}	0.32	0.31	0.31	0.31	0.28	0.25	0.28	0.25	0.27	0.25	0.27	0.24
	P11	M	5.1	5.1	5.1	5.1	5.1	5.0	5.1	5.1	5.1	5.1	5.1	5.1
		a_{max}	0.31	0.31	0.30	0.30	0.27	0.24	0.27	0.24	0.27	0.24	0.27	0.24

K&M stands for Kulhawy and Mayne 1990 and H&A stands for Hayati and Andrus 2009.

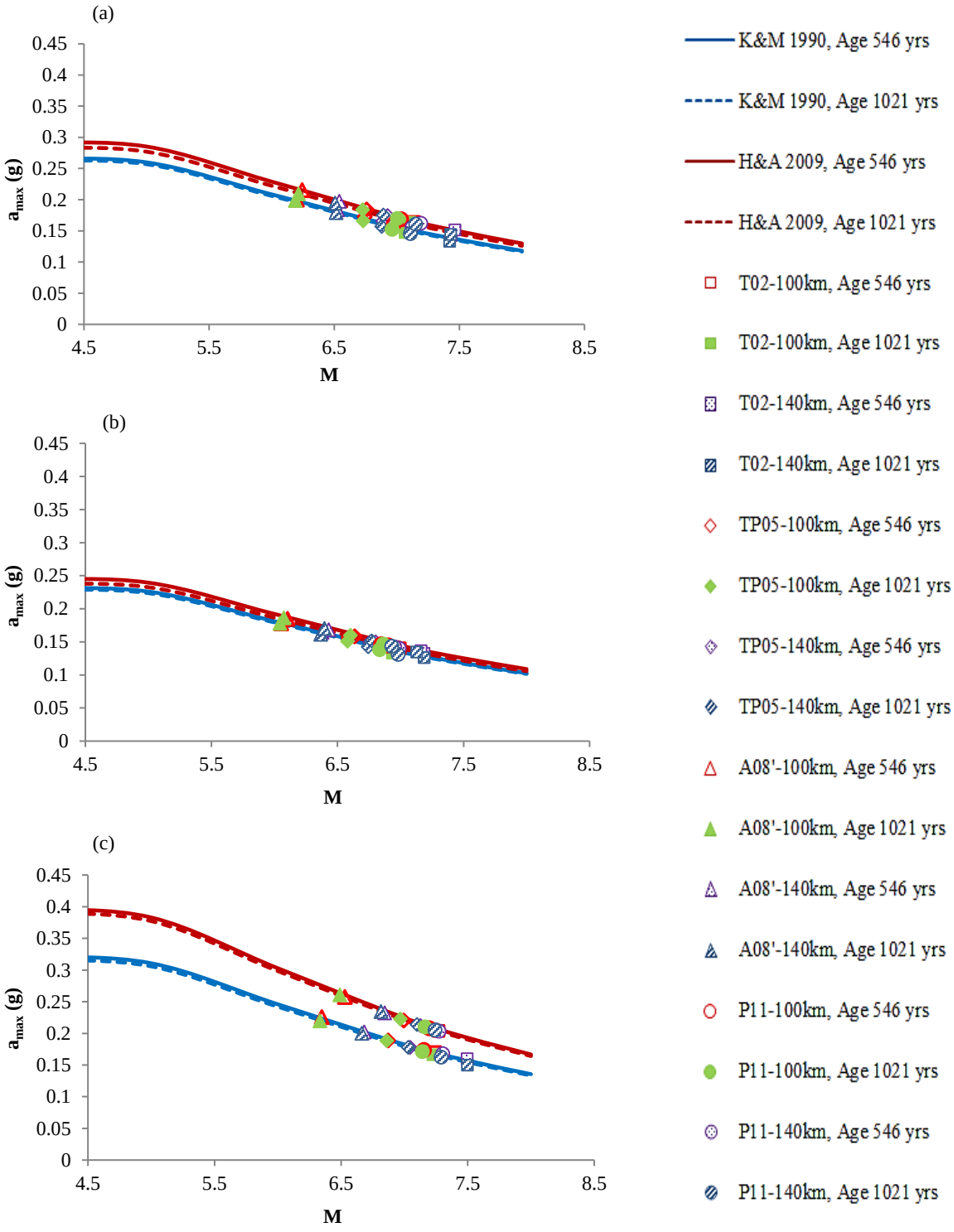

Figure 7.9 Combination of the cyclic stress method and GMPEs to find the minimum a_{max} and M for each test location at the Sampit site: (a) SAM-1, (b) SAM-2, and (c) SAM-3.

Table 7.6 Minimum a_{max}-M for each test location at the Sampit site, found using the combined methods of cyclic stress and GMPEs for different earthquake episodes.

Test Location	Model	Earthquake Magnitudes	No Age Correction		Age Corrected (Y.B.P.)							
					546±17				1021±30			
			Site-to-Source Distance		100 km		140 km		100 km		140 km	
			100 km	140 km	K&M	H&A	K&M	H&A	K&M	H&A	K&M	H&A
SAM-1	T02	M	7.3	7.6	7.1	7.1	7.4	7.5	7.1	7.1	7.4	7.4
		a_{max}	0.19	0.17	0.16	0.16	0.14	0.15	0.15	0.16	0.13	0.14
	TP05	M	6.9	7.1	6.7	6.8	6.9	6.9	6.7	6.7	6.9	6.9
		a_{max}	0.20	0.20	0.17	0.18	0.17	0.17	0.17	0.18	0.16	0.18
	A08'	M	6.4	6.7	6.2	6.2	6.5	6.5	6.2	6.2	6.5	6.5
		a_{max}	0.24	0.22	0.20	0.22	0.18	0.20	0.20	0.21	0.18	0.19
	P11	M	7.3	7.4	7.0	7.0	7.1	7.2	7.0	7.0	7.1	7.2
		a_{max}	0.19	0.18	0.16	0.17	0.16	0.16	0.15	0.17	0.15	0.16
SAM-2	T02	M	7.1	7.4	6.9	7.0	7.2	7.2	6.9	7.0	7.2	7.1
		a_{max}	0.16	0.15	0.14	0.14	0.13	0.14	0.13	0.14	0.13	0.13
	TP05	M	6.8	7.0	6.6	6.6	6.8	6.8	6.6	6.6	6.7	6.8
		a_{max}	0.18	0.17	0.16	0.16	0.15	0.15	0.15	0.16	0.14	0.15
	A08'	M	6.3	6.6	6.1	6.1	6.4	6.4	6.0	6.1	6.4	6.4
		a_{max}	0.21	0.19	0.18	0.18	0.16	0.17	0.18	0.19	0.16	0.17
	P11	M	7.0	7.1	6.8	6.9	7.0	7.0	6.8	6.9	7.0	6.9
		a_{max}	0.17	0.17	0.15	0.14	0.14	0.14	0.14	0.15	0.13	0.14
SAM-3	T02	M	7.4	7.2	7.2	7.3	7.5	7.2	7.2	7.2	7.5	7.3
		a_{max}	0.24	0.25	0.17	0.20	0.16	0.21	0.17	0.21	0.15	0.20
	TP05	M	7.1	7.3	6.9	7.0	7.0	7.1	6.9	7.0	7.0	7.1
		a_{max}	0.25	0.24	0.19	0.22	0.18	0.21	0.19	0.22	0.18	0.21
	A08'	M	6.7	7.0	6.3	6.5	6.7	6.8	6.3	6.5	6.7	6.8
		a_{max}	0.29	0.26	0.23	0.26	0.20	0.23	0.22	0.26	0.20	0.23
	P11	M	7.3	7.2	7.2	7.2	7.3	7.3	7.1	7.2	7.3	7.2
		a_{max}	0.24	0.25	0.17	0.21	0.17	0.20	0.17	0.21	0.16	0.21

K&M stands for Kulhawy and Mayne 1990 and H&A stands for Hayati and Andrus 2009.

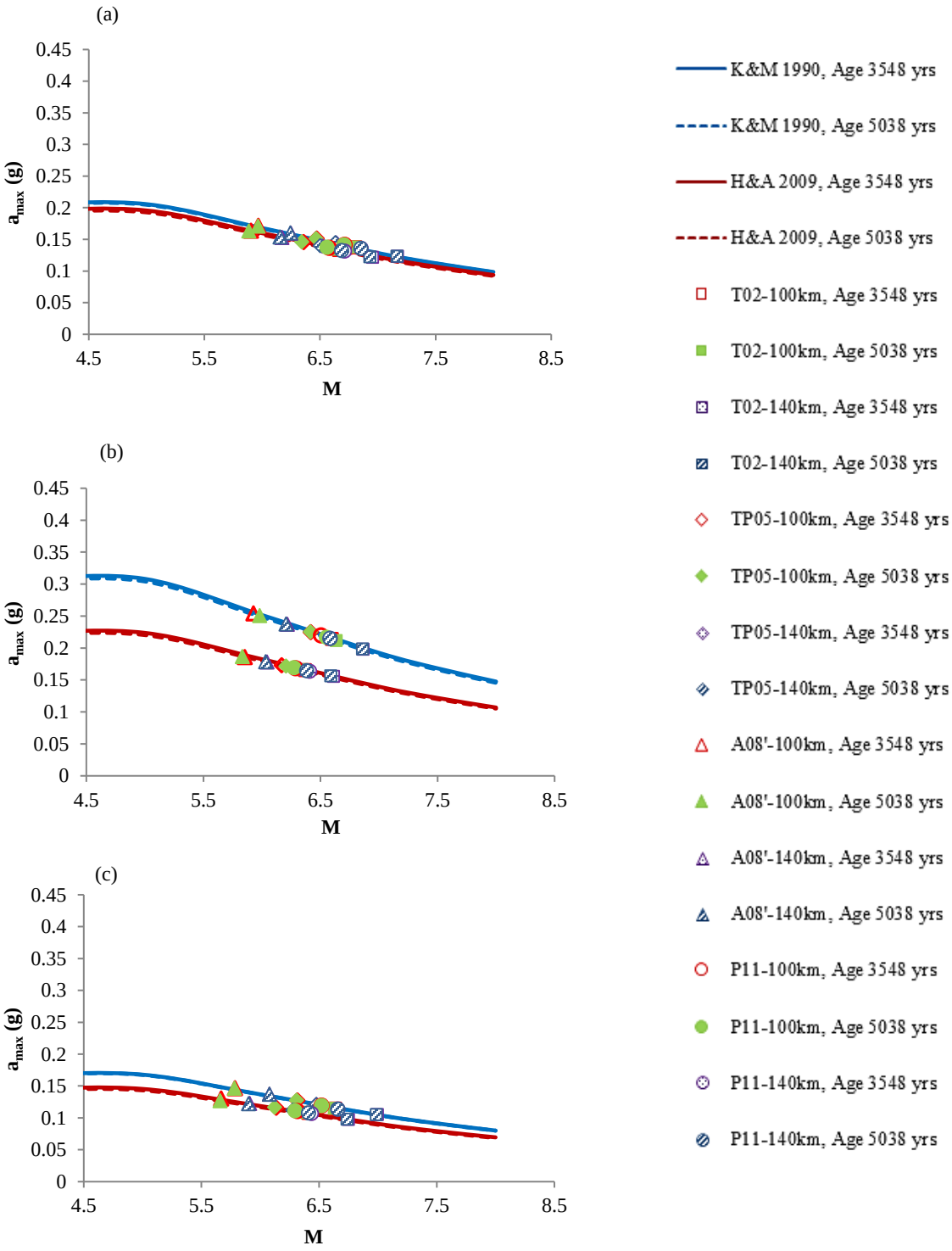

Figure 7.10 Combination of the cyclic stress method and GMPEs to find the minimum a_{max} and M for each test location at the Gapway site: (a) GAP-1, (b) GAP-2, and (c) GAP-3.

Table 7.7 Minimum a_{max}-M for each test location at the Gapway site, found using the combined methods of cyclic stress and GMPEs for different earthquake episodes.

Test Location	Model	Earthquake Magnitudes	No Age Correction		Age Corrected (Y.B.P.)							
					3548±66				5038±166			
			Site-to-Source Distance		100 km		140 km		100 km		140 km	
			100 km	140 km	K&M	H&A	K&M	H&A	K&M	H&A	K&M	H&A
GAP-1	T02	M	7.0	7.0	6.8	6.7	7.2	7.0	6.8	6.6	7.2	6.9
		a_{max}	0.16	0.16	0.14	0.13	0.12	0.12	0.14	0.13	0.12	0.12
	TP05	M	6.7	6.8	6.5	6.4	6.6	6.5	6.5	6.3	6.6	6.5
		a_{max}	0.18	0.17	0.15	0.15	0.14	0.14	0.15	0.15	0.14	0.14
	A08'	M	6.1	6.5	6.0	5.9	6.2	6.2	6.0	5.9	6.2	6.2
		a_{max}	0.20	0.19	0.17	0.16	0.16	0.15	0.17	0.16	0.16	0.15
	P11	M	6.9	7.0	6.7	6.6	6.9	6.7	6.7	6.6	6.9	6.7
		a_{max}	0.16	0.16	0.14	0.14	0.14	0.13	0.14	0.14	0.14	0.13
GAP-2	T02	M	6.7	7.0	6.6	6.4	6.9	6.6	6.6	6.3	6.9	6.6
		a_{max}	0.20	0.18	0.21	0.17	0.20	0.16	0.21	0.17	0.20	0.16
	TP05	M	6.4	6.6	6.4	6.2	6.6	6.3	6.4	6.2	6.6	6.3
		a_{max}	0.21	0.21	0.23	0.17	0.22	0.17	0.23	0.17	0.22	0.17
	A08'	M	6.0	6.2	5.9	5.9	6.2	6.0	6.0	5.8	6.2	6.0
		a_{max}	0.24	0.23	0.25	0.19	0.24	0.18	0.25	0.19	0.24	0.18
	P11	M	6.6	6.7	6.5	6.3	6.6	6.4	6.6	6.3	6.6	6.4
		a_{max}	0.20	0.20	0.22	0.17	0.22	0.16	0.22	0.17	0.22	0.16
GAP-3	T02	M	6.8	7.1	6.6	6.4	7.0	6.8	6.6	6.4	7.0	6.7
		a_{max}	0.13	0.11	0.11	0.11	0.10	0.10	0.11	0.11	0.10	0.10
	TP05	M	6.4	6.6	6.3	6.1	6.5	6.3	6.3	6.1	6.5	6.3
		a_{max}	0.14	0.13	0.13	0.12	0.12	0.11	0.13	0.12	0.12	0.11
	A08'	M	5.9	6.2	5.8	5.7	6.1	5.9	5.8	5.7	6.1	5.9
		a_{max}	0.15	0.14	0.15	0.13	0.14	0.12	0.15	0.13	0.14	0.12
	P11	M	6.7	6.8	6.5	6.3	6.7	6.4	6.5	6.3	6.7	6.4
		a_{max}	0.13	0.13	0.12	0.11	0.11	0.11	0.12	0.11	0.11	0.11

K&M stands for Kulhawy and Mayne 1990 and H&A stands for Hayati and Andrus 2009.

As shown in Figures 7.7 to 7.10 and the corresponding Tables 7.4 to 7.7, the earthquake magnitudes found using Kulhawy and Mayne 1990 and Hayati and Andrus 2009 are in a good agreement - M differed by up to 0.2, 0.5, 0.3, and 0.3 units and the a_{max} differed by up to 0.04, 0.05, 0.05, and 0.06g for Hollywood, Fort Dorchester, Sampit and Gapway sites, respectively. Also it is shown that, an increase in the time of soil aging

leads to a slight decrease in the required magnitude and peak ground acceleration for liquefaction initiation at time of earthquake. For instance, if the age of earthquake is not considered, using the Pezeshk et al. 2011 model, the a_{max}-M at HWD-4 is 0.36g-5.9; whereas, for the most recent and oldest earthquakes the range of earthquake magnitude is 5.7 to 5.8 and 5.5 to 5.7, respectively. The corresponding acceleration also decreases to range from 0.31 to 0.34g when the soil age is about 546±17 years B.P. and ranges from 0.30 to 0.34g when the soil age is about 5038±166 years B.P. Results for Hollywood site indicate that the T02 model predicts slightly larger earthquake magnitudes (around 5% larger) than the other three models.

The difference between M values for the range of site-to-source distance used in the analysis (a difference of 6 km (4 km to 10 km) at Fort Dorchester and difference of 40 km (100 km to 140 km) at Sampit and Gapway) is up to 0.7, 0.4 and 0.4 units at Fort Dorchester, Sampit and Gapway sites, respectively. Table 7.8 presents the range of minimum earthquake magnitude and peak ground acceleration at each test location at the four sites using the four attenuation models.

At the Fort Dorchester site, the A08' model predicted lower minimum earthquake magnitudes (up to 1.3 units) than the other three models. The A08' model also predicted lower earthquake magnitudes (up to 1 unit) at the Sampit and Gapway sites. Table 7.9 presents the range of minimum earthquake magnitude and peak ground acceleration at each test location for the attenuation models of T02, TP05 and P11 combined at Fort Dorchester, Sampit, and Gapway sites (based on the good agreement between T02, TP05 and P11).

Table 7.8 Range of minimum a_{max}-M at each test location found using the combined methods of cyclic stress and GMPEs.

Test Location	Model	Earthquake Magnitudes	No Age Correction	Age Corrected (Y.B.P)				
				Charleston Source				Sawmill Branch fault
				546±17	1021±30	3548±66	5038±166	3500
HWD-4	T02	M	6.1	6.0-6.1	5.9-6.0	5.9-6.0	5.9-6.0	-
		a_{max}	0.34	0.29-0.32	0.29-0.31	0.28-0.32	0.28-0.31	-
	TP05	M	5.9	5.7-5.8	5.7-5.8	5.6-5.7	5.6-5.7	-
		a_{max}	0.36	0.31-0.34	0.30-0.33	0.30-0.34	0.30-0.33	-
	A08'	M	5.8	5.7	5.6-5.8	5.6-5.7	5.6-5.7	-
		a_{max}	0.37	0.31-0.34	0.30-0.33	0.30-0.34	0.30-0.34	-
	P11	M	5.9	5.7-5.8	5.6-5.8	5.6-5.7	5.5-5.7	-
		a_{max}	0.36	0.31-0.34	0.30-0.33	0.30-0.34	0.30-0.34	-
HWD-5	T02	M	6.2	5.9-6.0	5.9	5.9	5.8-5.9	-
		a_{max}	0.31	0.26-0.28	0.26-0.27	0.25-0.26	0.25-0.26	-
	TP05	M	5.8	5.6-5.7	5.6	5.6	5.6	-
		a_{max}	0.33	0.28-0.29	0.28-0.29	0.27-0.28	0.27	-
	A08'	M	5.8	5.6	5.6	5.6	5.5	-
		a_{max}	0.34	0.28-0.30	0.28-0.29	0.27-0.28	0.27	-
	P11	M	5.9	5.6-5.7	5.6	5.5-5.6	5.5	-
		a_{max}	0.33	0.28-0.29	0.28-0.29	0.27-0.28	0.27	-
HWD-6	T02	M	6.5	6.2-6.3	6.2-6.3	6.2	6.2	-
		a_{max}	0.35	0.30-0.31	0.29-0.30	0.29	0.28-0.29	-
	TP05	M	6.1	5.9	5.9	5.8-5.9	5.8	-
		a_{max}	0.39	0.32-0.34	0.32-0.33	0.31-0.32	0.31	-
	A08'	M	6.1	5.9	5.9	5.8-5.9	5.8	-
		a_{max}	0.39	0.32-0.34	0.32-0.33	0.31-0.32	0.31	-
	P11	M	6.3	5.9-6.1	6.0	5.9	5.9	-
		a_{max}	0.37	0.32-0.33	0.31-0.32	0.30-0.31	0.30-0.31	-
FD-1	T02	M	5.9-6.2	-	-	-	-	5.6-5.9
		a_{max}	0.38-0.41	-	-	-	-	0.34-0.35
	TP05	M	5.9-6.1	-	-	-	-	5.4-5.8
		a_{max}	0.39-0.42	-	-	-	-	0.34-0.36
	A08'	M	5.4-5.7	-	-	-	-	4.9-5.3
		a_{max}	0.44-0.46	-	-	-	-	0.37-0.40
	P11	M	5.4-5.7	-	-	-	-	5.1-5.4
		a_{max}	0.44-0.46	-	-	-	-	0.36-0.39
FD-2	T02	M	5.5-5.7	-	-	-	-	5.6-6.1
		a_{max}	0.31-0.33	-	-	-	-	0.28-0.33
	TP05	M	6.0-6.1	-	-	-	-	5.9-6.3
		a_{max}	0.28-0.29	-	-	-	-	0.27-0.32
	A08'	M	4.5-4.8	-	-	-	-	4.6-5.2
		a_{max}	0.36	-	-	-	-	0.36-0.38
	P11	M	5.2	-	-	-	-	5.2-5.4
		a_{max}	0.34-0.35	-	-	-	-	0.34-0.36
FD-3	T02	M	5.2-5.4	-	-	-	-	5.2-5.9

Test Location	Model	Earthquake Magnitudes	No Age Correction	Age Corrected (Y.B.P)				
				Charleston Source				Sawmill Branch fault
				546±17	1021±30	3548±66	5038±166	3500
		a_{max}	0.28-0.29	-	-	-	-	0.21-0.25
	TP05	M	5.8-5.9	-	-	-	-	5.6-6.3
		a_{max}	0.24-0.26	-	-	-	-	0.19-0.24
	A08'	M	4.3-4.9	-	-	-	-	4.3-4.7
		a_{max}	0.30-0.31	-	-	-	-	0.25-0.27
	P11	M	5.1	-	-	-	-	5.1
		a_{max}	0.29-0.30	-	-	-	-	0.25-0.26
FD-7	T02	M	5.2-5.3	-	-	-	-	5.2-5.4
		a_{max}	0.30	-	-	-	-	0.23-0.26
	TP05	M	5.5-5.8	-	-	-	-	5.7-5.9
		a_{max}	0.27-0.28	-	-	-	-	0.21-0.24
	A08'	M	4.4-4.9	-	-	-	-	4.3-4.7
		a_{max}	0.31-0.32	-	-	-	-	0.24-0.28
	P11	M	5.1	-	-	-	-	5.0-5.1
		a_{max}	0.30-0.31	-	-	-	-	0.24-0.27
SAM-1	T02	M	7.3-7.6	7.1-7.5	7.1-7.4	-	-	-
		a_{max}	0.17-0.19	0.14-0.16	0.13-0.16	-	-	-
	TP05	M	6.9-7.1	6.7-6.9	6.7-6.9	-	-	-
		a_{max}	0.20	0.17-0.18	0.16-0.18	-	-	-
	A08'	M	6.4-6.7	6.2-6.5	6.2-6.5	-	-	-
		a_{max}	0.22-0.24	0.18-0.22	0.18-0.21	-	-	-
	P11	M	7.3-7.4	7.0-7.2	7.0-7.2	-	-	-
		a_{max}	0.18-0.19	0.16-0.17	0.15-0.17	-	-	-
SAM-2	T02	M	7.1-7.4	6.9-7.2	6.9-7.2	-	-	-
		a_{max}	0.15-0.16	0.13-0.14	0.13-0.14	-	-	-
	TP05	M	6.8-7.0	6.6-6.8	6.6-6.8	-	-	-
		a_{max}	0.17-0.18	0.15-0.16	0.14-0.16	-	-	-
	A08'	M	6.3-6.6	6.1-6.4	6.0-6.4	-	-	-
		a_{max}	0.19-0.21	0.16-0.18	0.16-0.19	-	-	-
	P11	M	7.0-7.1	6.8-7.0	6.8-7.0	-	-	-
		a_{max}	0.17	0.14-0.15	0.13-0.15	-	-	-
SAM-3	T02	M	7.2-7.4	7.2-7.5	7.2-7.5	-	-	-
		a_{max}	0.24-0.25	0.16-0.21	0.15-0.21	-	-	-
	TP05	M	7.1-7.3	6.9-7.1	6.9-7.1	-	-	-
		a_{max}	0.24-0.25	0.18-0.22	0.18-0.22	-	-	-
	A08'	M	6.7-7.0	6.3-6.8	6.3-6.8	-	-	-
		a_{max}	0.26-0.29	0.20-0.26	0.20-0.26	-	-	-
	P11	M	7.2-7.3	7.2-7.3	7.1-7.3	-	-	-
		a_{max}	0.24-0.25	0.17-0.21	0.16-0.21	-	-	-
GAP-1	T02	M	7.0	-	-	6.7-7.2	6.6-7.2	-
		a_{max}	0.16	-	-	0.12-0.14	0.12-0.14	-
	TP05	M	6.7-6.8	-	-	6.4-6.6	6.3-6.6	-
		a_{max}	0.17-0.18	-	-	0.14-0.15	0.14-0.15	-
	A08'	M	6.1-6.5	-	-	5.9-6.2	5.9-6.2	-
		a_{max}	0.19-0.20	-	-	0.15-0.17	0.15-0.17	-
	P11	M	6.9-7.0	-	-	6.6-6.9	6.6-6.9	-

Test Location	Model	Earthquake Magnitudes	No Age Correction	Age Corrected (Y.B.P)				
				Charleston Source				Sawmill Branch fault
				546±17	1021±30	3548±66	5038±166	3500
		a_{max}	0.16	-	-	0.13-0.14	0.13-0.14	-
GAP-2	T02	M	6.7-7.0	-	-	6.4-6.9	6.3-6.9	-
		a_{max}	0.18-0.20	-	-	0.16-0.21	0.16-0.21	-
	TP05	M	6.4-6.6	-	-	6.2-6.6	6.2-6.6	-
		a_{max}	0.21	-	-	0.17-0.23	0.17-0.23	-
	A08'	M	6.0-6.2	-	-	5.9-6.2	5.8-6.2	-
		a_{max}	0.23-0.24	-	-	0.18-0.25	0.18-0.25	-
	P11	M	6.6-6.7	-	-	6.3-6.6	6.3-6.6	-
		a_{max}	0.20	-	-	0.16-0.22	0.16-0.22	-
GAP-3	T02	M	6.8-7.1	-	-	6.4-7.0	6.4-7.0	-
		a_{max}	0.11-0.13	-	-	0.10-0.11	0.10-0.11	-
	TP05	M	6.4-6.6	-	-	6.1-6.5	6.1-6.5	-
		a_{max}	0.13-0.14	-	-	0.11-0.13	0.11-0.13	-
	A08'	M	5.9-6.2	-	-	5.7-6.1	5.7-6.1	-
		a_{max}	0.14-0.15	-	-	0.12-0.15	0.12-0.15	-
	P11	M	6.7-6.8	-	-	6.3-6.7	6.3-6.7	-
		a_{max}	0.13	-	-	0.11-0.12	0.11-0.12	-

Table 7.9 presents the range of minimum earthquake magnitude and peak ground acceleration at each test location for each episode, for all attenuation models combined. The difference in earthquake magnitude and peak ground acceleration between different test locations at Hollywood, Fort Dorchester, Sampit, and Gapway sites are up to 0.4, 0.4, 0.3, and 0.3 units and 0.07g, 0.16g, 0.07g, and 0.1g, respectively. The results from each test location at each site are combined for the age of earthquake and the range of M and a_{max} are shown in Table 7.10.

Table 7.9 Range of minimum a_{max}-M at each test location.

Test Location	Earthquake Magnitudes	No Age Correction	Age Corrected (Y.B.P)				
			Charleston Source				Sawmill Branch fault
			546±17	1021±30	3548±66	5038±166	3500
HWD-4	**M**	5.8-6.1	5.7-6.1	5.6-6.0	5.6-6.0	5.5-6.0	-
	a_{max}	0.34-0.37	0.29-0.34	0.29-0.33	0.28-0.34	0.28-0.34	-
HWD-5	**M**	5.8-6.2	5.6-6.0	5.6-5.9	5.5-5.9	5.5-5.9	-
	a_{max}	0.31-0.34	0.26-0.30	0.26-0.29	0.25-0.28	0.25-0.27	-
HWD-6	**M**	6.1-6.5	5.9-6.3	5.9-6.3	5.8-6.2	5.8-6.2	-
	a_{max}	0.35-0.39	0.30-0.34	0.29-0.33	0.29-0.32	0.28-0.31	-
FD-1	**M**	5.4-6.2	-	-	-	-	5.1-5.9
	a_{max}	0.38-0.46	-	-	-	-	0.34-0.39
FD-2	**M**	5.2-6.1	-	-	-	-	5.2-6.3
	a_{max}	0.28-0.35	-	-	-	-	0.27-0.36
FD-3	**M**	5.1-5.9	-	-	-	-	5.1-6.3
	a_{max}	0.24-0.30	-	-	-	-	0.19-0.26
FD-7	**M**	5.1-5.8	-	-	-	-	5-5.9
	a_{max}	0.27-0.31	-	-	-	-	0.21-0.27
SAM-1	**M**	6.9-7.6	6.7-7.5	6.7-7.4	-	-	-
	a_{max}	0.17-0.20	0.14-0.18	0.13-0.18	-	-	-
SAM-2	**M**	6.8-7.4	6.6-7.2	6.6-7.2	-	-	-
	a_{max}	0.15-0.18	0.13-0.16	0.13-0.16	-	-	-
SAM-3	**M**	7.1-7.4	6.9-7.5	6.9-7.5	-	-	-
	a_{max}	0.24-0.25	0.16-0.22	0.15-0.22	-	-	-
GAP-1	**M**	6.7-7.0	-	-	6.4-7.2	6.3-7.2	-
	a_{max}	0.16-0.18	-	-	0.12-0.15	0.12-0.15	-
GAP-2	**M**	6.4-7.0	-	-	6.2-6.9	6.2-6.9	-
	a_{max}	0.18-0.21	-	-	0.16-0.23	0.16-0.23	-
GAP-3	**M**	6.4-7.1	-	-	6.1-7.0	6.1-7.0	-
	a_{max}	0.11-0.14	-	-	0.10-0.13	0.10-0.13	-

The results at the Hollywood site are compared with those obtained from earlier studies of Martin and Clough 1994 that did not consider the effect of the age of the soil deposit and Gheibi and Gassman 2015 that used pre-earthquake tip resistance data found using Mesri et al. 1990 and Kulhawy and Mayne 1990 time dependent approaches. Also shown are the results from a re-analysis of the data from Gheibi and Gassman 2015. M and a_{max} were re-calculated using the post-earthquake values of tip resistance and the Kulhawy and Mayne 1990 study to account for aging. This is consistent with the approaches to account for aging and back-calculate a_{max} used in Section 7.3. The primary

difference between the study herein and the re-analysis of Gheibi and Gassman 2015 is the method to find M: GMPE's were used in this study; whereas, an approach based on the Energy Intensity equation (Pond and Martin 1997) was used previously.

Table 7.10 Summary of estimated minimum peak ground acceleration and earthquake magnitudes at the Hollywood, Fort Dorchester, Sampit, and Gapway sites.

Site	Study	Earthquake Magnitudes	No Age Correction	Age Corrected (Y.B.P)				
				Charleston Source				Sawmill Branch fault
				546±17	1021±30	3548±66	5038±166	3500
HWD	This Study	M	5.8-6.5	5.6-6.3	5.6-6.3	5.5-6.2	5.5-6.2	-
		a_{max}	0.31-0.39	0.26-0.34	0.26-0.33	0.25-0.34	0.25-0.34	-
	Gheibi and Gassman (2015)	M	7-7.2	5.7-6.7	5.5-6.5	5.3-6.5	5.2-6.5	-
		a_{max}	0.23-0.35	0.17-0.3	0.17-0.30	0.17-0.29	0.16-0.29	-
	Re-analysis of Gheibi and Gassman (2015)	M	7-7.2	6.7-6.9	6.6-6.9	6.6-6.8	6.6-6.8	-
		a_{max}	0.23-0.3	0.20-0.26	0.20-0.26	0.20-0.26	0.19-0.25	-
	Martin and Clough (1994)	M	7.5	-	-	-	-	-
		a_{max}	0.25	-	-	-	-	-
FD	This Study	M	5.1-6.2	-	-	-	-	5.0-6.3
		a_{max}	0.24-0.46	-	-	-	-	0.19-0.39
	Chapter 5	M	-	-	-	-	-	5.1-6.2
		a_{max}	-	-	-	-	-	0.19-0.40
SAM	This Study	M	6.8-7.6	6.6-7.5	6.6-7.5	-	-	-
		a_{max}	0.15-0.25	0.13-0.22	0.13-0.22	-	-	-
	Leon et al. 2005	M	-	6.2-7.0	6.2-6.8	-	-	-
	Gheibi and Gassman 2014	a_{max}	-	-	0.10-0.18	-	-	-
GAP	This Study	M	6.4-7.1	-	-	6.1-7.2	6.1-7.2	-
		a_{max}	0.11-0.21	-	-	0.10-0.23	0.10-0.23	-
	Leon et al. 2005	M	-	-	-	5.6-6.4	5.5-6.2	-
	Gheibi and Gassman 2014	a_{max}	-	-	-	0.10-0.14	0.11-0.18	-

At Fort Dorchester, results found using GMPEs are similar to the results found using the energy stress and cyclic stress methods presented in Chapter 5. Peak ground acceleration and earthquake magnitudes found using GMPEs at Sampit and Gapway sites

are also compared to those found by earlier studies of Leon et al. 2005 for the earthquake magnitude and Gheibi and Gassman 2014 for the peak ground acceleration values. Minimum earthquake magnitudes found using GMPEs at Sampit and Gapway sites are up to 0.7 and 1 units more than the previous findings using the energy stress equation by Leon et al. 2005.

Talwani and Schaeffer 2001 found evidence of prehistoric earthquakes (sand blows) associated with the Charleston Source, at more than one site. In particular, the earthquakes that occurred about 546±17 and 1021±30 years B.P. have caused sand blows at both Hollywood and Sampit sites. Similarly, prehistoric earthquakes that occurred about 3548±66 and 5038±166 years B.P. caused sand blows at both Hollywood and Gapway sites. Regardless of the site-specific geotechnical in-situ data, the final estimation of minimum a_{max} and M for each earthquake should be sufficient to liquefy the soil and cause sandblows at both sites.

Figure 7.11 is summary of the findings that indicate the range of minimum a_{max}-M for prehistoric earthquakes in the SCCP. Results in Figure 7.11 were found using in-situ geotechnical data and four Ground Motion Prediction Equations (T02, TP05, A08', P11) and indicate range of minimum a_{max}-M for each prehistoric earthquake associated with two sources of Charleston and Sawmill Branch fault. Results for each earthquake were found based on the required minimum a_{max} and M found at both sites that have evidence of sand blows associated with that earthquake.

As an example, using the soil profile and geotechnical in-situ data (i.e. cone penetration test) at the Hollywood site, the minimum earthquake magnitude of the earthquake that occurred about 546±17 years B.P. was found to range from 5.6 to 6.3. On

the other hand, using the geotechnical in-situ data at the Sampit site, the range of minimum earthquake magnitude for the same prehistoric earthquake was found to range from 6.6 to 7.5. The maximum value of the estimated lower bound (max (5.6,6.6)) and estimated upper bound (max (6.3,7.5)) were selected as the final estimation. Finally, the minimum earthquake magnitude of the prehistoric earthquake that occurred about 546±17 years B.P. and has liquefied the soil at both sites, was found to range from 6.6 to 7.5. The same procedure was conducted to find the minimum earthquake magnitude and peak ground acceleration values for the other prehistoric earthquakes.

As shown, for the Sawmill Branch fault, the minimum earthquake magnitude and peak ground accelerations are estimated to range from 5 to 6.3 and 0.19 to 0.39g. For the Charleston Source, the minimum earthquake magnitudes for earthquakes that occurred about 546±17 and 1021±30 years B.P. range from 6.6 to 7.5 and for the earthquakes that occurred about 3548±66 and 5038±166 years B.P. range from 6.1 to 7.2.

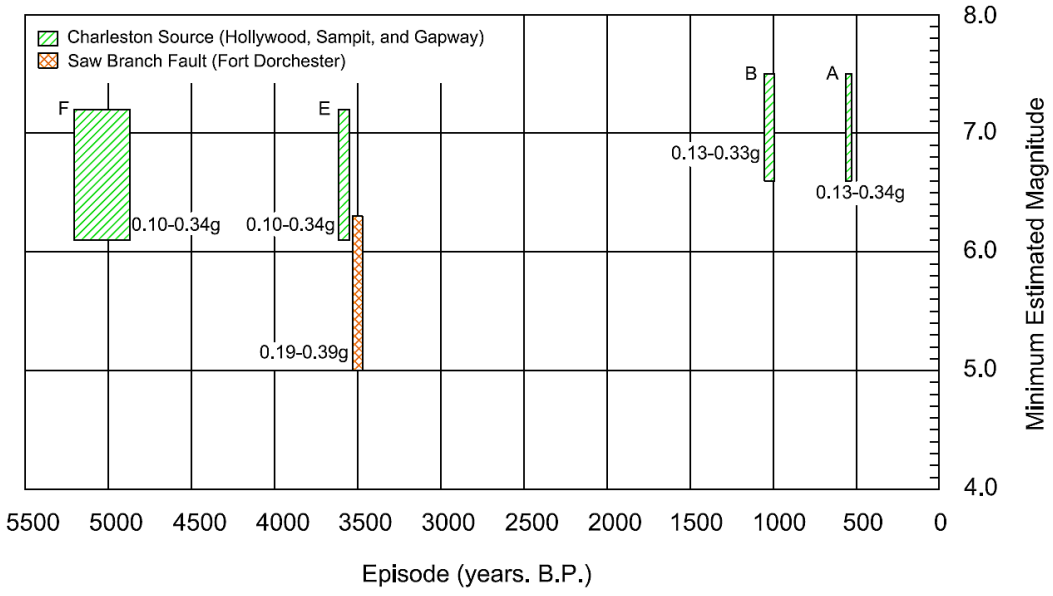

Figure 7.11 Minimum earthquake magnitudes for prehistoric earthquakes in SCCP found using GMPEs.

7.6 CONCLUSION

The minimum earthquake magnitudes and peak ground accelerations associated with prehistoric earthquakes at the Hollywood, Fort Dorchester, Sampit and Gapway sites in the South Carolina Coastal Plain were back analysed using in-situ geotechnical data, four Ground Motion Prediction Equations (T02, TP05, A08', P11) and two time-dependent procedures (Kulhawy and Mayne 1990 and Hayati and Andrus 2009) to correct for the age of the earthquake. It was shown that results obtained using Kulhawy and Mayne 1990 and Hayati and Andrus 2009 time-dependent approaches are in a general agreement.

Results indicated that at the Hollywood site, the magnitudes found using GMPE's are an order of magnitude less than those found using the Energy Intensity equation. At the Hollywood site, when the age of the earthquake was not considered, the minimum magnitude ranged from 5.8 to 6.5 and the corresponding peak ground acceleration ranged from 0.31 to 0.39g. When the age of the earthquake was considered, the earthquake magnitude was found to be 0.2 to 0.3 units lower depending on earthquake age and the GMPE model. For the most recent prehistoric earthquake with the age of 546±17, the magnitude ranged from 5.6 to 6.3 with corresponding acceleration ranging from 0.26 to 0.34g.

At the Fort Dorchester site, earthquake magnitudes found using both methods are in a good agreement. The earthquake at Fort Dorchester is estimated to have occurred 3,500 years B.P. or earlier and the minimum earthquake magnitude is estimated to range from 5 to 6.3. Results at the Sampit and Gapway sites indicate that the minimum earthquake magnitudes are estimated to range from 6.6 to 7.5 and 6.1 to 7.2, respectively.

Earthquake magnitudes for these two sites are estimated to be the same for earthquakes that occurred 546±17 and 1021±30 years B.P.

Minimum earthquake magnitudes for the prehistoric earthquakes in the SCCP associated with the Charleston Source range from 6.6 to 7.5 for earthquakes that occurred 546±17 and 1021±30 years B.P. and range from 6.1 to 7.2 for the earthquakes that occurred 3548±66 and 5038±166 years B.P. Earthquakes associated with Sawmill Branch fault are estimated to occur at least 3500 years ago with the minimum earthquake magnitude range from 5 to 6.3.

CHAPTER 8

CONCLUSION

8.1 Summary and Conclusions

The primary objective of the dissertation was to determine the proper combination of minimum earthquake magnitude and peak ground acceleration (a_{max}-M) required to initiate liquefaction for prehistoric earthquakes in the Charleston area. Many researchers have shown that aging leads to an increase in liquefaction resistance through mechanical mechanisms such as particle rearrangement and interlocking as well as chemical mechanisms such as cementation. To develop a regional view of a_{max}-M for prehistoric earthquakes in the SCCP, it was proposed to use three different approaches: Mesri et al. 1990, Kulhawy and Mayne 1990 and Hayati and Andrus 2009, to account for soil age in the back-calculation of the prehistoric minimum earthquake magnitude and peak ground acceleration at four sites in the SCCP: Sampit and Gapway (Chapter 3), Hollywood (Chapter 4), and Fort Dorchester (Chapter 5). The Hayati and Andrus 2009 method is the newest of the three methods and accounts for the effect of soil age on the cyclic resistance ratio (see Section 2.5 for a summary of the method). Studies were needed to compare the results from this method to those already found at Sampit and Gapway by Leon et al. 2005 using the Mesri et al. 1990 and Kulhawy and Mayne 1990 methods, and also to obtain results for the Hollywood and Fort Dorchester sites; sites that had not yet been studied with regard to aging.

Peak ground acceleration of the prehistoric earthquakes at the Sampit and Gapway sites were reassessed in Chapter 3 using newer liquefaction analysis method of Idriss and Boulanger 2008 and compared with previous findings from Hu et al. 2002b and Leon et al. 2005. Results indicated that the newer method of liquefaction analysis

resulted in accelerations that were about 50% less than those found by Leon et al. 2005 for M=5 and about 23% less for M=7.5.

Minimum earthquake magnitudes associated with prehistoric earthquakes that occurred about 546±30, 1021±30, 3548±66, and 5038±166 years B.P. at the Hollywood site were back-calculated in Chapter 4 using two approaches (Mesri et al. 1990 and Kulhawy and Mayne 1990) to consider the effect of soil aging and the updated method of liquefaction analysis used in Chapter 3. The results were compared with earlier studies by other researchers (Obermeier et al. 1987, Talwani and Cox 1985, Weems et al. 1986, and Martin and Clough 1994). It was shown that minimum earthquake magnitudes associated with the most recent episode (546±17 years B.P.) at the Hollywood site ranged from 5.7 to 6.7. The corresponding accelerations ranged from 0.16 to 0.30g.

In Chapter 5, the most recent aging approach of Hayati and Andrus 2009 was used in addition to the previously used methods that consider the effect of soil aging (Mesri et al. 1990 and Kulhawy and Mayne 1990) to back-calculate the minimum earthquake magnitudes at the Fort Dorchester site; a site with a recently discovered sand blow (Talwani et al. 2011). The minimum earthquake magnitude and peak ground accelerations obtained using the Mesri et al. 1990 method to account for age were not in agreement with the approaches of Kulhawy and Mayne 1990 and Hayati and Andrus 2009 at the Fort Dorchester site. Given the agreement with the results found using the Kulhawy and Mayne 1990 and the Hayati and Andrus 2009 relations for age, and also considering the study by Wells and Coppersmith 1994, the minimum magnitude was found to be 5.6 and the corresponding peak ground acceleration ranged from 0.21 to 0.36g.

In Chapter 7, minimum earthquake magnitudes and peak ground accelerations at the Hollywood, Fort Dorchester, Sampit, and Gapway sites were estimated by combining the cyclic stress method with Ground Motion Prediction Equations (GMPEs) to find a regional assessment of a_{max}-M in the SCCP. GMPEs define peak ground acceleration as a function of earthquake magnitude and site-to-source distance and can lead to a more robust risk assessment. As there are many combinations of a_{max}-M found from the cyclic stress method sufficient to induce liquefaction, the results of both methods are combined by intersection of the results to provide a reasonable combination of a_{max}-M. Four regionally proper GMPEs (T02, TP05, A08', and P11) were selected from the U.S. Geological Survey (USGS) updated hazard map report (Petersen et al. 2014) and used in combination with cyclic stress method and the methods of Kulhawy and Mayne 1990 and Hayati and Andrus 2009 to account for the effect of soil aging.

Results at the Hollywood, Fort Dorchester, Sampit and Gapway sites were compared with previous studies that back-calculated the minimum accelerations and magnitudes at these sites based on the cyclic stress, energy intensity and energy stress methods. At the Hollywood site, the minimum magnitudes found using GMPE's are an order of magnitude less than those found by Gheibi and Gassman 2015 using the energy intensity equation. At the Fort Dorchester site, the minimum earthquake magnitudes found using GMPE's are similar to those found using the energy stress method in chapter 5. Minimum earthquake magnitudes found using GMPEs are up to 0.7 units more at Sampit and 1 unit more at Gapway than previously findings by Leon et al. 2005 using the energy stress method.

Regional assessment of a_{max}-M for the Charleston area indicated that when the source of the earthquake is associated with the Charleston Source, the minimum earthquake magnitude and peak ground accelerations for the earthquakes that occurred about 546±17 and 1021±30 years B.P., were estimated to range from 6.6 to 7.5 and 0.13 to 0.34g, respectively. Earthquakes that occurred about 3548±66 and 5038±166 years B.P. were estimated to have minimum earthquake magnitude range from 6.1 to 7.2 and minimum peak ground acceleration of about 0.10 to 0.34g. For the earthquakes associated with the Sawmill Branch Fault that occurred about 3500 years ago or earlier, the minimum earthquake magnitudes were estimated to range from 5 to 6.3 and the corresponding peak ground acceleration ranged from 0.19 to 0.39 g.

8.2 Future Research

To further advance our understanding of the seismic hazard in the SCCP, future areas of research include:

1. Study aging mechanisms. The soil mineralogy and grain characteristics of soil deposits in the SCCP need to be studied to better understand the aging mechanism at each site. An initial study by Hasek and Gassman 2016 examined the mesoscopic and microscopic characteristics of liquefiable soils at the Hollywood, Sampit, and Four Hole Swamp sites and found no evidence of chemical aging in form of cementation between soil particles. Given the significance of paleoliquefaction study, further studies are needed to better understand the aging mechanism and find a site specific aging factor at each site. This will reduce uncertainties associated with aging approaches and will lead to a better estimation of earthquake magnitude and peak ground acceleration in the SCCP.

2. Utilize shear wave velocity. Shear wave velocity data has been shown to further our understanding of the liquefaction potential assessment since both shear wave velocity and liquefaction resistance parameters are influenced by similar factors (Andrus and Stokoe 2000; Andrus et al. 2006). CPT data were used in this study and it is suggested to utilize the shear wave velocity data at Hollywood, Fort Dorchester, Sampit, and Gapway sites that have been collected by Heidari and Andrus 2012, Hossain et al. 2013 and Hayati et al. 2008 and back-calculate minimum earthquake magnitudes and peak ground accelerations of the prehistoric earthquakes in the Charleston region. Results can be compared with the findings from this study to find a more robust assessment of a_{max}-M for the regional prehistoric earthquakes in the SCCP.

3. Increase the study area. Obtaining geotechnical data from more sites where sand blows have been discovered in the SCCP will extend the region of study. It is also suggested to find minimum a_{max}-M using regionally proper GMPEs for the prehistoric earthquakes at two sites where the CPT data have already been obtained; the Four Hole Swamp and Ten Mile Hill sites.

4. Study the site-to-source distance. GMPEs estimate peak ground acceleration as a function of earthquake magnitude and site-to-source distance. Site-to-source distance is one of the uncertainties associated with paleoseismic analysis since the exact locations of earthquakes are not known. It is suggested to use GMPEs to find minimum a_{max}-M for different site-to-source distances at each site. It is expected to find similar a_{max}-M for different sites for the same earthquake with different site-to-source distances. Results will be used to find the nearest estimation of site-to-source distance for each site.

REFERENCES

Aboye, S. A., Andrus, R. D., Ravichandran, N., Bhuiyan, A.H., and Harman, N. (2015). "Seismic site factors and design response spectra based on conditions in Charleston, South Carolina." *Earthquake Spectra,* 31 (2): 723-744.

Abrahamson, N., and Silva, W., (2008). "Summary of the Abrahamson & Silva NGA ground-motion relations." Earthquake Spectra, 24 (1): 67–97.

Ambraseys, N. N. (1988). "Engineering seismology." *Earthquake Engineering and Structural Dynamics,* Vol 17: 1-105.

American Society for Testing and Materials (ASTM). (2007). "Designation D422-63(2007)e2, Standard Test Method for Particle-Size Analysis of Soils." *Annual Book of ASTM Standards,* West Conshohocken, PA. doi: 10.1520/D0422-63R07E02

American Society for Testing and Materials (ASTM). (2009). "Designation D2488-09a, Standard Practice for Description and Identification of Soils (Visual-Manual Procedure)." *Annual Book of ASTM Standards*. 4.08. West Conshohocken, PA. doi: 10.1520/D2488-09A

American Society for Testing and Materials (ASTM). (2010). "Designation D4318-10e1, Standard Test Methods for Liquid Limit, Plastic Limit, and Plasticity Index of Soils." *Annual Book of ASTM Standards*. 4.08. West Conshohocken, PA. doi: 10.1520/D4318

American Society for Testing and Materials (ASTM). (2011). "Designation D1586-11, Standard Test Method for Standard Penetration Test (SPT) and Split-Barrel Sampling of Soils." *Annual Book of ASTM Standards*. 4.08. West Conshohocken, PA. doi: 10.1520/D1586-11

American Society for Testing and Materials (ASTM). (2011). "Designation D2487-11, Standard Practice for Classification of Soils for Engineering Purposes (Unified Soil Classification System)." *Annual Book of ASTM Standards.* 4.08. West Conshohocken, PA. doi: 10.1520/D2487-11

American Society for Testing and Materials (ASTM). (2012). "Designation D5778-12, Standard Test Methods for Electronic Friction Cone and Piezocone Penetration Testing of Soils." *Annual Book of ASTM Standards*. 4.08. West Conshohocken, PA. doi: 10.1520/D5778-12

American Society for Testing and Materials (ASTM). (2014). "Designation D854-14, Standard Test Methods for Specific Gravity of Soil Solids by Water Pycnometer." *Annual Book of ASTM Standards*. 4.08. West Conshohocken, PA. doi: 10.1520/D0854-14

Andrews, D. CA., and Martin, G. R. (2000). "Criteria for liquefaction of silty soils." *Proc. 12th World Conference on Earthquake Engineering*, Upper Hut, New Zealand.

Andrus, R. D., Fairbanks, C. D., Zhang, J., Camp III, W. M., Casey, T. J., Cleary, T. J., and Wright, W. B. (2006). "Shear wave velocity and seismic response of near-surface sediments in Charleston, South Carolina." *Bulletin of Seismological Society of America,* 96 (5): 1897-1914.

Andrus, R. D., and Stokoe, K. H. (2000). "Liquefaction resistance of soils from shear wave velocity." *Journal of Geotechnical and Geoenvironmental Engineering*, ASCE, 126 (11).

Arango, I., and Migues, R. E. (1996). "Investigation of the seismic liquefaction of old sand deposits." *National Science Foundation Grant no. CMS-94-16169*, March 1996.

Atkinson, G. (2008). "Ground-motion prediction equations for eastern North America from a referenced empirical approach: Implications for epistemic uncertainty." *Bulletin of the Seismological Society of America.*, 98: 1304-1318.

Atkinson, G. M., and Boore, D.M. (1995). "New ground motions relations for eastern North America." *Bulletin of the Seismological Society of America.*, 85: 17-30.

Atkinson, G. M., and Boore, D.M. (2011). "Modifications to existing ground-motion prediction equations in light of new data." *Bulletin of the Seismological Society of America.*, 101 (3): 1121-1135.

Baser, T., McCartney, J. S., Moradi, A. Smits, K. M., and Lu, N. (2016) "Impact of a thermo-hydraulic insulation layer on the long-term response of the soil-borehole thermal energy storage systems" *Geo-Chicago 2016*. PP. 125-134.

Baxter, C. DP., and Mitchell, J. K. (2004). "Experimental study on the aging of sands." *Journal of Geotechnical and Geoenvironmental Engineering*, 132 (10): 1051-1062.

Boore, D. M., and Atkinson, G. M. (2008). "Ground-motion prediction equations for the average horizontal component of PGA, PGV, and 5%-damped PSA at spectral periods between 0.01 s and 10.0 s." *Earthquake Spectra*, 24 (1): 99–138.

Boulanger, R. W., and Idriss, I. M. (2006). "Liquefaction susceptibility criteria for silts and clays." *Journal of Geotechnical and Geoenvironmental Engineering*, 132 (11): 1413- 1426.

Bradley, B. A. (2010). "NZ-specific pseudo-spectral acceleration ground motion prediction equations based on foreign models." *Department of Civil and Natural Resources Engineering*, University of Canterbury, Christchurch, New Zealand, 324 pp.

Bray, J. D., and Sancio, R. B. (2006). "Assessment of the liquefaction susceptibility of fine-grained soils." *Journal of Geotechnical and Geoenvironmental Engineering*, 132 (9): 1165-1177.

Campbell, K. W. (2001). "Development of semi-empirical attenuation relationships for the CEUS." *USGS Annual Technical Summary.*

Campbell, K. W. (2003). "Prediction of strong ground motion using the hybrid empirical method and its use in the development of ground motion (attenuation) relations in eastern North America." *Bulletin of Seismological Society of America,* 93 (3): 1012-1033.

Cetin, K. O., Seed, R. B., Der Kiureghian, A., Tokimatsu, K., Harder, L. F., Kayen, R. E., and Moss, R. E. S. (2004). "Standard penetration test-based probabilistic and deterministic assessment of seismic soil liquefaction potential." *Journal of Geotechnical and Geoenvironmental Engineering*, ASCE 130 (12): 1314-340.

Chiou, B. S. J., and Youngs, R. R (2008). "An NGA model for the average horizontal component of peak ground motion and response spectra." *Earthquake Spectra*, 24 (1): 173-215.

Cox, J. H. M. (1984). "Paleoseismology studies in South Carolina." *Masters Thesis, University of South Carolina,* Columbia, SC.

Doar III, W. R. (2007). "Vibracore logs from the Fort Dorchester site." *South Carolina Department of Natural Resources*, South Carolina Geological Survey (interagency communication).

Dura-Gomez, I. and Talwani, P. (2009). "Finding faults in the Charleston area, South Carolina: 1, Seismological data." *Seismological Research. Letters.,* 80 (5): 883-900.

Dutton, C. E. (1888). The Charleston Earthquake of August 31, 1886. *United States Geological Survey*, 203-528; Ninth Annual Report of the United States Geological Survey to the Secretary of the Interior: 1887-1888.

Ellis, C., and De Alba, P. (1999). “Acceleration distribution and epicentral location of the 1755 Cape Ann earthquake from case histories of ground failure.” *Seismological Research Letters*, 70 (6): 758-773.

Gassman, S. L., Sasanakul, I., Pierce, C. E., Gheibi, E., Ovalle Villamil, W., Rahman, M., and Starcher, R. (2016). “Geosystem failures from a 1000-yr flood event: pipe culvert.” *Proc., 5th Annual Southeastern GSA Section Meeting,* doi: 10.1130/abs/2016SE-273421

Ghavami, M., Javadi, S., and Zhao, Q. (2016) “Laboratory characterization of the saturated conductivities of compacted clay-organobentonite mixtures” *Geo-Chicago*. doi: 10.1061/9780784480144.045

Gheibi, E., and Bagheripour, M. H. (2010). "Evaluation of the equivalent number of cycles in liquefaction potential study using energy approach." *Proc., 4th International Conference on Geotechnical Engineering and soil Mechanics, Tehran, Iran.* doi: 10.13140/RG.2.1.5174.7841/1

Gheibi, E., and Bagheripour, M. H. (2011). "Alterations of equivalent number of cycles in depth of soil profile." *Proc., 6th International Conference of Seismology and Earthquake Engineering (SEE6),* doi: 10.13140/RG.2.2.16539.67360

Gheibi, E., and Bagheripour, M. H. (2011). "Effect of parameters on equivalent number of cycles using nonlinear seismic site response analysis." *Advanced Materials Research,* 255: pp. 2365-2369. doi: 10.4028/www.scientific.net/AMR.255-260.2365

Gheibi, E., Bagheripour, M. H., and Gheibi, A. (2011). "Soil liquefaction potential assessment using nonlinear site response analysis." *Proc., 6th International Conference of Seismology and Earthquake Engineering (SEE6),* doi: 10.13140/RG.2.2.29961.44641

Gheibi, E., and Gassman, S. L. (2014). "Back analysis of prehistoric earthquake accelerations at the Hollywood site in the South Carolina Coastal Plain." *Proc., 86th annual meeting of the Eastern Section of the Seismological Society of America,* Seismological Society of America. doi: 10.13140/2.1.2796.2560

Gheibi, E., and Gassman, S. L. (2014). "Reassessment of prehistoric earthquake accelerations at Sampit and Gapway sites in the South Carolina Coastal Plain." *Proc., 10NCEE,* doi: 10.4231/D3PV6B73Z

Gheibi, E., and Gassman, S. L. (2015). "Magnitudes of prehistoric earthquakes at the Hollywood, South Carolina, site." *IFCEE 2015*: pp. 1246-1256. doi: 10.1061/9780784479087.112

Gheibi, E., and Gassman, S. L. (2016). "Application of GMPEs to estimate the minimum magnitude and peak ground acceleration of prehistoric earthquakes at Hollywood, SC." *Engineering Geology,* 214: 60-66. doi: 10.1016/j.enggeo.2016.09.016

Gheibi, E., Gassman, S. L., Hasek, M., and Talwani, P. (2013). "Effect of aging on back analysis of a Charleston-area prehistoric earthquake magnitude." *Proc., 85th annual meeting of the eastern section of the seismological society of America*, Seismological Society of America.

Gheibi, E., Gassman, S. L., and Tavakoli, A. (2014). "Using regression model to predict cyclic resistance ratio at South Carolina Coastal Plain (SCCP)." *Proc., 22nd Annual Southeast SAS Users Group Conference (SESUG 2014),* Institute for Advanced Analytics. doi: 10.13140/2.1.4893.4081

Gheibi, E., Gassman, S. L., Hasek, M., and Talwani, P. (2017). "Assessment of paleoseismic shaking that caused sand blow at Fort Dorchester, SC." *Bulletin of Earthquake Engineering*, Submitted.

Gheibi, E., Sasanakul, I., Sanin, M., and Puebla, H. (2016). "Effect of temperatures on the dynamic properties of asphaltic core for an earth dam." *Geo-Chicago 2016:* pp. 266-275. doi: 10.1061/9780784480151.027

Green, R. A., Maurer, B. W., Bradley, B. A., Wotherspoon, L., and Cubrinovski, M. (2013). "Implications from liquefaction observations in New Zealand for interpreting paleoliquefaction data in the central eastern United States (CEUS)." *U.S. Geological Society Final Technical Report Award No. G12AP20002.*

Green, R. A., Obermeier, S. F., and Olson, S. M. (2005). "Engineering geologic and geotechnical analysis of paleoseismic shaking using liquefaction effects: field examples." *Engineering Geology,* 76: 263-293.

Hasek, M. J. (2016). "Liquefaction potential as related to the aging of SC outer coastal plain sands." *Ph.D. Dissertation Submitted to the University of South Carolina*, Columbia. SC.

Hasek, M. J., and Gassman S. L. (2016). "Characterization of soils at paleoliquefaction sites in the South Carolina Coastal Plain using petrographic and scanning electron microscopy." *Southeastern Geology,* 52(1): 1-19.

Hayati, H., and Andrus, R. D. (2008). "Liquefaction potential map of Charleston, South Carolina base on the 1886 earthquake." *Journal of Geotechnical and Geoenvironmental Engineering*, 134 (6): 815-828.

Hayati, H., and Andrus, R. D. (2009). "Updated liquefaction resistance correction factors for aged sands." *Journal of Geotechnical and Geoenvironmental Engineering*, 135(11): 1683-1692. doi: 10.1061/ASCEGT.1943-5606.0000118

Hayati, H., Andrus, R. D., Gassman, S. L., Hasek, M. J., Camp, W.M., and Talwani, P. (2008). "Characterizing the liquefaction resistance of aged soils." *GEESD IV*, Sacramento, CA.

Heidari, T., and Andrus, R. D. (2012). "Liquefaction potential assessment of pleistocene beach sands near Charleston, South Carolina." *Journal of Geotechnical and Geoenvironmental Engineering*, 138(10): 1196-1208. doi: 10.1061/(ASCE)GT.1943-5606.0000686

Hossain, A. M., Andrus, R. D., and Camp, W. M. (2013). "Correcting liquefaction resistance of unsaturated soil using wave velocity." *Journal of Geotechnical and Geoenvironmental Engineering*, 139(2): 277-287. doi: 10.1061/(ASCE)GT.1943-5606.0000770

Hu, K., Gassman, S. L., and Talwani, P. (2002a). "In-situ properties of soils at paleoliquefaction sites in the South Carolina Coastal Plain." *Seismological Research Letters*, 73 (6): 964-978.

Hu, K., Gassman, S. L., and Talwani, P. (2002b). "Magnitudes of prehistoric earthquakes in the South Carolina Coastal Plain from geotechnical data." *Seismological Research Letters*, 73 (6): 979-991.

Idriss, I. M. (1990). "Response of soft soil sites during earthquake." *In H. Bolton Seed: Memorial Symposium Proceedings.* BiTechPublishers, Richmond, BC, 2: 273-289.

Idriss, I. M. (1999). "Presentation notes: an update of the Seed-Idriss simplified procedure for evaluating liquefaction potential." *Proceeding of TRB Workshop on New Approaches to Liquefaction.* Annual Publication No. FHWARD-99-165, Federal Highway Administration, Washington, D.C.

Idriss, I. M., and Boulanger, R. W. (2008). "Soil liquefaction during earthquakes." *Monograph MNO-12, Earthquake Engineering Research Institute.* Oakland, CA.

Ishihara, K. (1985). "Stability of natural soil deposits during earthquakes." *Proc. 11th Conference on Soil Mechanics and Foundation Engineering*. International Society of Soil Mechanics and Foundation Engineers San Francisco, CA: 321-376.

Joshi R. C., Achari, G., Kaniraj, S. R., and Wijeweera, H. (1995). "Effect of aging on the penetration resistance of sands." *Canadian Geotechnical Journal*, 32 (5): 767-782.

Khabiri, M. M., Khishdari, A., and Gheibi, E. (2016). "Effect of tyre powder penetration on stress and stability of the road embankments." *Road Materials and Pavement Design*, 1-14. doi: 10.1080/14680629.2016.1194879

Khosravi, A., Gheibi, A., Rahimi, M., McCartney, J. S., and Haeri, S. M. (2016). "Impact of void ratio and state parameters on the small strain shear modulus of unsaturated soils." *Japanese Geotechnical Society Special Publication,* 2(4): 241-246. doi: 10.3208/jgssp.IRN-03

Khosravi, A., Rahimi, M., Shahbazan, P., Pak, A., and Gheibi, A. (2016). "Characterizing the variation of small strain shear modulus for silt and sand during hydraulic hysteresis." *Proc. E3S Web of Conferences,* EDP Sciences, 14018. doi: 10.1051/e3sconf/20160914018

Kulhawy, F. H., and Mayne, P. W. (1990). "Manual on estimating soil properties for foundation design." *Final Report, EL-6800, Electric Power Research Institute,* 1439-6.

Leon, E., Gassman, S. L., and Talwani, P. (2005). "Accounting for soil aging on assessing magnitudes and accelerations of prehistoric earthquakes." *Earthquake Spectra,* 21 (3): 737-759.

Leon, E., Gassman, S. L., and Talwani, P. (2006). "Accounting for soil age when assessing liquefaction potential." *Journal of Geotechnical and Geoenvironmental Engineering,* 132(3): 363-377.

Liao, S. C., and Withman, R. V. (1986). "Overburden correction factors for SPT in sand." *Journal of Geotechnical Engineering,* 112 (3): 373-77.

Lunne, T., Robertson, P. K., and Powel, J. J. (1997). "Cone penetration testing in geotechnical practice." *EF Spou/Blackie Academic, Routledge Publishers,* London, UK.

Malekzadeh, M., and Sivakugan, N. (2016) "One-dimensional electrokinetic stabilization of dredged mud" *Marine Georesources and Geotechnilogy,* doi: 10.1080/1064119X.2016.1213778

Malekzadeh, M., and Sivakugan, N. (2016) "Experimental study on intermittent electroconsolidation of singly and doubly drained dredged sediments" *International Journal of Geotechnical Engineering,* doi: 10.1080/19386362.2016.1181143

Martin, J. R. (1990). "Implications from a geotechnical investigation of liquefaction phenomena associated with seismic events in the Charleston, SC area" *PhD Dissertation, Virginia Polytechnic Institute and State University*.

Martin, J. R., and Clough, G. M. (1994). "Seismic parameters from liquefaction evidence." *Journal of Geotechnical Engineering,* 120 (8): 1345-1361.

McCartan, L., Lemon, E. M. Jr., and Weems, R. E. (1984). "Geologic map of the area between Charleston and Orangeburg, South Carolina." *United States Geological Survey*, Miscellaneous Investigations Map I-1472.

McCartney, J. S, Moradi, A., Smits, K. M., Massey, J., and Cihan, A. (2015) "Impact of coupled heat transfer and water flow on soil borehole thermal energy storage (SBTES) systems: experimental and modeling investigation" *Geothermics*. 57. PP. 56-72.

McVerry, G. H., Zhao, J. X., Abrahamson, N. A., and Sommerville, P.G. (2006). "New Zealand acceleration response spectrum attenuation relations for crustal and subduction zone earthquakes." *Bulletin of the New Zealand Society for Earthquake Engineering*, 39 (1): 1-58.

Mesri, G., Feng, T. W., and Banek, J.M. (1990). "Post densification penetration resistance of clean sands." *Journal of Geotechnical Engineering*, 116 (7): 1095-1115.

Michalowski, R. L., and Nadukuru, S. S. (2015). "Contact Fatigue: A key mechanism in time-dependent behavior of sand after dynamic compaction." *Geotechnical Special Publication*, 256, 2233-2241.

Mitchell, J. K. (1986). "Practical problems from surprising soil behavior." *The 20th Terzaghi Lecture, Journal of Geotechnical Engineering*, ASCE 112 (3): 259-289.

Mitchell, J. K., and Solymar, Z. V. (1984). "Time dependent strength gain in freshly deposited or densified sand." *Journal of Geotechnical Engineering, ASCE*. 110 (11): 1559-1576.

Mohammadi, B., and Shahabi, F. (2012). "The effect of edge delamination onset and growth on the post buckling behavior of laminated composites by using de-cohesive elements" *15th European Conference on Composite Materials, Venice, Italy.*

Mohammadi, B., and Shahabi, F. (2015). "On computational modeling of postbuckling behavior of composite laminates containing single and multiple through-the-width delaminations using interface elements with cohesive law" *Engineering Fracture Mechanics*, 152. doi: 10.1016/j.engfracmech.2015.04.005

Moradi, A., Smits, K. M., Lu, N., and McCartney, J. S. (2016) "Heat transfer in unsaturated soil with application to borehole thermal energy storage" *Vadose Zone Journal*. 15 (10). doi: 10.2136/vzj2016.03.0027

Moradi, A., Tootkaboni, M., and Pennell, K. G. (2015) "A variance decomposition approach to uncertainty quantification and sensitivity analysis of the Johnson and Ettinger model" *Journal of the Air & Waste Management Association*. 65 (2). PP. 154-164

Moss, R. E. S., Seed, R. B., Kayen, R. E., Stewart, J. P., Der Kiureghian, A., and Cetin, K. O. (2006). "CPT-based probabilistic and deterministic assessment of in situ seismic soil liquefaction potential." *Journal of Geotechnical and Geoenvironmental Engineering, ASCE*. 132 (8): 1032-051.

Obermeier, S. F., Olson, S. M., Pond, E., Green, R., Stark, T. D., and Mitchell, J. K. (2001). "Paleoliquefaction studies in continental settings: geologic and geotechnical factors in interpretations and back-analysis." *US Geological Survey Open-File Report 01-29*.

Obermeier S. F., and Pond, E. C. (1999). "Issues in using liquefaction features for paleoseismic analysis." *Seismological Research Letters.* 70 (1): 34-58.

Obermeier, S. F., Weems, R. E., and Jacobson, R. B. (1987). "Earthquake-induced liquefaction features in the coastal South Carolina region." *US Geological Survey Open File Report,* 87, 504.

Olson, S. M., Green, R. A., and Obermeier, S. F. (2005). "Geotechnical analysis of paleoseismic shaking using liquefaction features: a major updating." *Journal of Engineering Geology*. 76: 235-261.

Olson, S. M., Obermeier, S. F., and Stark, T. D. (2001). "Interpretation of penetration resistance for back-analysis at sites of previous liquefaction." *Seismological Research Letters,* 72(1): 46-59.

Petersen, M. D., Moschetti, M. P., Powers, P. M., Mueller, C. S., Haller, K. M., Frankel, A. D., Zeng, Y., Rezaeian, S., Harmsen, S. C., and Boyd, O. S., et al. (2014). "Documentation for the 2014 update of the United States national seismic hazard maps." *U.S. Geological Survey Open-File Rept.* 2014-1091, 243 pp.

Pezeshk, S., Zandieh, A., and Tavakoli, B. (2011). "Hybrid empirical ground-motion prediction equations for eastern north America using NGA models and updated seismological parameters." *Bulletin of Seismological Society of America,* 101(4): 1859-1870. doi: 10.1785/0120100144

Pond, E. C. (1996). "Seismic parameters for the central United States based on paleoliquefaction evidence in the Wabash Valley." *Ph.D. Dissertation, Virginia Polytechnic Institute*, Blacksburg, Virginia, pp.583.

Pond, E. C., and Martin, J. R. (1997). "Estimated magnitudes and accelerations associated with prehistoric earthquakes in the Wabash Valley region of the central United States." *Seismological Research Letters,* 68(4): 611-623.

Robertson, P. K. (1990). "Soil classification using the cone penetration test." *Canadian Geotechnical Journal,* 27: 151-158.

Robertson, P. K. (2009). "Interpretation of cone penetration tests-a unified approach." *Canadian Geotechnical Journal,* 46: 1337-1355.

Robertson, P. K., and Wride, C. E. (1998). "Evaluating cyclic liquefaction potential using the cone penetration test." *Canadian Geotechnical Journal.,* 35 (3): 442-459.

Regueiro, R. A., Zhang, B., and Shahabi, F. (2014). "Micromorphic continuum stress measures calculated from three-dimensional ellipsoidal discrete element simulations on granular media." *Geomechanics from Micro to Macro,* 195.

Saeedi, M., Li, L., and Moradi, A. (2012) "Effect of alternative electrolytes on enhanced electrokinetic remediation of hexavalent chromium in clayey soil" *International Journal of Environmental Research*. 7 (1). PP. 39-50.

Salamat-Talab, M., Shahabi, F., and Assadi, A. (2013). "Size dependent analysis of functionally graded microbeams using strain gradient elasticity incorporated with surface energy" Applied *Mathematical Modelling,* 37 (s 1-2): 507-526. doi: 10.1016/j.apm.2012.02.053

Salimi-Majd, D., Shahabi, F., and Mohamamdi, B. (2016). "Effective local stress intensity factor criterion for prediction of crack growth trajectory under mixed mode fracture conditions" *Theoretical and Applied Fracture Mechanics*. doi: 10.1016/j.tafmec.2016.01.009

SAS Institute Incorporated. (2013). "SAS for Windows 9.4. Cary." *NC: SAS Institute Inc.*

Sasanakul, I., Gassman, S. L., Pierce, C. E., Gheibi, E., Ovalle Villamil, W., Rahman, M., and Starcher, R. (2016). "Geosystem failures from a 1000-yr flood event: dams." *Proc., 5th Annual Southeastern GSA Section Meeting,* doi: 10.1130/abs/2016SE-273415

Schmertmann, J. H. (1987). "Discussion of "Time-dependent strength gain in freshly deposited or densified sand," by J. Mitchell, and Z. V. Solymar." *Journal of Geotechnical Engineering, ASCE,* 113 (2): 173-175.

Schmertmann, J. H. (1991). "The mechanical aging of soils." *Journal of the Geotechnical Engineering Division, ASCE,* 117 (9): 1288-1330.

Seed, H. B. (1979). "Soil liquefaction and cyclic mobility evaluation for level ground during earthquakes." *Journal of the Geotechnical Engineering Division, ASCE,* 105 (2): 201-255.

Seed, H. B., Harder, L. F., and Jong, H. (1988). "Re-evaluation of the slide in the lower San Fernando dam in the earthquake of February 9, 1971." *Report No. UBC/EERC-88/04.* University of California. Berkeley, Earthquake Engineering Research Center.

Seed, H. B., and Idriss, I. M. (1971). "Simplified procedure for evaluating soil liquefaction potential." *Journal of the Soil Mechanics and Foundations Division,* 97 (9): 1249–1273.

Seed, H. B., Lee, K. L., Idriss, I. M., and Makdisi, F. (1975). "The slides in the San Fernando dams during the earthquake of February 9, 1971." *Journal of Geotechnical Engineering Division, ASCE,* 101 (GT7): 651-688.

Seed, H. B., Tokimatsu, K., Harder, L. F., and Chung, R. M. (1984). "The Influence of SPT procedures in soil liquefaction resistance evaluations." *Report No. UBC/EERC-84/15.* University of California. Berkeley, Earthquake Engineering Research Center.

Shahsavari, M., and Grabinsky, M. (2014). "Cemented paste backfill consolidation with deposition-dependent boundary conditions." *Proc. 67th Canadian Geotechnical Conference.*

Shahsavari, M., Moghaddam, R., and Grabinsky, M. (2014). "Liquefaction screening assessment for as-placed cemented paste backfill." *Proc. 67th Canadian Geotechnical Conference,* doi: 10.13140/2.1.1450.5769

Shahsavari, M., and Sivathayalan, S. (2014). "Effects of overconsolidation and the direction of principal stresses on liquefaction susceptibility of Fraser River sand." *Proc. 67th Canadian Geotechnical Conference,* doi: 10.13140/2.1.3547.7281

Shahsavari, M., and Sivathayalan, S. (2014). "Post liquefaction response of initially overconsolidated Fraser River sand." *Proc. 67th Canadian Geotechnical Conference,* doi: 10.13140/2.1.4596.3046

Shooshpasha, I., Afzali Rad, M., Ghavami, M., Kamalijoo, H. (2011) "Study on bearing capacity of pile in liquefiable and unliquefiable soil layers" *Geo-Frontiers Congress,* doi: 10.1061/41165(397)380

Skempton A. W. (1986). "Standard penetration test procedures and the effects in sands of overburden pressure, relative density, particle size, aging and overconsolidation." *Geotechnique,* 36 (3): 425-447.

Somerville, P., Collins, N., Abrahamson, N., Graves, R., and Saikia, C. (2001). "Ground motion attenuation relations for the central and eastern united states." *Final Report to the US Geological Survey.*

Stark, T. D., Obermeier, S. F., Newman, E. J., and Stark, J. M. (2002). "Interpretation of ground shaking from paleoliquefaction features." *http://erp web.er.usgs.gov/reports/annsum/vol43/cu/ g0030.pdf, (2/08/03).*

Talwani, P., Amick, D. C., and Schaeffer, W. T. (1999). "Paleoliquefaction studies in the South Carolina Coastal Plain." *Technical Report NUREG/CR-6619,* 109. Nuclear Regulatory Commission, Washington, D.C.

Talwani, P., and Cox, J. (1985). "Paleoseismic evidence for recurrence of earthquakes near Charleston, South Carolina." *Science.,* 229 (4711): 379-381.

Talwani, P., Hasek, M., Gassman, S. L., Doar III, W. R., and Chapman, A. (2011). "Discovery of a sand blow and associated fault in the epicentral area of the 1886 Charleston earthquake." *Seismological Research Letters.* 82 (4): 589-598.

Tavakoli, B., and Pezeshk, S. (2005). "Empirical-stochastic ground-motion prediction for eastern north America." *Bulletin of Seismological Research Letter*, 95: 2283-2296.

Talwani, P., and Schaeffer, W. T. (2001). "Recurrence rates of large earthquakes in the South Carolina Coastal Plain based on the paleoliquefaction data." *Journal of Geophysical Research.,* 106 (B4): 6621-6642.

Toro, G. R., Abrahamson, N. A., and Schneider, J. F. (1997). "Model of strong ground motions from earthquakes in central and eastern north America: best estimated and Uncertainties." *Seismological Research Letters,* 68: 41-57.

Tuttle, M. P., Schweig, E. S., Sims, J. D., Lafferty, R. H., Wolf, L. W., and Haynes, M. L. (2002). "The earthquake potential of the New Madrid seismic zone." *Bulletin of the Seismological Society of America,* 92 (6): 2080-2089.

Weems, R. E., and Lemon, E. M. (1984). "Geologic map of the stallsville quadrangle, Dorchester and Charleston Counties, South Carolina." *United States Geological Survey*, Geologic Quadrangle, Map GQ-1581, 2 sheets.

Weems, R. E., Obermeier, S. F., Pavich, M. J., Gohn, G. S., and Rubin, M. (1986). "Evidence for three moderate to large prehistoric Holocene earthquakes near Charleston, South Carolina." *Proceeding of 3rd U.S. National Conference on Earthquake Engineering Charleston, South Carolina,* Earthquake Engineering Research Institute, Oakland, CA., 1: 3-13.

Wells, D. L., and Coppersmith, K. J. (1994). "New empirical relationships among magnitude, rupture length, rupture width, rupture area, and surface displacement." *Bulletin of the Seismological Society of America,* 84 (4): 974-1002.

Williamson, J. (2013). "Liquefaction potential of South Carolina Coastal Plain soils using dilatometer data." *Masters Thesis, University of South Carolina,* Columbia, SC.

Williamson, J. R. and Gassman, S. L. (2014). "Identification of liquefiable coastal plain soils using DMT, SPT and CPT profiles." *Proceeding of ASCE GeoCongress Special Publication*, Atlanta, GA.

Youd, T. L., and Hoose, S. N. (1977). "Liquefaction and geologic setting." *Proceedings of Sixth World Conference on Earthquake Engineering*, New Delhi, India, Vol. III.

Youd, T. L., and Idriss, I. M. (1997). "Proc. NCEER workshop on evaluation of liquefaction resistance of soils." *National Center for Earthquake Engineering Research Technical Report NCEER-97-0022*: 276.p.

Youd, T. L., Idriss, I. M., Andrus, R. D., Arango, I., Castro, G., Christian, J. T., Dobry, R., Finn, W. D. L., Harder, L. F., Hynes, M. E., Ishihara, K., Koester, J. P., Liao, S. S. C., Marcuson, W. F., Martin, G. R., Mitchell, J. K., Moriwaki, Y., Power, M. S., Robertson, P. K., Seed, R. B., and Stokoe, K. H. (2001). "Liquefaction resistance of soils: summary report from the 1996 NCEER and 1998 NCEER/NSF workshops on evaluation of liquefaction resistance of soils." *Journal of Geotechnical and Geoenvironmental Engineering, ASCE,* 127 (10): 817-33.

APPENDIX A

COPYRIGHT PERMISSIONS TO REPRINT

A.1 CHAPTER 3 COPYRIGHT PERMISSION

Copyright release Inbox x

emad gheibi <emadgheibi@gmail.com> Jul 13
to juliane

Dear Sir/Madam,

I have used my published paper in 10NCEE in my PhD dissertation and I need a letter that indicate I have received the permission to do so. I would appreciate it if you can provide me a confirmation so that I can re-use the paper below as one of the chapters in my dissertation:

Paper Title:

Reassessment of Prehistoric Earthquake Accelerations at Sampit and Gapway in the South Carolina Coastal Plain

Paper link:
https://nees.org/resources/11271

Thank you in advance

Emad Gheibi
PhD Candidate
Department of Civil and Environmental Engineering
University of South Carolina
300 Main Street, C109
Columbia, SC 29208
Ph: (803)-269-3133
emadgheibi@gmail.com

Juliane Lane <juliane@eeri.org> Jul 13
to me

Dear Emad,

Permission is granted to use the paper in your dissertation.

Please let us know if you need anything else.

Regards,
Juliane

From: emad gheibi [mailto:emadgheibi@gmail.com]
Sent: Wednesday, July 13, 2016 12:27 PM
To: juliane@eeri.org
Subject: Copyright release

A.2 CHAPTER 4 COPYRIGHT PERMISSION

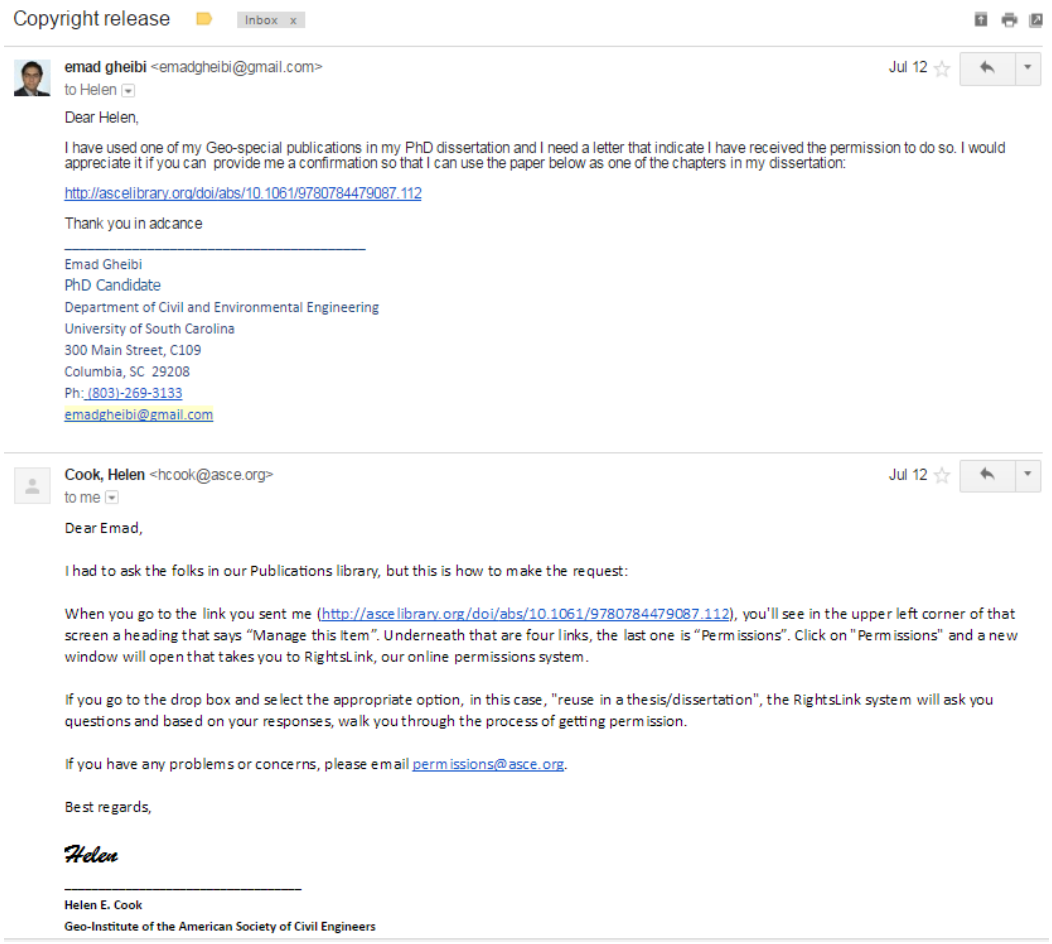

Copyright release Inbox x

emad gheibi <emadgheibi@gmail.com> Jul 12

to Helen

Dear Helen,

I have used one of my Geo-special publications in my PhD dissertation and I need a letter that indicate I have received the permission to do so. I would appreciate it if you can provide me a confirmation so that I can use the paper below as one of the chapters in my dissertation:

http://ascelibrary.org/doi/abs/10.1061/9780784479087.112

Thank you in adcance

Emad Gheibi
PhD Candidate
Department of Civil and Environmental Engineering
University of South Carolina
300 Main Street, C109
Columbia, SC 29208
Ph: (803)-269-3133
emadgheibi@gmail.com

Cook, Helen <hcook@asce.org> Jul 12

to me

Dear Emad,

I had to ask the folks in our Publications library, but this is how to make the request:

When you go to the link you sent me (http://ascelibrary.org/doi/abs/10.1061/9780784479087.112), you'll see in the upper left corner of that screen a heading that says "Manage this item". Underneath that are four links, the last one is "Permissions". Click on "Permissions" and a new window will open that takes you to RightsLink, our online permissions system.

If you go to the drop box and select the appropriate option, in this case, "reuse in a thesis/dissertation", the RightsLink system will ask you questions and based on your responses, walk you through the process of getting permission.

If you have any problems or concerns, please email permissions@asce.org.

Best regards,

Helen

Helen E. Cook
Geo-Institute of the American Society of Civil Engineers

Copyright Clearance Center RightsLink®

Home | Create Account | Help | Live Chat

ASCE AMERICAN SOCIETY OF CIVIL ENGINEERS

Conference Proceeding:	IFCEE 2015
Conference Proceeding Paper:	Magnitudes of Prehistoric Earthquakes at the Hollywood, South Carolina, Site
Author:	Emad Gheibi, Sarah L. Gassman
Publisher:	American Society of Civil Engineers
Date:	03/17/2015

Copyright © 2015, ASCE. All rights reserved.

LOGIN

If you're a copyright.com user, you can login to RightsLink using your copyright.com credentials. Already **a RightsLink user** or want to learn more?

Permissions Request

As an author of an ASCE journal article, you are permitted to reuse the accepted manuscript version of your article for your thesis or dissertation.

BACK CLOSE WINDOW

Copyright © 2016 Copyright Clearance Center, Inc. All Rights Reserved. Privacy statement. Terms and Conditions.
Comments? We would like to hear from you. E-mail us at customercare@copyright.com

A.3 CHAPTER 6 COPYRIGHT PERMISSION

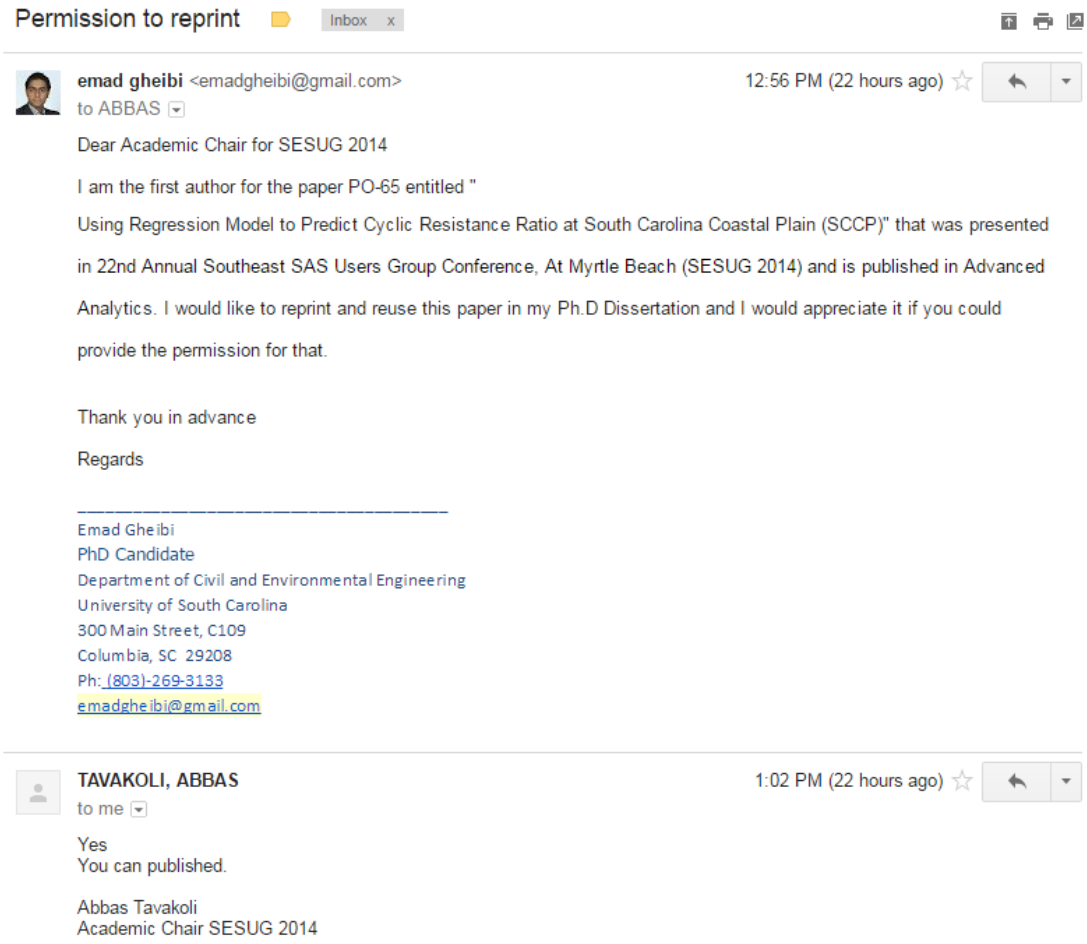

Permission to reprint Inbox x

emad gheibi <emadgheibi@gmail.com> 12:56 PM (22 hours ago)
to ABBAS

Dear Academic Chair for SESUG 2014

I am the first author for the paper PO-65 entitled "

Using Regression Model to Predict Cyclic Resistance Ratio at South Carolina Coastal Plain (SCCP)" that was presented in 22nd Annual Southeast SAS Users Group Conference, At Myrtle Beach (SESUG 2014) and is published in Advanced Analytics. I would like to reprint and reuse this paper in my Ph.D Dissertation and I would appreciate it if you could provide the permission for that.

Thank you in advance

Regards

Emad Gheibi
PhD Candidate
Department of Civil and Environmental Engineering
University of South Carolina
300 Main Street, C109
Columbia, SC 29208
Ph: (803)-269-3133
emadgheibi@gmail.com

TAVAKOLI, ABBAS 1:02 PM (22 hours ago)
to me

Yes
You can published.

Abbas Tavakoli
Academic Chair SESUG 2014

A.4 CHAPTER 7 COPYRIGHT PERMISSION

Copyright Clearance Center RightsLink®

Home | Account Info | Help | Live Chat

Title: Application of GMPEs to estimate the minimum magnitude and peak ground acceleration of prehistoric earthquakes at Hollywood, SC
Author: Emad Gheibi,S.M. ASCE,Sarah L. Gassman,M. ASCE
Publication: Engineering Geology
Publisher: Elsevier
Date: 30 November 2016

Logged in as:
Emad Gheibi
LOGOUT

Order Completed

Thank you for your order.

This Agreement between Emad Gheibi ("You") and Elsevier ("Elsevier") consists of your license details and the terms and conditions provided by Elsevier and Copyright Clearance Center.

Your confirmation email will contain your order number for future reference.

Get the printable license.

License Number	3971991290405
License date	Oct 18, 2016
Licensed Content Publisher	Elsevier
Licensed Content Publication	Engineering Geology
Licensed Content Title	Application of GMPEs to estimate the minimum magnitude and peak ground acceleration of prehistoric earthquakes at Hollywood, SC
Licensed Content Author	Emad Gheibi,S.M. ASCE,Sarah L. Gassman,M. ASCE
Licensed Content Date	30 November 2016
Licensed Content Volume	214
Licensed Content Issue	n/a
Licensed Content Pages	7
Type of Use	reuse in a thesis/dissertation
Portion	full article
Format	both print and electronic
Are you the author of this Elsevier article?	Yes
Will you be translating?	No
Order reference number	
Title of your thesis/dissertation	IMPROVED ASSESSMENT OF THE MAGNITUDE AND ACCELERATION OF PREHISTORIC EARTHQUAKES IN THE SOUTH CAROLINA COASTAL PLAIN
Expected completion date	Nov 2016
Estimated size (number of pages)	170
Elsevier VAT number	GB 494 6272 12
Requestor Location	Emad Gheibi 300 Main St. C109 COLUMBIA, SC 29208 United States Attn: Emad Gheibi
Total	0.00 USD

ORDER MORE | CLOSE WINDOW